Arabidopsis Tubby-like proteins: subcellular localization and participation in stress signaling and mutualistic interactions

Dissertation zur Erlangung des Doktorgrades
(Dr. rer. nat.)
der Naturwissenschaftlichen Fachbereiche der
Justus-Liebig-Universität Gießen

durchgeführt am
Institut für Phytopathologie
und Angewandte Zoologie

vorgelegt von
Dipl.-Biol. Marco Uwe Reitz

Gießen, September 2012

Dekan: Prof. Dr. Holger Zorn
1. Gutachter: Prof. Dr. Karl-Heinz Kogel
2. Gutachter: Prof. Dr. Aart J. E. van Bel

Parts of this work have already been published:

Reitz MU, Bissue JK, Zocher K, Attard A, Hückelhoven R, Becker K, Imani J, Eichmann R, Schäfer P (2012) The Subcellular Localization of Tubby-Like Proteins and Participation in Stress Signaling and Root Colonization by the Mutualist *Piriformospora indica*. Plant Physiol **160:** 349-364

Reitz MU, Pai S, Imani J, Schäfer P New insights into the subcellular localization of Tubby-like proteins and their participation in the *Arabidopsis – Piriformospora indica* interaction. Plant Signaling & Behaviour. eLocation ID: e25198 (Short Communication)

Table of contents

List of abbreviations

3D	Three-dimensional
aa	Amino acid(s)
ABA	Abscisic acid
AM	Arbuscular mycorrhiza
bp	Base pairs
BSA	Bovine serum albumin
dest	distilled
CaMV35S	Cauliflower mosaic virus 35S promoter
cDNA	Complementary DNA
CDS	Coding sequence
CLSM	Confocal laser scanning microscopy
CM	Complex medium
cTP	Chloroplast transit peptide
dai	Day(s) after inoculation
DEPC	Diethylpyrocarbonate
DMSO	Dimethyl sulfoxide
DNA	Desoxyribonucleic acid
DNAse	Desoxyribonuclease
dNTP	Desoxyribonucleoside triphosphate
EDTA	Ethylene diamine tetraacetic acid
EF-Tu	Elongation factor Tu
e.g.	Exempla grata
ER	Endoplasmic reticulum
ET	Ethylene
ETI	Effector triggered immunity
EtOH	Ethanol
FBP	F-box protein
FP	Fluorescent protein
Fwd	Forward
GA	Gibberellic acid
GFP	Green fluorescent protein
GPCR	G protein-coupled receptor
GUS	β-glucuronidase
h	Hour/hours
hat	Hours after treatment
HR	Hypersensitive response
HSP	Heat shock protein
IP_3	Inositol 1,4,5-trisphosphate
ISB	L-alpha-glycerophospho-D-myo-inositol-4,5-bis-phosphate
ISR	Induced systemic resistance
IAA	Indole-3-acetic acid
JA	Jasmonic acid
kDa	Kilo Dalton
LB	Lysogenic broth
LRR	Leucin-rich repeat

MAMP	Microbe-associated molecular pattern
MOPS	3-(N-Morpholino)propanesulfonic acid
MQ H_2O	Milli-Q water
mRNA	Messenger RNA
MS medium	Murashige & Skoog medium
MTI	MAMP-triggered immunity
NB	Nucleotide binding
NLS	Nuclear localization signal
OD	Optical density
PAMP	Pathogen-associated molecular pattern
PDB	Potato dextrose broth
PCR	Polymerase chain reaction
PEG	Polyethylene glycol
PH	Pleckstrin homology
PIP_2	Phosphatidylinositol 4,5-bisphophate
PLC	Phospholipase C
PLSCR	Phospholipid scramblase
PM	Plasma membrane
PPI(s)	Polyphosphoinositide(s)
PR	Pathogenesis-related
PRR	Pathogen recognition receptor
PTI	PAMP-triggered immunity
qRT-PCR	Quantitative real-time PCR
rev	Reverse
RLK	Receptor-like kinase
RNA	Ribonucleic acid
RNase A	Ribonuclease A
ROS	Reactive oxygen species
rpm	Rounds per minute
R protein	Resistance protein
RT	Room temperature
SA	Salicylic acid
SAR	Systemic aquired resistance
SCF	SKP1/Cullin/F-box
SD	Standard deviation
SDS	Sodium dodecyl sulfate
SE	Standard error
TAIR	The Arabidopsis Information Resource
TBE	Tris-Borate-EDTA
TLP	Tubby-like protein
Tris	Tris-(hydroxymethyl)-aminomethane
TUSP	Tubby superfamily protein
UPR	Unfolded protein response
UTR	Untranslated region
WT	Wild-type
YFP	Yellow fluorescent protein

1. Introduction

Plants are constantly exposed to a variety of biotic and abiotic stresses. As sessile organisms they have evolved mechanisms to quickly perceive and react to these adverse conditions. Especially, salt and drought stress have become a major problem for plant growth with salt stress alone affecting about 6% of the land area (Munns, 2002) and causing tremendous losses in agriculture (e.g. Zhu, 2003; Parida and Das, 2005). More and more land becomes salinated, which is alarming as the loss of arable land is accompanied by an ever faster growing population. Increasing the salt and drought tolerance of crop plants is therefore a vital global issue in agriculture. One way for plants to protect themselves against such unfavourable conditions is to live in a mutualistic symbiosis with mycorrhizal or endophytic fungi (Rodriguez et al., 2004). The basidiomycete *Piriformospora indica* has been shown to colonize roots of a variety of plant species. It confers several beneficial traits to its hosts including higher tolerance to salt and drought stress and serves as a model organism to investigate beneficial plant-fungal interactions (reviewed in e.g. Schäfer and Kogel, 2009; Qiang et al., 2012a). It is therefore most desirable to get a better comprehension of the interaction between plants and *P. indica* to identify compounds which may improve plant growth and stress tolerance.

The complementation of the *Arabidopsis thaliana* (in the following only called *Arabidopsis*) genome in 2000 revealed an estimated number of about 25000 genes in this model plant (The Arabidopsis Genome Initiative, 2000). Despite extensive research and the development of various high throughput methods, the function of many proteins encoded by these genes is still unknown or is investigated only slightly. In a recent study, Luhua et al. (2008) constitutively expressed 41 proteins of unknown function in *Arabidopsis*. More than 70% of these proteins led to increased tolerance to oxidative stress and more than 50% had an influence on osmotic and salinity tolerance. A high potential for the breeding and engineering of tolerant crop plants can therefore be expected to be present in yet uncharacterized proteins and it is essential to acquire more information about them. One relatively unknown gene family in plants with such potential encompasses the Tubby-like proteins (TLPs), which have recently been linked to biotic and abiotic stress responses.

1.1 The Tubby-like protein gene family

Two different abbreviations were used for Tubby-like proteins in the literature. Often respective plant proteins are designated as TLPs while TULP is generally used for animals and *Chlamydomonas rheinhardtii*, though this is not followed consequently. For an easier understanding, TLP will be used in this work for all proteins of this family.

1.1.1 TUBBY and Tubby-like proteins in animals: Discovery and diseases

In 1990, Coleman and Eicher described a late-onset obesity syndrome designated as Tubby, which had spontaneously arisen in an inbred mouse (*Mus musculus*) strain at The Jackson Laboratory. Obesity in the mutants was accompanied by insulin resistance and infertility (Coleman and Eicher, 1990). In addition, the mice showed cochlear and retinal degeneration (Heckenlively et al., 1995; Ohlemiller et al., 1995). It turned out that the Tubby syndrome was caused by a G to T transversion in a donor splice site in a gene designated *Tubby*. This led to a mutated TUBBY protein lacking the last 44 amino acids, which were replaced by 24 intron-derived new amino acids (Kleyn et al., 1996; Noben-Trauth et al., 1996). Later it could be demonstrated that *tubby* knockout mice showed the same symptoms as the original tubby mice (Stubdal et al., 2000).

The TUBBY protein was found to be conserved throughout mammals and became the prototype of a family of similar proteins (e.g. North et al., 1997; Ikeda et al., 2002; Mukhopadhyay and Jackson 2011). In addition to TUBBY, four TLPs were identified in mammalian organisms, designated as TLP1 to TLP4 (North et al., 1997; Nishina et al., 1998; Li et al., 2001). TLP4 was named Tubby superfamily protein (TUSP) in earlier publications and is more distantly related to the other members of the family (Li et al., 2001). TLPs seem to play fundamental roles in mammals, as demonstrated by disease phenotypes caused by mutations in some TLPs (reviews Ikeda et al., 2002; Carroll et al., 2004; Mukhopadhyay and Jackson, 2011). For example, embryonic lethality with several neural defects was found in *tlp3* knockout mice (Ikeda et al., 2001) and genetic ablation of *MmTLP1* caused retinal degeneration (Ikeda et al., 2000). In humans, mutations in *TLP1* are the origin of a type of retinitis pigmentosa, a disease marked by progressive degeneration of photoreceptors (Banerjee et al., 1998; Hagstrom et al., 1998; Lewis et al., 1999). Apoptosis of neurons is most likely the cause for the observed vision and hearing

deficits in mice, as well as for embryonic lethality (Ikeda et al., 2000; Stubdal et al., 2000; Ikeda et al., 2001).

1.1.2 TLPs in animals: Structure and function

The three-dimensional (3D) structure of the C-terminal part of mouse TUBBY was resolved in 1999 by Boggon and colleagues. The structure consisted of a 12-stranded anti-parallel β-barrel, filled with a central hydrophobic α-helix. This new structural motif was called Tubby domain and became the hallmark of all members of the TLP family (Boggon et al., 1999). The domain was shown to bind to polyphosphoinositides (PPIs) phosphorylated at adjacent positions of the inositol ring. It was suggested that *in vivo* phosphatidylinositol 4,5-bisphosphate (PIP_2), which is mainly present in the plasma membrane (PM), constitutes the PPI bound by the Tubby domain. Concomitantly, MmTUBBY and *Homo sapiens* (Hs) TLP3 were detected at the PM (Santagata et al., 2001). Both proteins responded to signaling from heterotrimeric G proteins of the $G_{\alpha/11}$-family by a change in their subcellular localization, implying detachment from the PM. Activation of the G proteins occurred by stimulation of G protein-coupled receptors (GPCRs) through application of a respective neurotransmitter. PM dislodgement was shown to be mediated by phospholipase C (PLC) activity, proteins capable of hydrolyzing PIP_2 (Santagata et al., 2001). The Tubby domain of MmTUBBY as well as that of TLP1 has been shown to bind to double stranded DNA and the N-termini of both proteins activated transcription from a GAL4 DNA binding site when fused to the GAL4 DNA binding domain. Together, this led to the suggestion that TLPs may act as transcriptional regulators, which, in a resting state, are sequestered at the PM (Boggon et al., 1999; Santagata et al., 2001). However, no target genes or a direct involvement in transcriptional regulation *in vivo* has been demonstrated until now.

Because of its selective and specific binding to PIP_2 the TUBBY protein has been employed as a biosensor for PIP_2 in mammals when coupled to different fluorescent proteins (Nelson et al., 2008; Quinn et al., 2008; Szentpetery et al., 2009). Although amino acid sequence alignments revealed a conservation of the identified PIP_2 binding pocket in all animal TLPs (Santagata et al., 2001), TLP2 and TLP4 have only been detected in the cytosol till now (Li et al., 2001; Mukhopadhyay et al., 2010), while TLP1 was detected in the cytosol and nucleus (He et al., 2000; Mukhopadhyay et al., 2010). However, TUBBY has also not always been detected at the PM. In some studies the protein has been found to be located solely in the cytosol or in the cytosol and the nucleus (He et al., 2000; Ikeda et al., 2002; Mukhopadhyay et al., 2010). It was

suggested that subcellular localization of TUBBY might be regulated by cell type and/or developmental status (Ikeda et al., 2002).

In addition to transcriptional regulation, TLPs have been implicated to function in vesicular trafficking (Hagstrom et al., 1999; Ikeda et al., 2000; Norman et al., 2009; Mukhopadhyay et al., 2010). TLP3 was found to be located in cilia (Norman et al., 2009; Mukhopadhyay et al., 2010), which function as sensory signaling compartments (Pazour and Rosenbaum, 2002). Ciliary localization was dependent on interaction with a protein complex till then only known to regulate retrograde transport within cilia (intraflagellar transport complex-A; IFT-A). Transport of GPCRs into cilia was shown to be regulated by IFT-A and TLP3. In addition to interaction between TLP3 and IFT-A, GPCR transport also depended on the phospholipid binding capacity of TLP3. Therefore, TLP3 was suggested to work as bridging molecule between IFT-A and vesicles carrying GPCRs (Mukhopadhyay et al., 2010). Another role for TLPs as bridging molecules was described by Caberoy and co-workers (Caberoy et al., 2010a; Caberoy et al., 2010b; Caberoy et al. 2012). All mouse TLPs were reported to be present in the extracellular matrix (Caberoy and Li, 2009). TUBBY and TLP1 bound apoptotic debris via their Tubby domain. Interestingly, this was independent of the phospholipid binding capacity of TUBBY. Simultaneously, the proteins interacted with transmembrane receptors via amino acids in their N-terminal part, thereby facilitating phagocytosis (Caberoy et al., 2010a; Caberoy et al., 2010b; Caberoy et al. 2012). Mouse TUBBY was also shown to be phosphorylated by the insulin receptor in response to the hormone and suggested to act as adapter between the receptor and other proteins, amongst them a PLCγ enzyme (Kapeller et al., 1999).

In contrast to the conserved C-terminal Tubby domain, mammalian TLPs possess variable N-terminal regions. In TLP4 a WD40 repeat region and a suppressor of cytokinine signaling (SOCS) domain were detected in the N-terminal part (Li et al., 2001). SOCS domains confer substrate specificity to ElonginC-cullin-SOCS-box E3 ligases, which work in protein degradation (Kile et al., 2002). In addition to TLP3, TUBBY and TLP2 also bound to IFT-A by a conserved region within their N-terminal parts (Mukhopadhyay et al., 2010) and as described, TUBBY and TLP1 interact with receptors regulating phagocytosis (Caberoy et al., 2010a; Caberoy et al., 2010b; Caberoy et al. 2012). Furthermore, nuclear localization signals have been reported to be present in the N-terminal parts of TUBBY, TLP1, TLP3 and TLP4 (Boggon et al., 1999; He et al., 2000; Santagata et al., 2001; Li et al., 2001).

Taken together, animal TLPs seem to play crucial roles in neuronal function and development. But despite mounting data, no comprehensive view concerning their direct biochemical functions has emerged until now. It was suggested that TLPs might be multifunctional proteins and/or integrate information from several signaling pathways (Ikeda et al., 2002; Carroll et al., 2004).

1.1.3 Phylogenetic classification of the gene family

The structure for the *Arabidopsis* protein At5g01750 was resolved by the CESG structural genomic project (http:://www.uwstructuralgenomics.org) and proved strikingly similarity to that of the Tubby domain (Bateman et al., 2009). At5g01750 belongs to the DUF567 family of uncharacterized proteins, which consists of 21 members in *Arabidopsis*. The family is closely related to that of the phospholipid scramblases (PLSCRs). Using At5g01750 as template, the structure of PLSCR proteins was thus suggested to be also similar to that of the Tubby domain (Bateman et al., 2009). PLSCR proteins have first been identified to mediate transbilayer movement of membrane phospholipids (Zhou et al., 1997). In addition, functions in cellular signaling have been demonstrated (e.g. Zhou et al., 2005; Amir-Moazami et al., 2008). PLSCR1 for example, a protein bound to the inner side of the PM by *S*-acylation, was also found to activate transcription in the nucleus (Zhou et al., 2005). In that, it resembles the subcellular localization dynamics of MmTUBBY (Santagata et al., 2001; Bateman et al., 2009). In contrast to TLPs, which are only present in eukaryotes, the DUF567/PLSCR family also exists in prokaryotes. It was therefore suggested that scramblases are evolutionary older and TLPs might have evolved from an ancestral scramblase-like protein (Bateman et al., 2009). Besides that, a Tubby domain like structure has not been reported for any other protein family.

TLPs seem to be present in most uni- and multicellular organisms, including plants (e.g. Kleyn et al., 1996; Nishina et al., 1998; Riechmann et al., 2000; Li et al., 2001; Gagne et al., 2002; Lai et al., 2004; Jain et al., 2007; Liu, 2008; Yang et al., 2008; Lai et al., 2012). Fungi represent an exception as so far only one TLP has been identified in a single species (Liu, 2008; Lai et al., 2012). A phylogenetic tree for the gene family employing sequences from various species across the eukaryotic kingdoms was generated by Liu (2008) using the conserved C-terminal TLP sequence. Two major clades, an animal- and a plant specific one, were identified. In addition, a small mixed clade was found. This clade contained genes from algae, higher plants, a fungal and one excavata species. Interestingly, one TLP from the green alga *C. rheinhardtii* was present in

the mixed and one in the plant-specific clade, although the algal TLP is only distantly related to TLPs from higher plants.

In comparison to the five TLPs of mammals, the gene family has undergone expansion in higher plants. 11 TLPs have been identified in *Arabidopsis* (AtTLPs) and poplar (*Populus trichocarpa* / PtTLPs), respectively, and 14 were reported for rice (*Oryza sativa* / OsTLPs) (Lai et al., 2004; Jain et al., 2007; Liu, 2008; Yang et al., 2008). Two different assignments of names for OsTLPs to respective gene loci have been introduced in literature (Liu, 2008; Yang et al., 2008). This study will follow the nomenclature used by Yang et al. (2008).

A characteristic that discerns many plant from animal TLPs is the presence of an F-box domain in their N-terminal part. The F-box is a protein-protein interaction domain. Often F-box proteins (FBPs) have been found as parts of SCF (SKP1/Cullin/F-box) complexes. These are E3 ligases involved in the ubiquitin-proteasome pathway of protein degradation (Kipreos and Pagano, 2000). Higher plants harbor large numbers of FBPs. Within the 600-700 and about 700 identified FBPs of *Arabidopsis* and rice, TLPs have been shown to form separate phylogenetic groups. This was not only the case when the full-length amino acid sequences were employed for the generation of a phylogenetic tree but also when the F-box sequences were used (Gagne et al., 2002; Jain et al., 2007). In plants, most TLPs possess an F-box. This is preceded by a leading sequence and linked to the Tubby domain by a short conserved linker. Interestingly, these sequences are encoded by the first exon in nearly all plant TLPs identified so far (Lai et al., 2004; Liu, 2008; Yang et al., 2008). This indicates that they may have arisen from a common ancestor (Lai et al., 2004). Both identified TLPs from *C. rheinhardtii* lack an F-box, as do two more TLPs identified in green algae (Yang et al., 2008; Lai et al., 2012). Therefore, the question remains when plant TLPs acquired this domain during evolution.

Yang et al. (2008) proposed a phylogenetic tree in which the TLPs from *Arabidopsis*, rice and poplar are arranged in three major clades (A-C). Clade C contains three TLPs (AtTL8, OsTLP4 and PtTLP1). None of these feature an F-box. It was suggested that they originate from a common ancestor of monocots and dicots (Yang et al., 2008). Interestingly, these three genes were also the higher plant representatives existing in the mixed-clade generated by Liu (2008). The only member present in clade B is AtTLP4. At the moment it is not clear if this is a true gene or a pseudogene (Lai et al., 2004). Clade A was further subdivided (clades A1 to A4). At least one TLP per species is present in each of these four clades. This indicates that the principal phylogenetic structure within clade A was also present before the monocot/dicot split. Two

poplar TLPs within clade A lacked an F-box (PtTLP7 and -10), while the domain was present in all other members. In addition, PtTLP7 and -10 were found to be orthologous to AtTLP7, which in turn harbors an F-box domain. It was therefore concluded that the domain was lost in the two poplar genes during evolution, rather than not have been present at all (Yang et al., 2008). Interestingly, while the total number of TLPs is similar in the three plant species, their allocation to the different clades is not. For example, two PtTLPs, three AtTLPs and six OsTLPs can be found in clade A1. Similar differences are also present in the other clades, except clade C. It was suggested that the variations arose from species specific expansion of the gene family (Yang et al., 2008). This might imply differential functions for at least some TLPs from different plant species.

1.1.4 TLPs in plants

C. reinhardtii is considered a model organism for green algae. Moreover, as it possesses flagella which are almost identical to human cilia, it serves also as model in studies concerning this organelle (Pazour and Rosenbaum, 2002). Transcription of the *C. reinhardtii* protein TLP2 was strongly induced during flagellar regeneration and a role for the protein in ciliary function was proposed (Stolc et al., 2005). The same protein was recently also identified in the *C. reinhardtii* nuclear proteome (Winck et al., 2012), which might indicate a function as transcriptional regulator. In addition, a Tubby-like protein was induced during proliferation of the dinoflagellate *Alexandrium catenella* (Toulza et al., 2010).

The first detailed study on TLPs in higher plants came from Lai et al. in 2004, which dealt with the gene family in *Arabidopsis*. An evaluation of publicly available microarray data suggested a role of some AtTLPs in hormone and environmental stress signaling. For example, expression of AtTLP9 was reduced in the *abscisic acid insensitive 1* mutant (Pei et al., 1997) as compared to wild-type plants, but was induced by cadmium treatment in ecotype *Col*-0 (Lai et al., 2004). Nevertheless, observed transcriptional changes rarely exceeded a two to threefold induction or decrease. *Arabidopsis* lines bearing a T-DNA insertion within the *AtTLP9* gene germinated some hours earlier as respective controls and germination rates were not as affected by the phytohormone abcsisic acid (ABA) as in wild-type plants. Opposite effects were observed in transgenic lines overexpressing *AtTLP9*. Also, *AtTLP9* transcription was transiently induced during seed germination (Lai et al., 2004). Besides developmental processes like seed dormancy, ABA is a key regulator of plant responses to environmental stresses such as drought and high

salinity (e.g. Parida and Das, 2005; Fujita et al., 2006). AtTLP9 was shown to be transcriptionally co-regulated and to interact with the *Arabidopsis* protein XERICO. Plants overexpressing XERICO showed higher contents of endogenous ABA and were more drought tolerant than wild-type plants. Like plants overexpressing AtTLP9, seedlings overexpressing XERICO were hypersensitive to ABA treatment (Ko et al., 2006). More hints towards a role of plant TLPs in abiotic stress signaling came from chickpea (*Cicer arietanum*). A TLP from this species, designated CaTLP1, was found to accumulate in the extracellular matrix in response to dehydration (Bhushan et al., 2007; Wardhan et al., 2012). Wardhan et al. (2012) reported further, that an YFP-tagged version of the protein was also detected in the root cell wall of stably transformed *Arabidopsis* plants. In response to dehydration, an increase of fluorescence in the nuclei of root cells was described. In addition, tobacco plants overexpressing CaTLP1 displayed higher growth rates, ABA insensitivity and increased tolerance to salt and osmotic stress. Interestingly, these plants were also more resistant to treatment with hydrogen peroxide (H_2O_2) (Wardhan et al., 2012).

Information on a possible involvement of TLPs in biotic interactions came from two studies in rice. Transcription of all 14 identified *OsTLPs* was induced after infection of rice plants with the causative agent of bacterial blight disease, *Xanthomonas oryzae* pv. *oryzae* (Cai et al., 2008; Kou et al., 2009). Furthermore, OsTLP12 was found to bind a pathogen responsive *cis*-element in the promoter of *OsWRKY13*, a gene involved in pathogen resistance. In addition, a GFP-tagged version was reported to locate to the cytoplasm and nucleus of transiently transformed onion epidermal cells (Cai et al., 2008). This was the first demonstration of a TLP binding to a specific DNA sequence. However, it was not investigated if OsTLP12 had actual influence on the transcription of *OsWRKY13*. As mentioned above, for mammals, it is not yet clear if TLPs actually act as transcriptional regulators (Mukhopadhyay and Jackson, 2011). In addition to OsTLP12, CaTLP1 was found to bind to double stranded DNA, but failed to activate transcription from a GAL4 binding site when fused to a GAL4 DNA binding domain (Wardhan et al., 2012). The same was observed for AtTLP9 (Lai et al., 2004). Also, AtTLP7 was found to associate with a plant promoter in a yeast-one-hybrid screen for root stele transcription factor – promoter interactions (Gaudinier et al., 2011). Therefore, as reported for animals, while DNA binding has been demonstrated for some plant TLPs, a direct effect on transcription has not been identified.

As many plant TLPs feature an F-box domain, they might act in protein degradation as part of SCF complexes (e.g. Gagne et al., 2002; Lai et al., 2004; Yang et al., 2008; Lai et al., 2012). Indeed, in yeast-two-hybrid assays AtTLP9 and AtTLP10 have been shown to interact with *Arabidopsis* SKP-1 like protein 1 (ASK1) a part of SCF complexes in *Arabidopsis* (Risseeuw et al., 2003; Lai et al., 2004). It remains to be shown if TLPs are actually part of SCF complexes and act in protein degradation.

For AtTLP8 a direct upstream regulator has been identified. Consensus binding sequences for the LEAFY transcription factor have been detected in the promoter region of AtTLP8. LEAFY was found to bind the promoter of AtTLP8 and to positively regulate its transcription (William et al., 2004). As LEAFY regulates the switch from vegetative to reproductive development (Weigel and Nilsson, 1995), the obtained results suggest a role of AtTLP8 in this process.

Unlike for mammalian TLPs a PM localization has not been reported for plant TLPs. Lai et al. (2012) used the same yeast assay which had been employed to demonstrate PM targeting of MmTUBBY (Santagata et al., 2001), but failed to show PM targeting for AtTLP2, -8 and -9. Nevertheless, an amino acid sequence alignment of AtTLPs with MmTUBBY revealed putative PIP_2 binding sites in the majority of the *Arabidopsis* TLPs (Lai et al., 2004).

Together, while first studies gave hints towards the function of TLPs in plants and indicate to possible roles in development and stress signaling, many questions concerning this interesting gene family remain unresolved.

1.2 Reactive oxygen species (ROS)

1.2.1 Synthesis and detoxification

The term ROS comprises several species of oxygen radicals and non-radical but reactive oxygen molecules. The best known are the hydroxyl ($OH^{\bullet}$) and superoxide anion ($O_2^{\bullet-}$) radicals, singlet oxygen ($^1O_2$) and hydrogen peroxide (H_2O_2) (e.g. Van Breusegem et al., 2001; Quan et al., 2008; Triantaphylidés and Havaux, 2009). The latter is the by far best characterized ROS at the moment. A variety of environmental stresses, such as pathogen attack, cold, high light, drought and high salt conditions lead to a rise in plant ROS levels. The main sites of ROS generation are chloroplasts, mitochondria, peroxisomes and the cell wall (Van Breusegem et al., 2001; Pfannschmidt, 2003; Laloi et al., 2004; Torres, 2010). ROS often emerge as side products of metabolic processes. For example, singlet oxygen is constitutively produced during photosynthesis in photosystem II (Apel and Hirt, 2004).

Several ROS arise in a sequence of subsequent reduction events. Superoxide radicals have only a half-life of about two to four µs (Sutherland, 1991) and readily turn into H_2O_2, a process that can even be accelerated by the activity of some enzymes. The comparibly long half-life of this ROS enables the molecule to diffuse some way within the cell. And in contrast to superoxide, H_2O_2 is able to cross membranes (Sutherland 1991; Van Breusegem et al., 2001). The much more reactive and harmful hydroxyl radicals occur in the presence of metal ions and H_2O_2 (Van Breusegem et al., 2001; Quan et al., 2008).

ROS levels are tightly regulated by a network involving at least 152 different genes (Mittler et al., 2004). This 'reactive oxygen gene network' was described as redundant and flexible. Redundancy is indicated, as the loss of one component has been shown to cause increased production of proteins with similar function. Flexibility was suggested as different stresses lead to specific transcriptional responses within the network (Mittler et al., 2004). In addition to several classes of enzymes, the antioxidants ascorbate and glutathione play vital roles in the detoxification of ROS. The term antioxidant comprises every molecule capable of quenching ROS without being turned into a destructive radical itself (Noctor and Foyer, 1998). ROS detoxifying enzymes can be found throughout the cell (Quan et al., 2008). *Arabidopsis* ascorbate peroxidases for example catalyze the conversion of H_2O_2 to water in an ascorbate dependent manner. They have been predicted to be present in the cytosol, chloroplasts, mitochondria and peroxisomes (Mittler et al., 2004).

Besides being generated as by-products, especially superoxide radicals and H_2O_2 can also actively be produced by plant cells, for example by manipulating the network of ROS detoxifying enzymes. Furthermore, plants are equipped with ROS generating enzymes. For instance NADPH-dependent oxidases in the PM produce $O_2^{\bullet-}$ and superoxide dismutases, present in several cellular compartments, transform $O_2^{\bullet-}$ into H_2O_2 (Simon-Plas et al., 2002; Torres et al., 2002; Mittler et al., 2004).

1.2.2 Damage and signaling

As reactive molecules, all ROS are potentially harmful for plant cells and can lead to oxidative stress. ROS react with a large variety of biomolecules like proteins, lipids and DNA. Excess protein damage in the photosystem causes inhibition of photosynthesis and lipid peroxidation can damage membranes. The consequences of oxidative stress can lead to cell death and may

ultimately kill the plant (Van Breusegem et al., 2001; Triantaphylidés and Havaux, 2009; Apel and Hirt, 2004).

But ROS have also emerged as important signaling compounds, where specific manipulation and tight control of ROS levels is a prerequisite. H_2O_2 was demonstrated to act in a great variety of signaling processes. It was shown to be involved in acclimatory signaling leading to elevated tolerance to abiotic stresses (e.g. Van Breusegem et al., 2001; Mittler et al., 2004), but also, for example, in regulation of stomatal closure (Pei et al., 2000; Kwak et al., 2003), photorespiration, photosynthesis (Noctor and Foyer, 1998) and root cell expansion (Kwak et al., 2003). ROS signaling is intertwined with many other signaling networks. For instance, ROS have been shown to influence hormone signaling, such as mediated by the stress hormone ABA. In turn, ROS signaling itself is highly affected by many hormones (Mittler et al., 2011). How H_2O_2 is perceived by the cell is still not completely resolved, and even less is known for other ROS. For H_2O_2 three mechanisms of perception have been proposed: (i) through redox-sensitive transcription factors, such as NPR1; (ii) inhibition of phosphatases; (iii) perception by as yet unknown receptors (Mittler et al., 2004).

ROS are also involved in biotic interactions and have significant roles during establishment of symbiotic interactions (Torres, 2010). In plant defense responses, ROS occur for instance during the oxidative burst, a fast accumulation of superoxide and H_2O_2 upon recognition of a pathogen. It was shown that PM localized NADPH-oxidases are responsible for the extracellular production of superoxide during this process (Torres et al., 2002).

1.3 Plant innate immunity

Plants are equipped with a multilayered defense system to ward off invading microorganisms like fungi, oomycetes, bacteria and viruses. A first line of defense is composed of preformed structures such as the epicuticular waxes, cell walls or preformed anti-microbial components (Wittstock and Gershenzon, 2002; Zipfel, 2008). In addition, innate immunity involves two layers of inducible cell-autonomous defense reactions. The first is called microbe-associated molecular pattern (MAMP)-triggered immunity. The second is designated as effector triggered immunity.

1.3.1 MAMP-triggered immunity (MTI)

The terms MAMP and MTI have mainly replaced the older terms pathogen-associated molecular pattern (PAMP) and PAMP-triggered immunity (PTI), since PAMPs were shown not to be restricted to pathogenic microorganisms. MAMPs are typically conserved in a larger group of microorganisms. They have vital functions within the respective organism and are therefore highly invariable. Another characteristic is that they do not occur in plants (Nürnberger et al., 2004). The best-characterized MAMP is the eubacterial protein flagellin, a structural component of the bacterial flagellum. A conserved sequence consisting of 22 amino acids at the N-terminus of the protein, flg22, has been shown to elicit defense responses in many plant species (Felix et al., 1999). Similar, the bacterial elongation factor Tu (EF-Tu) triggers immune reactions in Brassicaceae. In this case a conserved epitope of 18 amino acids (elf18) is sufficient to elicit defense responses in *Arabidopsis* (Kunze et al., 2004). In addition to these, various other MAMPs have been identified. Besides proteins from bacteria, plants do also sense, for example, bacterial lipopolysaccharides, chitin and β-glucans from fungi, and proteins from oomycetes (reviewed e.g. in Nürnberger et al., 2004; Abramovitch et al., 2006; Boller and Felix, 2009). Plants seem to sense most MAMPs through PM localized pattern recognition receptors (PRRs) (Boller and Felix, 2009). The *Arabidopsis* receptors for flg22 and elf18, FLS2 and EFR, are both receptor-like kinases (RLKs) with an extracellular leucine rich repeat (LRR) domain (Chinchilla et al., 2006; Zipfel et al., 2006). Nevertheless, not all PRRs seem to be RLK-LRR proteins (Zipfel, 2008; Boller and Felix, 2009).

MAMP recognition initiates several immune responses like Ca^{2+} influx, activation of mitogen activated protein kinase (MAPK) signaling, ROS production, callose deposition at infection sites and transcriptional induction of defense genes (Nürnberger et al., 2004). In addition, growth inhibition in seedlings was observed (Felix et al., 1999; Gómez-Gómez et al., 1999). Besides pathogens, MTI has also been shown to be active against beneficial microbes (Van Wees et al., 2008; Jacobs et al., 2011)

1.3.2 Effector-triggered immunity (ETI)

To successfully infect plants, pathogens have evolved ways to avoid MTI. A widespread way is the secretion of proteins called effectors to interfere with defense responses. Plenty of such effectors have been identified, not only from pathogens (Abramovitch et al., 2006; Chisholm et al., 2006), but for example also from a mycorrhizal fungus (Kloppholz et al., 2011). However,

plants have developed ways to recognize the effector proteins. This leads to a fast activation of strong defense responses. In this case the respective effector is also called avirulence (Avr) factor, because its presence causes increased host resistance. On the plant side, effector detection is carried out by resistance (R) proteins. In most cases these proteins feature a nucleotide binding (NB) and a C-terminal LRR domain and are therefore called NB-LRR proteins. R proteins do not necessarily interact with their effector counterparts. In several cases it was shown that they survey the status of plant proteins (Jones and Dangl, 2006; Rafiqi et al., 2009). If these are targeted by an effector, for example by phosphorylation or degradation, the change is recognized by the R protein, which in turn triggers immune responses. This mechanism is known as guard hypothesis (Van der Biezen and Jones, 1998; Dangl and Jones, 2001) or more recently as guard model (e.g. Innes, 2004). ETI defense responses can be considered as amplified version of MTI often involving plant cell death. During evolution pathogens got rid of Avr proteins or developed new effectors to suppress ETI. Conversely, plants developed new R proteins to detect these pathogens again. This led to the proposed 'zigzag' model of plant immunity and describes an ongoing arms race between plants and pathogens (Jones and Dangl, 2006).

1.3.3 Systemic resistance

Defense to invading microorganisms occurs locally at the infection site and the surrounding tissue. But in addition to this, systemic responses involving plant organs distant to the site of pathogen contact take place. Well studied forms of such mechanisms are systemic acquired resistance (SAR) and induced systemic resistance (ISR). SAR is triggered by pathogens and is mainly dependent on salicylic acid (SA) signaling and induction of SA regulated production of pathogen related (PR) proteins with anti-microbial activities (Durrant and Dong, 2004). ISR is initiated by beneficial rhizobacteria and the mechanism is dependent on the plant hormones jasmonic acid (JA) and ethylene (ET). In contrast to SAR, no or only minor changes in transcriptional regulation can be detected in systemic tissue of unchallenged plants. But after pathogenic infection, accelerated defense responses were observed, leading to enhanced resistance (Pieterse et al., 1996; Pieterse et al., 1998; Van Wees et al., 2008). An ISR-like mechanism was also shown to be responsible for increased resistance of plants colonized by the mutualistic fungus *P. indica* against leaf infecting powdery mildews (Stein et al., 2008).

1.4 *Piriformospora indica*

1.4.1 Mutualistic plant – microbe interactions

Associations between plants and microorganisms like fungi can be classified as pathogenic, parasitic and mutualistic (Newton et al., 2010). In a pathogenic relation one partner actively harms the other to gain nutrients. Parasites initiate damage to their host organisms as a side effect caused by their presence and consumption of resources, which might have otherwise been accessible to the host. On the other side, both partners benefit in a mutualistic interaction (Brundrett, 2004; Newton et al., 2010). This effect is not restricted to nutrients, but can also comprise for example a safer habitat for the microorganism or increased tolerance to biotic or abiotic stresses in plants. Nevertheless, these categories should only be regarded as stereotypes. Indeed, it has been shown that many microorganisms can be involved in different types of interactions, depending on their host and environmental conditions (Newton et al., 2010).

The best known type of mutualistic interaction between autotrophic plants and fungi are mycorrhizas. Indeed, 70-90% of land plants live in association with the most common mycorrhizal type, the arbuscular-mycorrhiza (AM), formed by members of the Glomeromycota. AMs are characterized by tree-shaped fungal structures formed within plant cells, known as arbuscules, which are thought to be the main side of interaction and nutrient exchange between both organisms (Brundrett, 2004; Parniske, 2008). In addition, there are other types of mycorrhizas, for example ericoid and orchid mycorrhizas, distinguished by specific morphological traits, interaction partners and physiological attributes (Brundrett, 2004). All mycorrhizas involve transfer of nutrients between both organisms (Brundrett, 2004). In contrast to this, many root colonizing fungi do not form distinct colonization structures. As they do not cause disease symptoms but rather more confer beneficial traits to their hosts, they are classified as endophytes (Wilson, 1995). In the case of the basidiomycete *P. indica*, features reminiscent of orchid mycorrhizas have been described, but in other traits the fungus differs from mycorrhizas (Varma et al., 1999; Deshmukh et al., 2006; Schäfer and Kogel, 2009; Jacobs et al., 2011; Qiang et al., 2012b). At the moment, *P. indica* is commonly considered as a mutualistic endophyte (e.g. Qiang et al., 2012a; Weiß et al., 2011; Zuccaro et al., 2011).

1.4.2 Sebacinales: A newly defined fungal order with a great biodiversity

P. indica was first discovered in the Indian Thar desert in 1997 (Verma et al., 1998). It was classified as a member of the Sebacinaceae family, within the newly defined order Sebacinales (Weiß et al., 2004). Until recently, the Sebacinaceae belonged to the Auriculariales, a group of wood decaying fungi, but molecular phylogenetic studies revealed that they should constitute an own order (Weiß and Oberwinkler, 2001; Weiß et al., 2004). Sebacinales have been identified on all continents and seem to be present in all ecosystems (e.g. Weiß et al., 2004; Selosse et al., 2009; Weiß et al., 2011). For example, using a PCR-based method Weiß et al. (2011) identified sebacinalean sequences in root samples from all tested 27 plant families collected on four different continents. Importantly, the model plant *Arabidopsis thaliana* was also shown to be associated with Sebacinales, providing more practical relevance to studies with *P. indica* on this plant species (Weiß et al., 2011). Till now, only beneficial fungi have been identified in this order (Schäfer and Kogel, 2009). In addition to an endophytic lifestyle, a unique number of mycorrhizal types can be found within the Sebacinales (Weiß et al., 2004). Fungi of this order have been described to form orchid mycorrhizas (e.g. Selosse et al., 2002; Huynh et al., 2009), ectomycorrhizas (e.g. Glen et al., 2002; Urban et al., 2003; Tedersoo et al., 2003), ericoid mycorrhizas (Allen et al., 2003; Selosse et al., 2007), arbutoid mycorrhizas (Selosse et al., 2007) and jungermannoid mycorrhizas with liverworts (Kottke et al., 2003). Taken together, the Sebacinales may play significant roles in many ecosystems worldwide (Weiß et al., 2004). The order has informally been divided into two clades (A and B). *P. indica*, like the majority of endophytic Sebacinales, was placed in the evolutionary more basal clade B (Weiß et al., 2004).

1.4.3 Beneficial traits conferred by *P. indica*

Studies on plant – *P. indica* interactions are simplified by the fact that the fungus can be cultivated axenically (Verma et al., 1998). Although a natural host plant has not yet been identified, *P. indica* was shown to colonize a broad range of mono- and dicotyledonous plants causing a variety of beneficial effects (e.g. Varma et al., 1999; Peskan-Berghöfer et al., 2004; Waller at al., 2005; Quiang et al., 2012a). For example, enhanced fresh weight and seed yield was reported for barley plants associated with the mutualist (Waller et al., 2005; Deshmukh et al., 2006). Increased fresh weight was also observed for various other plant species colonized by *P. indica*, including *Arabidopsis*, maize, parsley, wheat and tobacco plants (Varma et al., 1999; Peskan-Berghöfer et al., 2004; Serfling et al., 2007). In addition, the fungus caused earlier

flowering (Peskan-Berghöfer et al., 2004; Das et al., 2012), promoted root formation in cuttings (Druege et al., 2007) and increased survival rates in micropropagated plantlets (Sahay and Varma, 1999). Another important feature of *P. indica* colonized plants is a higher resistance to pathogens (e.g. Qiang et al., 2012a). For example, in association with *P. indica* barley plants were more tolerant to the necrotrophic fungal root pathogens *Fusarium graminearum* and *Fusarium culmorum* as well as to the hemi-biotrophic root pathogen *Cochliobolus sativus* (Waller et al., 2005; Deshmukh and Kogel, 2007). As no antifungal activity was observed for *P. indica in vitro* (Waller et al., 2005), resistance against these pathogens does not seem to be caused by antibiosis (Oelmüller et al., 2009). A higher tolerance to *F. culmorum* was also demonstrated for wheat, although the effect was much more distinct when plants were grown in sand instead of soil (Serfling et al., 2007). The positive traits conferred by *P. indica* may generally be influenced by environmental conditions. In addition to the mentioned effects on *F. culmorum* resistance, Serfling et al. (2007) reported further differences in growth promotion and disease resistance depending on plant growth conditions. Furthermore, when tomato plants were grown under high light conditions a positive effect on concentrations of Pepino mosaic virus was observed in *P. indica* colonized plants. In contrast, adverse *P. indica* effects on resistance to the virus were observed when plants were grown under low light conditions (Fakhro et al., 2010). Strikingly, an increased resistance to pathogens was also observed in plant organs not colonized by *P. indica* (Waller et al., 2005; Serfling et al., 2007; Fakhro et al., 2010; Qiang et al., 2012a). A closer investigation on this effect was performed using the *Arabidopsis* interaction with the powdery mildew *Golovinomyces orontii*. It was found that *P. indica* induced systemic resistance to *G. orontii* was independent of SA signaling but instead required JA signaling. It was concluded that an ISR-like response was responsible for the observed effect (Stein et al., 2008).

As mentioned before, *P. indica* colonized plants also displayed an elevated tolerance to abiotic stress conditions (e.g. Waller et al., 2005; Baltruschat et al., 2008; Sherameti et al., 2008a; Vadassery et al., 2009). For example, a positive effect on growth performance under salt stress was observed when wheat plants were inoculated with *P. indica*. It was suggested that this, at least in part, was caused by elevated proline levels in leaves from colonized plants, which may enable the cells to maintain higher water potentials in order to increase water uptake and reduce oxidative damage (Zarea et al., 2012). In addition, Waller et al. (2005) and Baltruschat et al. (2008) reported higher biomasses of barley plants co-cultivated with *P. indica* and exposed to salt stress as compared to plants grown without the fungus. This effect might, also at least in part, be

mediated by altered antioxidant capacities in colonized plants. As expression of monodehydroascorbate reductase 2 (MDAR2) and dehydroascorbate reductase 5 (DHAR5), two enzymes involved in ascorbate reduction, was also increased in *P. indica* inoculated *Arabidopsis* plants, especially under drought stress (Vadassery et al., 2009), modulating ROS levels and signaling might be a general effect elicited by the fungus in its host species. Yet, neither the mechanism by which *P. indica* alters the antioxidative capacity in plants nor the meaning of it for the interaction with its host are currently known. But as *mdar2* and *dhar5* mutants were hypersensitive to the fungus, ROS seem also to play a role in the colonization of plants by *P. indica* (Vadassery et al., 2009).

1.4.4 Root colonization

Detailed analyses about the way *P. indica* colonizes roots have been performed in barley and *Arabidopsis* (Peskan-Berghöfer et al., 2004; Deshmukh et al., 2006; Jacobs et al., 2011; Zuccaro et al., 2011; Qiang et al., 2012b). Fungal hyphae were mainly observed in the root maturation zone, but were hardly detected in the elongation zone or the meristematic region (Deshmukh et al., 2006; Jacobs et al., 2011). In the latter, a hypersensitive response-like defense reaction was observed in cells getting in contact with the fungus, indicating that plants can restrict *P. indica* colonization by immune responses (Schäfer and Kogel, 2009). It was suggested that because of its importance, the meristematic zone might be especially guarded by the immune system and therefore allows the plant to deny *P. indica* growth in this region (Schäfer and Kogel, 2009). In the maturation zone, fungal growth was restricted to the rhizodermis and the cortex, but was never observed in the stele or in aerial parts of the plant (Peskan-Berghöfer et al., 2004; Deshmukh et al., 2006; Jacobs et al., 2011; Zuccharo et al., 2011; Qiang et al., 2012b). In both plant species a bi-phasic colonization pattern was observed (Deshmukh et al., 2006; Jacobs et al., 2011; Qiang et al., 2012b). In a first stage, *P. indica* colonizes root cells in a biotrophic way. This was, for example, demonstrated by transmission electron microscopic studies, showing intracellular fungal hyphae surrounded by the PM of living plant cells (Jacobs et al., 2011; Qiang et al., 2012b). Under the applied conditions, this phase lasted till about three days after fungal inoculation. During the following second phase, fungal growth was dependent on plant cell death (Deshmukh et al., 2006; Quiang et al., 2012b). A first hint to this came from barley where fungal colonization led to transcriptional down regulation of the cell death inhibitor *BAX inhibitor-1* (*HvBI-1*). In line with this, barley plants overexpressing the protein showed strongly reduced

fungal colonization (Deshmukh et al., 2006). Recently, Qiang et al. (2012b) demonstrated that *P. indica* elicits plant cell death in *Arabidopsis* by increasing ER stress in colonized root cells, while simultaneously suppressing the unfolded protein response (UPR). Many proteins, especially those of the secretory pathway, are folded and modified within the ER (Liu and Howell, 2010). Stress conditions, such as biotic interactions, increase ER workload. This leads to more misfolded proteins and cell damage. To avoid this and adapt the ER working capacities, the UPR signaling pathway leads to increased synthesis of chaperones for protein folding in the ER and elevated degradation of misfolded proteins. In turn, the accumulation of too many falsely folded proteins triggers cell death (Moreno and Orellana, 2011). This colonization strategy had, till then, been unknown for plant colonizing microorganisms. It is important to note that *P. indica*, even in its cell-death dependent colonization phase, does not cause disease symptoms. As monocotyledonous barley and dicotyledonous *Arabidopsis* are evolutionary quite distant species, the observations suggest that *P. indica* might use similar strategies for colonization of various plant species.

Especially in *Arabidopsis*, but also in barley, numerous factors have been identified to influence plant colonization by *P. indica* (Sherameti et al., 2008a; Schäfer et al., 2009; Jacobs et al., 2011; Khatabi et al., 2012; Qiang et al., 2012b). In addition to the before mentioned, some examples are given below. In recent studies, it became obvious, that *P. indica* is able to suppress a broad repertoire of plant immune responses (Schäfer et al., 2009; Jacobs et al., 2011). A few mutants have been identified in *Arabidopsis* where immune suppression was, at least partially, alleviated, leading to reduced fungal colonization (Jacobs et al., 2011). In addition, several phytohormones have been shown to affect fungal proliferation in the plant. For example, JA and ET signaling positively affected fungal proliferation within plants and lower amounts of fungal DNA were detected in *Arabidopsis* mutants compromised in JA synthesis or signal transduction (Sherameti et al., 2008a; Jacobs et al., 2011; Khatabi et al., 2012). It was suggested that *P. indica* makes use of these signaling pathways to suppress SA mediated defenses, which have been shown to restrict fungal growth (Jacobs et al., 2011; Khatabi et al., 2012). Consistently, enhanced fungal proliferation was detected in mutants impaired in SA accumulation or signaling (Jacobs et al., 2011). In addition, ABA has been proposed to be employed in immune suppression by the fungus, inferred from transcriptional up-regulation of ABA controlled genes in response to *P. indica* (Sherameti et al., 2008b; Schäfer et al., 2009). ABA is a central regulator of plant tolerance against abiotic stresses with ABA-mediated responses possibly having priority over

immune reactions. Consistent with this, enhanced ABA signaling has been shown to increase susceptibility to several pathogens (Mauch-Mani and Mauch, 2005; Fujita et al., 2006). As *P. indica* itself produces auxin (Sirrenberg et al., 2007; Hilbert et al., 2012) and activates auxin signaling within the plant, this phytohormone was also suggested to have a positive effect on colonization (Schäfer et al., 2009; Hilbert et al., 2012). Gibberellic acid is also involved in the plant - *P. indica* interaction, but the role of this phytohormone seems to be more complex (Schäfer et al., 2009; Jacobs et al., 2011). Besides hormones, vacuolar processing enzymes (VPEs) have been shown to be necessary for *P. indica* induced cell death and proper plant colonization (Qiang et al., 2012b). A lot of additional factors involved in plant colonization by *P. indica* can be expected and their identification will further deepen our understanding of the interaction between *P. indica* and its hosts, thereby possibly allowing conclusions in respect to other mutualistic plant – microbe associations.

1.5 Objectives

Various factors have been identified to influence the interaction of plants with the mutualistic fungus *P. indica*. In recent microarray studies, transcription of a barley *TLP* was up-regulated in response to the fungus. Though little information is available at the moment, proteins of this family have been proposed to function in biotic and abiotic stress signaling. The first aim of this study was therefore to investigate if TLPs play a role in the colonization of plant roots by *P. indica*. Considering the availability of genetic tools, the model plant *Arabidopsis thaliana* was chosen for research. *Arabidopsis* T-DNA insertion lines each lacking one *AtTLP* gene were identified and tested for fungal colonization employing qRT-PCR. Furthermore, to investigate a possible role of TLPs in plant immune responses, the mutant lines were subjected to immune response assays as well as to infection with several pathogens.

The second part of this work was mainly focusing on the subcellular localization of AtTLPs to get possible hints towards their function. Proteins of interest were coupled to green fluorescent protein (GFP), transiently expressed in leaf epidermal cells and fluorescence was observed by confocal laser scanning microscopy. The technique was chosen over other methods like immuno-localization because it allows examinig several proteins in much shorter time and in several plant species. Special emphasis was put on AtTLP3 as representative member of the protein family. Various GFP-tagged truncated versions of this protein were employed to gain insights into mechanisms and structural features underlying its subcellular localization. In addition, re-

localization in response to extracellular signals has been shown to be important for TLP signaling in mammals. It was therefore interesting to examine localization dynamics of AtTLP3 in response to environmental stress conditions and phytohormones. This should give hints to signaling pathways the protein might be involved in. To complement these studies, effects of abiotic stresses were monitored in *attlp* T-DNA insertion lines.

Overall, this study aimed at getting new insights into the functions and characteristics of a currently poorly investigated gene family in plants, whose members have been shown to fulfill crucial tasks in mammals. Furthermore, it should expand our understanding of *P. indica* colonization in plants.

2. Materials and Methods

All chemicals and laboratory equipment used in this study were delivered by the following companies: Applied Biosystems (Foster City, CA, USA), Calbiochem (Bad Soden, Germany), DNA Cloning Service (Hamburg, Germany), Duchefa (Haarlem, The Netherlands), Eurofins MWG (Ebersberg, Germany), Fermentas (St. Leon-Rot, Germany), Finnzymes (Oy, Finland), Greiner (Frickenhausen, Germany), Invitrogen (Karlsruhe, Germany), Japan Tobacco Inc. (Higashibara, Japan), Leica (Wetzlar, Germany), Merck (Darmstadt, Germany), Pequlab (Erlangen, Germany), Promega (Madison, USA), Quanta Biosciences (Gaithersburg,USA), Roth (Karlsruhe, Germany), Sarstedt (Nümbrecht-Rommelsdorf, Germany), Sigma-Aldrich (Munich, Germany), WTW (Weilheim, Germany).

2.1 Basic molecular biological methods

2.1.1 Polymerase chain reaction (PCR)

Three different types of DNA polymerases have been used for amplification of DNA fragments from different templates. Respective standard protocols and programs are given below.

Phusion / Phire DNA Polymerase

PCR mixture (1x)	
5 x Buffer	10 µl
2 mM dNTPs	5 µl
Primer fwd 10µM	2 µl
Primer rev 10µM	2 µl
Polymerase	0.5 µl
Template	variable
MQ H_2O	add 50 µl

Cycler program		
98°C	30 sec	
98°C	10 sec	
x°C	30 sec	25-35 x
72°C	15-30 sec/kb	
72°C	5 min	

GoTaq DNA Polymerase

PCR mixture (1x)	
5x Buffer	4 µl
2 mM dNTPs	2 µl
Primer fwd 10µM	0.8 µl
Primer rev 10µM	0.8 µl
Polymerase	0.2 µl
Template	variable
MQ H_2O	add 20 µl

Cycler program		
95°C	2 min	
95°C	30 sec	
x°C	30 sec	25-35 x
72°C	1 min/kb	
72°C	5 min	

2.1.2 Agarose gel electrophoresis

Agarose gel electrophoresis was employed to separate and analyze DNA and RNA samples. DNA samples were mixed 1:10 with 10 x DNA loading buffer and were loaded onto a gel (1 x TBE buffer with 0.5-2 % (w/v) agarose and about 0.75-1 mg/ml ethidium bromide). The 1 kb Plus ladder (Invitrogen) was used as standard. Gels for RNA were composed of 1 x MOPS (3-(N-morpholino) propanesulfonic acid) buffer with 1% (w/v) agarose and 5% (v/v) formaldehyde. Prior to loading, RNA (0.5 mg) was mixed 1:1 with 2 x RNA loading dye (Fermentas) and heated to 95°C for 5 min. Separation was achieved by applying 80-120 V for about an hour.

10 x TBE (Tris-Borate-EDTA)
900 mM Tris
900 mM Boric acid
25 mM EDTA
add 1 l H_2O_{dest}, pH 8

10 x MOPS
200 mM MOPS
50 mM Sodium acetate
10 mM EDTA
pH 7.0
add 1 l DEPC-treatment overnight

2.1.3 Production of chemically competent *Escherichia coli* (*E. coli*) cells

Liquid lysogeny-broth medium (LB, modified after Bertani, 1951) (3 ml) was inoculated with *E. coli* DH5α cells from a TSS stock and grown overnight at 37°C and 220 rpm. The next day 1 ml of this culture was added to 50 ml LB medium and incubated for about 2 h at 37°C and 220 rpm. The OD_{600} (optical density) was determined in intervals using a spectrophotometer. The culture was centrifuged (5 min, RT, 4000 rpm) after an OD of 0.6 was reached. The supernatant was discarded and the bacterial pellet was carefully resuspended in 2.5 ml cold TSS buffer. Aliquots of this were stored at -80°C.

LB medium (1 l)	
Peptone	10 g
Yeast extract	5 g
NaCl	5 g
Agar-Agar	15 g (for plates only)
pH adjusted to 7 with NaOH if necessary	

TSS buffer
10% (w/v) PEG6000
5% (v/v) DMSO
20 mM $MgSO_4$

2.1.4 Transformation of chemically competent *E. coli* cells

TSS stocks of competent *E. coli* DH5α cells were thawed on ice. 5 to 50 ng of desired plasmid were added to 80 µl of competent cells and kept on ice for 30 min. Thereafter, cells were put for 45 sec on 42°C followed by 2 min on ice. 200 µl LB medium were added and cells were shaken for 2 h at 37°C at 220 rpm. Subsequently, cells were spread on solid LB medium containing respective antibiotics for selection and kept overnight at 37°C. Respective filter-sterilized antibiotics (i.e. 100 µg/ml ampicillin or 50 µg/ml kanamycin) were added to LB medium after autoclaving.

2.1.5 Colony PCR with *E. coli* cells

Single colonies from a transformation plate were picked with a sterile toothpick and transferred to a new LB plate containing respective antibiotics to generate a master plate for further use. The toothpick was then dipped briefly into a reaction tube containing PCR mixture. DCS polymerase (DNA Cloning Service) was used for all colony PCRs. The used annealing temperatures were chosen according to the employed primers.

DCS polymerase PCR mixture (1x)	
10 x Buffer	1 µl
25 mM $MgCl_2$	1 µl
2 mM dNTPs	1 µl
Primer fwd 10µM	0.2 µl
Primer rev 10µM	0.2 µl
Polymerase	0.1 µl
MQ H_2O	add 10 µl
Template	see text

Cycler program		
95°C	5 min	
95°C	30 sec	30 x
x°C	30 sec	
72°C	1 min/kb	
72°C	5 min	

2.1.6 Quick extraction of plant DNA

Leaves were crushed with a small pestle in 2 ml reaction tubes and incubated for 5-10 min in DNA extraction buffer. Tubes were centrifuged (10 min, RT, 13000 rpm) after adding 500 µl chloroform. The emerging upper phase was transferred to a new tube, 500 µl isopropanol were added and samples were incubated for 2 min at RT. After a second step of centrifugation (10 min, RT, 13000 rpm) the supernatant was discarded and 500 µl 70 % (v/v) ethanol were added to wash the pellet. Subsequently, tubes were centrifuged (5 min, RT, 13000 rpm). The supernatant was

discarded and 50-100 µl of Milli-Q water were added. DNA concentrations were determined after vortexing using a NanoDrop (Pequlab) and samples were stored at -20°C.

DNA extraction buffer
200 mM Tris-HCl ph 7.5
250 mM NaCl
25 mM EDTA
0.5% (v/v) SDS

2.1.7 Whole RNA extraction

Plant and fungal material was homogenized under liquid nitrogen and stored at -80°C until use. RNA was extracted using the TRIzol reagent (Invitrogen). 1 ml TRIzol was added to about 200-300 mg of powdered sample, vortexed viciously and incubated at RT for 2-3 min. 200 µl chloroform were added, samples were shaken and centrifuged (20 min, 4°C, 14000 rpm) after incubation for another 2-3 min at RT. The aqueous upper phase was transferred to a new reaction tube containing 500 µl isopropanol. RNA was precipitated by centrifuging the samples (30 min, 4°C, 14000 rpm). The pellet was washed once with 70 % (v/v) ethanol and dried shortly at RT. Then 30 µl of RNAse free water were added and RNA was dissolved for 5 min at 64°C. Samples were stored at -80°C after determination of RNA concentrations using a NanoDrop (Peqlab).

2.1.8 cDNA synthesis

Extracted RNA was transcribed to double stranded cDNA using the qScript cDNA synthesis kit (Quanta Biosciences) according to manufacturer's instructions. To remove any residual amounts of DNA, samples were digested with DNase I (Fermentas), following manufacturer's instructions. cDNA samples were stored at -20°C.

2.1.9 Quantitative real-time PCR (qRT-PCR)

A 7500 Fast Real-Time PCR System (Applied Biosystems) was used to perform qRT-PCR. A standard curve was generated for every primer pair using 10 ng, 1 ng, 0,1 ng and 0,01 ng of cDNA or genomic DNA as template. Only primer pairs with accurate amplification efficiencies were used in qRT-PCR. Every sample was measured in triplicates.

PCR mixture (1x)	
Green JumpStart Taq ReadyMix (SigmaAldrich)	10 µl
Primer fwd 10µM	0.5 µl
Primer rev 10µM	0.5 µl
Template	variable
MQ H_2O	add 20 µl

For qRT-PCR, the cycler program contained two phases. The first consisted of a standard PCR amplification. Fluorescence was determined at the end of each cycle. In the second phase, a melting curve was recorded between 66°C and 95°C.

Cycler program		
95°C	5 min	
95°C	15 sec	
60°C	30 sec	40 x
72°C	30 sec	
95°C	15 sec	
66°C	30 sec	melting curve record
95°C	30 sec	
25°C	15 sec	

2.2 Plant growth conditions

2.2.1 *Arabidopsis thaliana* growth conditions

Arabidopsis thaliana (L.) ecotype *Columbia*-0 (N60000) was used as wild-type (WT) in all experiments unless noted otherwise. For aseptically grown plants, seeds were surface sterilized with 70% (v/v) ethanol for 1 min followed by a subsequent exposure to sodium hypochlorite (3% active chlorine) for 5 min. Next, seeds were washed 8 – 10 times with sterile water. If not stated otherwise, seeds were placed on solid ½ Murashige-Skoog (MS) medium without vitamins (Duchefa), 0.4 % (w/v) Gelrite (Roth) in squared petri dishes (Greiner Bio-One) and grown vertically. For soil grown plants, seeds were placed in pots on top of a 3:1 soil-sand mixture (Fruhstorfer Erde Typ P; Quarzsand). Only one plant was grown per pot. After sowing, all seeds were kept at 4°C in the dark for 48 h to synchronize germination. Plants were cultivated under short-day conditions (22/18°C day/night cycle, 8 hours light, 180 µmol m^{-2} s^{-1} photon flux density, 60% rel. humidity).

2.2.2 *Nicotiana benthamiana* growth conditions

N. benthamiana plants were grown in soil (Fruhstorfer Erde Typ T) in a growth chamber under long day conditions (24°C, 16 hours light, 180 µmol m^{-2} s^{-1} photon flux density, 80% rel. humidity). After about four weeks, plants were transferred to larger pots with new soil (Fruhstorfer Erde Typ I).

Table 2.1: T-DNA insertion lines used in this study

Name	AGI code	Line	T-DNA Insertion Site
attlp1-1	At1g76900	N674227 (salk_026655C)	Promoter
attlp2-1	At2g18280	N663531 (salk_103619C)	Exon 4
attlp2-2		N654211 (salk_058100C)	Promoter
attlp3-1	At2g47900	N678667 (salk_072994C)	Exon 1
attlp3-2		N676958 (salk_131745C)	Promoter
attlp5-1	At1g43640	N675664 (salk_069659C)	Intron 1
attlp5-2		N462147 (GK-648C11)	Exon 4
attlp6-1	At1g47270	N855060 (WiscDsLox421A6)	Promoter
attlp7-1	At1g53320	N666743 (salk_092324)	Intron 1
attlp8-1	At1g16070	N668671 (salk_093284)	Promoter
attlp8-2		N507790 (salk_007790)	Promoter
attlp9-1	At3g06380	N665383 (salk_016678C)	Exon 4
attlp9-2		N659871 (salk_051138C)	Promoter
attlp10-1	At1g25280	N612155 (salk_112155)	5' UTR
attlp10-2		N550916 (salk_050916)	5' UTR
attlp11-1	At5g18680	N662879 (salk__070225C)	Exon 1
attlp11-2		N663172 (salk_085537C)	Intron 1

2.3 *attlp* mutant lines

2.3.1 *Arabidopsis* T-DNA insertion lines

All seeds were received from the Nottingham *Arabidopsis* Stock Centre (Scholl et al., 2000). It was aimed to obtain two lines per *AtTLP* gene except for *AtTLP4*, which was suggested to be a pseudogene (Lai et al., 2004). If possible, lines with a T-DNA insertion within the coding region of the respective gene were selected. If not available, insertion sites within introns, the 5'UTR or promoters, respectively, were chosen. Homozygous plants were obtained for lines *attlp1-1* (N674227), *attlp2-1* (N663531), *attlp2-2* (N654211), *attlp3-1* (N678667), *attlp3-2* (N676958),

attlp5-1 (N675664), *attlp7-1* (N666743), *attlp8-1* (N668671), *attlp9-1* (N665383) and *attlp9-2* (N659871), *attlp11-1* (N662879) and *attlp11-2* (N663172). Lines *attlp9-1* (N665383) and *attlp9-2* (N659871) were previously described in Lai et al. (2004). Segregating plants were obtained for lines *attlp5-2* (N462147), *attlp6-1* (N855060), *attlp8-2* (N507790), *attlp10-1* (N612155) and *attlp10-2* (N550916) (for more information see Table 2.1). All lines were selfed and screened for homozygosity by PCR using T-DNA specific primers (LBb1.3 for SALK lines, LB_GABI for GABI-Kat lines and p745 for WiscDsLox lines) in combination with primers flanking the putative insertion site (Table 2.2). GoTaq DNA polymerase (Promega) was used for all reactions.

Table 2.2: Primers used for screening of T-DNA insertion lines

T-DNA Insertion Line	Left border primer 5' - 3'	Right border primer 5' - 3'
LBb1.3	ATTTTGCCGATTTCGGAAC	/
LB_GABI	ATATTGACCATCATACTCATTGC	/
p745	AACGTCCGCAATGTGTTATTAAGTTGTC	/
attlp1-1	TTTGATTTCATCTTTGGGCAG	GAAACAAAGACTCCAGATTCTGG
attlp2-1	GGATAGGTCTGGTTTTCTGGG	ATGATTGCCTTTGCATGACTC
attlp2-2	CCTTGTGATTGCGAATTTTTC	AAGATCGGAAAGAGAAAACGC
attlp3-1	GGAACCCAAGACGTTAAGCTC	TCGTTGAGATCTCGTTCGTTC
attlp3-2	ATTTAGACTTCAATTCGGCCC	CCCTAATAAACCCACATTCGG
attlp5-1	TTTTGGTGAAAAATGGTATACATC	CTCAGAAACGACATTTTTCCG
attlp5-2	GCATATAGGGGGAACATCAAC	TGCATTATGCACTCTATCCCC
attlp6-1	ACCTGATTTTATCTGCTCCCC	GGCTTCTACCTTCTCCTTTGG
attlp7-1	TGAAAATGATCCTTTTGCCAG	CGCTTGCGTTTCTAAGAAATG
attlp8-1	TCCATCATTCCATTTTGGAAG	TCTGGATGGATTGCTTTCAAG
attlp8-2	TTGCAGTGATGACTGCTTCAG	ATGGGTCCTTCAAAATCAACC
attlp9-1	AACAAACCTTCCCTCTTCCTG	CAAAGAGAAGCAACGCGTATC
attlp9-2	TTATGGCCGGTCAAAAGTATC	AGCTTTTGTTGAGCTGAGCAC
attlp10-1	AGCTAAGGCAATTCTGAGTC	ATTGAATGGGGTTAGGTATG
attlp10-2	AAATGCCCCAAAATTGAGATC	ATTGAATGGGGTTAGGTATG
attlp11-1	TAGCGTCGGTTGAAACAAAAG	AGGCTGCAGAAGATACACACC
attlp11-2	AAAAGGGACCTTTCCACACAC	CATCTCTCTCAAGCAGGTTCG

2.3.2 Analysis of *AtTLP* transcription in mutant lines by semi-quantitative reverse-transcription (RT)-PCR

Semi-quantitative RT-PCR was used to study *AtTLP* transcript abundance in *attlp* and wild-type plants. *Col*-2 (N907) was used as wild-type for *attlp6-1*. Total RNA was isolated from three-week-old whole plants using TRIzol (Invitrogen) reagent (see 2.1.7) and cDNA was synthesized employing the qScript cDNA synthesis kit (Quanta Biosciences) using oligo dT primers. The *Arabidopsis Ubiquitin5* (*AtUbi5*) transcript was used as a loading control. Phire DNA polymerase (Finnzymes) was used for all reactions (Table 2.3)

Table 2.3: Primers used for semi-quantitative RT-PCR

Gene	Forward Primer 5' - 3'	Reverse Primer 5' - 3'
AtTLP1	ATGTCGTTCCGTAGCATA	TTATTCGCAAGCAAGTTTTGTG
AtTLP2	ATGTCTTTGAAAAGCATCCTTCG	TTACCCTTCACATGCCGG
AtTLP3	ATGTCCTTCAAGAGTCTCATTCAGG	TCATTCACATGCTATCTTGGTGTC
AtTLP5	ACGAAGACATATCGTTTCTC	GCATATCGTAAACGGTTCCT
AtTLP6	ATGGATTTGTCGCTTTTGTTG	TCATTCGCAGACTGGCTTC
AtTLP7	AATGCCTTTGTCACGGTCCC	TCACTCGCAGGCAAGTTTAGTG
AtTLP8	AAGCAATCCATCCAGAAAGG	TCAAACAGTACAACAAAGCTTG
AtTLP10	CAAAGAGAAATGTCGTTTCGAG	CTATTCACAAGCAAGCTTGG
AtTLP11	GTATGACCTTACGTAGCTTAATCC	TCATTCACAAGCGATTCTAGTC
UBI5	CCAAGCCGAAGAAGATCAAG	ATGACTCGCCATGAAAGTCC

2.3.3 Generation of *attlp* double mutants

The double mutant lines *attlp1/5* and *attlp9/11* were generated by crossing homozygous plants of *attlp1-1* and *attlp5-1* and *attlp9-1* and *attlp11-1*, respectively. For that, sepals, petals and stamens from flowers of recipient plants were removed using a fine forceps. For pollination, opened flowers of donor plants were cut and carefully applied to the pistil of prepared recipient flowers. Crossings were done during the morning. F1 progeny was selfed and F2 plants were screened for plants homozygous for both T-DNA insertions as well as for azygous plants showing no T-DNA insertions at all (for primer sequences see Table 2.2). For this, the same conditions were applied as described in 2.3.1. F3 seeds of such plants were harvested and stored at 4°C until use.

2.4 β-glucuronidase (GUS) plants and histochemical GUS staining

2.4.1 Generation of AtTLP$_{Prom}$:*GUS* lines

For generation of pCX-AtTLP3$_{Prom}$:*GUS* a stretch of 1032 base pairs (bp) upstream of the translational start site of *AtTLP3* (AT2G47900) was PCR amplified from genomic DNA using primers 5'-CCATTAAAGCGGCGAAAGTG-3' (forward primer) and 5'-GGCTCTG-AATTCTAACTAATAACGA-3' (reverse primer). For generation of pCX-AtTLP5$_{Prom}$:*GUS* a stretch of 1231 bp upstream of the translational start site of *AtTLP5* (AT1G43640) was PCR amplified from genomic DNA using primers 5'- TTTTGGTGAAAAATGGTATACATC-3' (forward primer) and 5'- TTTTCCGAATACCAAAGATTCTA-3' (reverse primer). Phusion DNA polymerase (Finnzymes) was employed for both reactions. The pCXGUS-P vector (Chen et al., 2009) was digested with *Xcm*I (Fermentas). Vector and PCR products were gel purified (Wizard® SV Gel and PCR Clean-Up System, Promega). 3' terminal adenine overhangs were added to the PCR products (A-tailing). T4 DNA ligase (Fermentas) was employed to ligate A-tailed PCR fragments into digested pCXGUS-P. After that, the vector was introduced into competent *E. coli* cells. Selection was carried out on LB plates supplemented with 50 mg/ml kanamycin. Single colonies were tested in colony PCR and the vector was gained via minipreparation of plasmid DNA (PureYieldTM Plasmid Miniprep System (Promega). M13 fwd (5'-GTTTTCCCAGTCACGAC-3') was employed for both constructs in combination with the respective reverse primer used in cloning. Plasmids were sent for sequencing to verify sequences. pCX-AtTLP3$_{Prom}$:*GUS* and pCX-AtTLP5$_{Prom}$:*GUS* were electroporated into *Agrobacterium tumefaciens* strain LBA4404pSB1 (kindly provided by Japan; Komari et al., 1996) using *E. coli* Pulser, (Biorad) according to manufacturer's instruction. The transformed cells were plated on YEP agar medium (0.1% (w/v) yeast extract; 0.5% (w/v) beef-extract; 0.5% (w/v) sucrose; 0.5% (w/v) casein hydrolysate; 2 mM $MgCl_2$) containing 5 mg/l tetracyclin, 25 mg/l rifampicin and 50 mg/l kanamycin and subsequently incubated at 28°C in the dark for two days. Growing antibiotica-resistant colonies of Agrobacteria were subcultured in liquid medium and then screened by PCR amplification using the same primers as for *E. coli*. Plant transformation and regeneration was performed as described by the standard vacuum infiltration method (Bechtold et al., 1993). Briefly, a single colony of *Agrobacterium* was grown over night at 28°C in 10 ml YEB medium (0.1% (w/v) yeast extract; 0.5% (w/v) beef-extract; 0.5% (w/v) sucrose; 0.5% (w/v) casein hydrolysate; 2 mM $MgCl_2$) with appropriate antibiotics (5 mg/l tetracycline; 25 mg/l rifampicin; 50 mg/l kanamycin). Subsequently, the culture was cultivated in 250 ml fresh YEB

medium for 6 h until the relative density of OD_{600}: 1.8. Agrobacteria were harvested by centrifugation and then suspended in infiltration medium consisting of ½ MS-salts, vitamins, 5% (w/v) sucrose, 2.3 µM 6-benzylaminopurine (6-BAP), and 0.01% silwet-L77, pH 5.8, to a final density (OD_{600}) of 1.1 - 1.3. *Arabidopsis Col*-0 plants were infiltrated as described by Bechtold et al. (1993). T1 seeds of transgenic *Arabidopsis* plants were surface-sterilized as described. Seeds were germinated on ½ MS-medium including vitamins supplemented with 0.5% (w/v) sucrose, 0.4% (w/v) Gelrite (Duchefa) and kanamycin (50 mg/l) in a growth chamber under photoperiodic conditions of 16 h light (180 µmol m^{-2} s^{-1} photon flux density) and 22°C day / 18°C night temperatures. Kanamycin resistant transgenic plants were transferred to soil and propagated. T2 seeds of two independent transgenic lines per construct were harvested and used for further experiments.

A-tailing	
Purified PCR product	15 µl
10 x buffer	2 µl
10 mM ATP	1 µl
DCS polymerase	1 µl
25 mM $MgCl_2$	1 µl

Cycler program	
70°C	20 min

2.4.2 GUS staining procedure

Histochemical staining of GUS activity was performed as described in Jefferson et al. (1987) with modifications. T2 plants of two independent transgenic lines for $AtTLP3_{Prom}$:*GUS* and $AtTLP5_{Prom}$:*GUS*, respectively, were grown under sterile conditions in glasses on solid ½ MS medium with vitamins (Duchefa) supplemented with 1% (w/v) sucrose and 1% (w/v) agar-agar under short day conditions. To obtain flowers and siliques, several two-week-old plants were transferred to pots containing soil/sand mixture and were further cultivated in a greenhouse. *Arabidopsis Col*-0 plants were grown as control. For staining, whole plants or plant organs were harvested, immediately transferred to staining solution (0,1% (v/v) Triton X-100, 2 mM potassium ferrocyanide, 2 mM potassium ferricyanide, 1 mM X-Gluc (Duchefa) and 100 mM sodium phosphate buffer, pH 7.0), vacuum infiltrated and kept overnight or until sufficient staining was reached at 37°C. To remove chlorophyll, plants were washed three times for several hours in 70% (v/v) ethanol and finally stored in 50 % (v/v) glycerol. Images were acquired using a Leica DFC 300 FX digital camera mounted on a Leica MZ 16 F stereomicroscope. For this, plant material was put in petri dishes containing 25% (v/v) glycerol.

2.5 *Piriformospora indica*

2.5.1 Cultivation

The isolate *P. indica* DSM11827 (German collection of microorganisms and cell cultures in Braunschweig, Germany) was used in all experiments. This isolate comes down from the original isolate deposited in 1997 after the discovery of the fungus in the Indian Thar desert (Verma et al., 1998). Chlamydospores, kept as glycerol stocks at -80°C, were spread on modified *Aspergillus* complex medium (CM medium) to generate master plates. Spores harvested from these were used to cultivate the fungus in greater amounts. For all experiments, *P. indica* chlamydospore suspension obtained from master plates was spread on solid CM medium and grown for 3-4 weeks at 24°C in the dark. To obtain chlamydospores, 0,002 % (v/v) Tween20 in sterilized water was added and the plates were carefully scratched with a spatula. This was performed two times per plate. Spore suspension was collected in a 50 ml tube and filtered through Miracloth (Calbiochem) to remove residual mycelium. Thereafter, spore suspension was centrifuged (7 min, RT, 3500 rpm) and spores were washed thrice with sterile Tween20-water. Spore densities were determined using a Fuchs-Rosenthal counting chamber and adjusted to 500000 spores/ml.

CM medium (1 l)	
20 x salt solution	50 ml
Glucose	20 g
Peptone	2 g
Yeast extract	1 g
Casamino acids	1 g
1000 x microelements	1 ml
Agar-Agar	15 g

20 x salt solution (1 l)	
$NaNO_3$	120 g
KCl	10.4 g
$MgSO_4$ x 7 H_2O	10.4 g
KH_2PO_4	30.4 g

1000 x microelements (1 l)	
$MnCl_2$ x 4 H_2O	6 g
H_3BO_3	1.5 g
$ZnSO_4$ x 7 H_2O	2.65 g
KI	750 mg
Na_2MO_4 x 2H_2O	2.4 mg
$CuSO_4$ x 5 H_2O	130 mg

2.5.2 Inoculation of *Arabidopsis* roots and quantification of fungal colonization by qRT-PCR

Arabidopsis plants were grown aseptically for three weeks on vertically placed squared petri dishes. For inoculation, 1 ml spore suspension per petri dish was pipetted on top of the roots. Plants were cultivated further on and roots were harvested at indicated time points. For that, plants were carefully pulled out of the medium and roots were directly cut off into liquid nitrogen. About 200 plants were used per line and time point. Fungal and plant genomic DNA was co-extracted using the DNAeasyKit (Quiagen). 40 ng DNA served as template for qRT-PCR analyses. Fungal colonization was determined by the $2^{-\Delta Ct}$ method (Schmittgen and Livak, 2008) by subtracting the raw Ct values of *P. indica ITS* from those of *AtUbi5* (for primer sequences and AGI codes see Table 2.4). Data were analyzed by Student's *t*-test.

2.5.3 Gene expression analysis by qRT-PCR in *P. indica* inoculated plants

Experiments were carried out as described in Jacobs et al. (2011). For this, *Col*-0 and *attlp3-1* plants were grown under sterile conditions and three-week-old plants were either inoculated with *P. indica* or mock treated. For mock treatment, 1 ml 0,002 % (v/v) sterile Tween20-water per plate was pipetted on top of the roots. About 200 plants were used per line, time point and treatment. Plants were further cultivated and root material was harvested at 0, 1, 3, and 7 days after inoculation (dai) and immediately transferred into liquid nitrogen. Total RNA was extracted and aliquots were used for cDNA synthesis. 10 ng of cDNA were used as template for qRT-PCR. The $2^{-\Delta Ct}$ method was used to determine differential gene expression of immune and stress marker genes by relating the Ct values of respective primers to that of the housekeeping gene *AtUbi5*. For expression of *AtTLPs*, only *Col*-0 plants and time points 1, 3, and 7 dai were used (for primer sequences and AGI codes see Table 2.4).

Table 2.4: Primers used for qRT-PCR

Gene	AGI code	Forward Primer 5' - 3'	Reverse Primer 5' - 3'
AtTLP2	At2g18280	AGTCTCTTCCTCTCCTTCAC	ATCACCCTCTCATGTTCTTCAG
AtTLP3	At2g47900	TTTCCTATCTCCCTCAAACAG	GACATCATCGCAGTTTAAGG
AtTLP5	At1g43640	GAAAGAGGAAGAAGGAAAGGT	CAGAAGCTACAGTCACTCTC
AtTLP7	At1g53320	AGATAAGCCCTCAAGTTCCAG	GAAGCAACAGTAACTCGTCC
AtTLP8	At1g16070	TGAAGTCTCAATCGATGAAGG	TTCAACGAACTTGAATGCTCTG
AtTLP9	At3g06380	CCAGTCTTTAGGTCTCACTC	AGTATGATCCTCTCAGATGTC
AtTLP10	At1g25280	CGCAGTAACATCTCCTTCTC	CGGAAATTCAAACACCAGCA
AtTLP11	At5g18680	GGCTACTTATGAACGAAACC	CATTGAACCAGTGAATCCCT
CBP60g	At5g26920	AAGAAGAATTGTCCGAGAGGAG	GGCGAGTTTATGAAGCACAG
DREB2A	At5g10695	GATGTAGTTTCAGAGGAGTTAGG	CGGAGAAGGGTTTAGATTCAC
HSP70	At5g05410	ATGTGTTTGGTGTTCGTGTG	ATTTACGTCAACCACTTGAACC
ITS	-	CAACACATGTGCACGTCGAT	CCAATGTGCATTCAGAACGA
MYB51	At1g18570	ACCAACCTCGAATCTTCTCTG	TTTCAACACAAGACTCCTCCA
OXI1	At3g25250	TCATCTACATTGGCCGTGTC	CGTCGCTCCATACAACATCT
UBI5	At3g62250	CCAAGCCGAAGAAGATCAAG	ATGACTCGCCATGAAAGTCC
VSP2	At5g24770	CAAACTAAACAATAAACCATACCATAA	GCCAAGAGCAAGAGAAGTGA
WRKY29	At4g23550	TCCGGTACGTTTTCACCTTC	AGAGACCGAGCTTGTGAGGA
ZAT12	At5g59820	GTTTCATTCGTTCCAAGCCT	GTGTCTCCTCATGTGTCCTC

2.6 Pathogenicity assays

2.6.1 *Botrytis cinerea*

Conidial spores of *Botrytis cinerea* strain B05.10 were kept at -80°C. For all experiments, spore suspension was spread on HA-agar plates (1% (w/v) malt extract; 0.4% (w/v) glucose; 0.4% (w/v) yeast extract; 1.5% (w/v) agar). Plates were sealed with parafilm and the fungus was grown for 7-12 days at 24°C with 12 h light as described previously (Doehlemann et al., 2006). To get conidial spores, mycelium was covered with sterile water and scratched slightly with a spatula. Spore suspension was collected through Miracloth (Calbiochem) to remove residual mycelium and centrifuged (3 min, RT, 2500 rpm). Then, spores were resuspended in ½ PDB (½ potato dextrose broth: 12 g in ddH_2O/l; Duchefa) and spore density was adjusted to 200000 spores/ml using a Fuchs-Rosenthal counting chamber. *Arabidopsis* plants were grown on soil under short day conditions. Leaves from 6-7-week-old plants were detached and placed in translucent plastic boxes containing 250 ml of 1 % (w/v) agar-agar. Control and test lines were kept in the same box. 5 µl spore suspension were pipetted onto the middle vein of each leaf. Boxes were covered with translucent lids. To maintain high humidity, lids were sprayed with water and boxes were

sealed with Parafilm. Digital photographs were taken at different time points with a Canon EOS450D camera. For this purpose, plastic lids were shortly removed, again sprayed with water and plastic boxes were resealed after taking the pictures. Lesion diameters were determined using ImageJ software to measure lesion diameter (Abramoff et al., 2004).

2.6.2 *Phytophtora parasitica*

Phytophthora parasitica Dastur isolate 310 was isolated from tobacco in Australia and maintained in the *Phytophthora* collection at INRA, Sophia Antipolis, France. *P. parasitica* growth conditions and production of zoospores were performed as described by Galiana et al. (2005). In short, roots of *Arabidopsis* plantlets were grown *in vitro* and inoculated with 500 motile *P. parasitica* zoospores according to Attard at al. (2010). Disease symptoms were scored over three weeks using a wilting disease index ranked from 1 (healthy plant) to 7 (dead plant) (Attard et al., 2010). The analysis was carried out on 18 to 35 inoculated plants. All experiments were performed twice.

2.6.3 *Erysiphe cruciferarum*

For *Erysiphe cruciferarum* inoculation, *Arabidopsis* plants were grown at 22°C and 65% relative humidity in a 10 h photoperiod with 120 µmol m^{-2} s^{-1} light in a 2:1 soil sand mixture (Fruhstofer Erde, Typ P; Quarzsand, granulation: 0.1-0.5 mm). *Erysiphe cruciferarum* was grown on *Col*-0, to maintain constant aggressiveness, and, simultaneously, on susceptible *phytoalexin deficient 4* (*pad4*) mutants, for strong conidia production. For inoculation, *Arabidopsis* plants were placed under an inoculation box, covered with a polyamide net (0.2 mm^2). Conidia were brushed off of *pad4* plants through the net until a density of 3-4 conidia/mm^2 was reached. Inoculated plants were kept in a growth chamber under the above conditions. Leaves were photographed at 11 days after inoculation.

2.7 3D homology modelling

Modelling of the three-dimensional (3D) structure of AtTLP3 was done using the project mode of the protein structure homology-modelling server Swiss Model (Peitsch, 1995; Arnold et al., 2006; Kiefer et al., 2009) in combination with the program DeepView (Swiss Pdb-Viewer). Suitable template structures were searched via the Swiss Model server. Resulting 3D structure templates were: 1C8Z (C-terminal domain of mouse brain Tubby protein; Boggon et al. 1999), 1S31 (Crystal structure analysis of the human Tub protein isoform a), 1I7E (Mouse brain Tubby protein bound to PIP_2; Santagata et al., 2001) and 3C5N (Human TULP1 in complex with IP3). For homology modelling of AtTLP3, the crystal structures of 1C8Z as well as 1S31 were used as templates. The comparison of the amino acid sequences of the used proteins revealed an identity of 38% and 35%, respectively. Visualization of the protein molecules was done using PyMOL.

2.8 Stress treatments

2.8.1 flg22-triggered seedling growth inhibition

Arabidopsis plants were grown under sterile conditions for 10-12 days on solid ½ MS medium supplemented with 1% (w/v) sucrose and 0.4% Gelrite (Roth) and subsequently inoculated with *P. indica* spore suspension or mock-treated. Plants were further cultivated for additional five days, to allow the fungus to spread and colonize plants. After that, plants of approximately the same size were transferred to petri dishes (Greiner Bio-One; Ø: 5 cm) containing a sterile filter paper and 5 ml liquid ½ MS medium plus 1% (w/v) sucrose. One half of the petri dishes were further supplemented with 1 µM flg22, whereas the others served as control (mock treatment). Three petri dishes were prepared per line and treatment, each containing five plants. To avoid loss of liquid, petri dishes were sealed with gas permeable Nescofilm (Bio-Rad). The flg22 peptide was used as described (Gómez-Gómez et al., 1999; Kunze et al., 2004). flg22 was stored as 10 mM water stocks at -20°C. For all experiments, a working solution was prepared freshly. To get a 1 µM solution, 1.5 µl flg22 stock solution was pre-dissolved in 0.1 M NaCl, 0.1% (w/v) BSA (bovine serum albumin, Roth), and then filled up to 15 ml with liquid ½ MS medium. Plant fresh weights were determined at 10 days after treatment.

2.8.2 elf18-triggered seedling growth inhibition

Experiments were essentially performed as described in 2.8.1 with some modifications. *Arabidopsis* plants were transferred to liquid medium after 21 days, without inoculation with *P. indica*. Plant fresh weights were determined 9 days after treatment. The elf18 peptide was handled like flg22 (Kunze et al., 2004).

2.8.3 Abiotic stress evoked root growth inhibition

Arabidopsis plants were grown aseptically on vertically placed squared petri dishes containing solid ½ MS medium (Duchefa) supplemented with 1% (w/v) sucrose and 1% (w/v) agar-agar. Plates were placed in a growth chamber under short day conditions for 8 days. To test for salt and osmotic stress sensitivity, plants of similar size were transferred to new plates, containing ½ MS medium as described above plus indicated concentrations of NaCl, mannitol or H_2O_2. After that, root tips were marked with a pen. Plants were further grown under described conditions. From 3 days after relocation onward, a photograph was made of each plate once a day using a Canon EOS450D digital camera and root tips were marked again in a different colour after taking the picture. ImageJ software (Abramoff et al., 2004) was employed to measure root lengths and root elongation was calculated by substracting root length at day 0 (directly after relocation) from that of the respective day.

2.8.4 Determination of electrolyte leakage

Analysis of relative electrolyte leakage was performed as described in Lee et al. (2007) with modifications. *Arabidopsis* plants were grown on soil for 4-5 weeks. Leaf discs of same size (0.5 mm) were excised using a hole puncher, washed in deionized water and forwarded to 50 ml tubes containing test solutions (0 mM, 5 mM and 20 mM H_2O_2 (Merck) in deionized water). Three tubes per line and concentration were prepared and 15 leaf discs were used per tube. Samples were placed under constant light in a growth cabinet and electrical conductivity was determined at 48 hours after treatment (hat) using a conductivity meter (Cond 315i, WTW) to obtain L_t values. Subsequently, samples were heated for 20 min to 80-90°C to kill all cells and after cooling down to RT, total electrical conductivity was measured again (L_0). Relative electrolyte leakage was calculated as L_t/L_0 x 100%.

2.8.5 Gene expression analysis in H_2O_2 treated plants

For qRT-PCR gene expression analysis in response to H_2O_2 (Merck), *Arabidopsis Col*-0 plants were aseptically grown in round petri dishes on solid ½ MS medium (Duchefa) supplemented with 1% (w/v) sucrose and 1% (w/v) agar-agar (Roth) under short day conditions for 8 days. Thereupon, plants were transferred to 6-well plates (Greiner Bio-One), with each well containing 5 ml of liquid ½ MS medium (Duchefa) supplemented with 1 % (w/v) sucrose. 15-20 plants were cultivated per well for additional 3 days before treatment. For that, 1 ml of the same medium was added per well, containing appropriate amounts of H_2O_2 (Merck) to reach a final concentration of 0 mM, 1 mM or 10 mM H_2O_2. Whole plants were harvested at 0, 1, 5 and 24 hat and immediately transferred to liquid nitrogen. Total RNA was extracted and aliquots were used for cDNA synthesis. 10 ng of cDNA were used as template for qRT-PCR as described above for fungal quantification. The $2^{-\Delta Ct}$ method was used to determine differential gene expression of *AtTLP3* as described in 2.5.3.

2.9 Subcellular localization studies

2.9.1 Molecular cloning of *AtTLP* coding sequences (CDS)

Arabidopsis Col-0 plants were grown aseptically for three weeks. Whole plants were harvested, total RNA was extracted and aliquots were transcribed to cDNA and stored at -20°C. To obtain the CDS of *HvTLP12* (GenBank: AK251904.1) total RNA extracted from one-week-old plants of barley cultivar Golden Promise was used to generate cDNA. Aliquots of this were used to PCR amplify coding sequences of all *AtTLP* genes and *HvTLP12* using Phusion DNA polymerase (Finnzymes). 50-500 ng cDNA were used as template. Primers were designed to start with the first ATG and end with the respective stop codon. In some cases terminal restriction sites were added for the purpose of cloning. In case of *AtTLP5*, *-8*, *-10*, *-11* and *HvTLP12* this yielded no PCR product. Therefore, primers were designed to anneal in cDNA regions outside the coding sequence. In case of *AtTLP4* no PCR product was obtained at all. 3' terminal adenine overhangs were added to the PCR products (A-tailing). The DNA was separated on an agarose gel, purified using the Wizard® SV Gel and PCR Clean-Up System (Promega) and ligated into pGEM-T using the pGEM-T system (Promega). Ligation was performed as described in the manual with a fragment:vector ratio of 3:1 and incubated overnight at 4°C. The ligation reaction was used to transform competent *E. coli* DH5α cells. The bacteria were plated on LB plates supplemented with 100 mg/ml ampicillin for selection. Additionally 40 µl IPTG/X-Gal were spread on each

plate to perform blue/white screening following the instructions of the pGEM-T system manual. White colonies were tested in colony PCR using primers M13 fwd (5'-GTTTTCCCAGTCACGAC-3') and M13 rev (5'-AACAGCTATGACCATGA -3'). Positive clones were used for DNA minipreparation (Pure Yield Miniprep Kit, Promega). Plasmids were sent for sequencing to verify correctness of sequences.

Table 2.5 Primers used for cloning of CDS

Construct	Forward Primer 5' - 3'	Reverse Primer 5' - 3'
AtTLP1 XbaI/SbfI	TCTAGAATGTCGTTCCGTAGCATA	CCTGCAGGTTATTCGCAAGCAAGTTTTGTG
AtTLP2 XbaI/SbfI	TCTAGAATGTCTTTGAAAAGCATCCTTCG	CCTGCAGGTTACCCTTCACATGCCGG
AtTLP3 XbaI/SalI	TCTAGAATGTCCTTCAAGAGTCTCATTCAGG	GTCGACTCATTCACATGCTATCTTGGTGTC
AtTLP5	ACGAAGACATATCGTTTCTC	GCATATCGTAAACGGTTCCT
AtTLP6 XbaI/SbfI	TCTAGAATGGATTTGTCGCTTTTGTTGCC	CCTGCAGGTCATTCGCAGACTGGCTTC
AtTLP7 XbaI/SbfI	TCTAGAATGCCTTTGTCACGGTCCC	CCTGCAGGTCACTCGCAGGCAAGTTTAGTG
AtTLP8	AAGCAATCCATCCAGAAAGG	TCAAACAGTACAACAAAGCTTG
AtTLP9 XbaI/SbfI	TCTAGAATGACGTTCCGAAGTTTACTC	CCTGCAGGTTATTCACAGGCAATTCTGGTTT
AtTLP10	CAAAGAGAAATGTCGTTTCGAG	CTATTCACAAGCAAGCTTGG
AtTLP11	GTATGACCTTACGTAGCTTAATCC	TCATTCACAAGCGATTCTAGTC
HvTLP12	GCAGATATGTCTTTCCGCAG	GCTACTGGTCTATTCATTCACAC

2.9.2 Generation of *AtTLP-GFP* constructs

A modified pamPAT vector backbone (AY436765) containing GFP behind the CaMV35S promoter was used to clone *AtTLP* sequences in front of the *GFP* sequence. It was confirmed that no frameshift was created by fusing *AtTLPs* with *GFP*. Respective parts of *AtTLP* coding sequences were amplified from pGEM-T-*AtTLP* vectors using Phusion DNA polymerase (Finnzymes) (for primer sequences see Table 2.6). Stop codons were removed when full-length coding sequences were used. A *Sal*I restriction site was added to the 5' end of all forward primers and a *Not*I site was added to the 5' end of all reverse primers. PCR fragments were gel purified and digested with *Sal*I/*Not*I. Similar, the vector backbone was also digested with *Sal*I/*Not*I and gel purified. For ligation, PCR fragments and vector were incubated overnight at 4°C using T4 DNA ligase (Fermentas). For generation of pam-MCS-AtTLP3$_{Prom}$::*AtTLP3Δ116-406-GFP*, the pam-MCS-35S::*AtTLP3Δ116-406-GFP* vector was digested with *AscI* and *XhoI* to remove the CaMV35S promoter. A stretch of 1032 bp upstream of the translational start site of *AtTLP3* was PCR amplified from genomic DNA using Phusion DNA polymerase (Finnzymes), adding *Asc*I and *Xho*I as terminal restriction sites. After digestion of the PCR fragment with the respective

enzymes, it was ligated into the opened vector backbone. In any case, the ligation reaction was used for transformation of competent *E. coli* DH5α cells. Bacteria were spread on LB plates containing 100 mg/ml ampicillin. Bacterial clones were tested in colony PCR. For this, a gene specific forward primer (Table 2.6) was used in combination with primer GFP5'rev2 (5'-GTTGGCCATGGAACAGGTAG-3'). Positive clones were used for DNA minipreparation (Pure Yield Miniprep Kit, Promega). Plasmids were sent for sequencing to verify correctness of sequences.

2.9.3 Generation of *GFP-TLP* constructs

A modified pamPAT vector backbone (AY436765) containing a GFP without stop codon behind the CaMV35S promoter was used to clone *TLP* sequences behind *GFP*. It was confirmed that no frameshift was created by fusing *TLPs* to *GFP*. Respective parts of the *AtTLP* and *HvTLP12* coding sequences were amplified from pGEM-T-*AtTLP* and the pGEM-T-*HvTLP12* vectors using Phusion DNA polymerase (Finnzymes) (for primer sequences see Table 2.6). A *Not*I restriction site was added to the 5' end of all forward primers and an *Xma*I restriction site was added to the 5' end of all reverse primers. To avoid frameshift, a single nucleotide was added between restriction site and the TLP sequence in all forward primers. PCR fragments were gel purified and digested with *Not*I/*Xma*I. The sequence for *AtTLP3(Δ1-115) (K187A/R189A)* was synthesized at Eurofins MWG with *Not*I and *Xma*I added as terminal restriction sites and digested with both enzymes. Similar, the vector backbone was also digested with *Not*I/*Xma*I and gel purified. For ligation, DNA fragments and vector were incubated overnight at 4°C using T4 DNA ligase (Fermentas). The ligation reaction was used for transformation of competent *E. coli* DH5α cells. Bacteria were spread on LB plates containing 100 mg/ml ampicillin. Bacterial clones were tested in colony PCR. For this, a gene specific reverse primer (Table 2.6) was used in combination with primer GFP3'fwd2 (5'- TGGAAGCGTTCAACTAGCAG-3'). Positive clones were used for DNA minipreparation (Pure Yield Miniprep Kit, Promega) and plasmids were sent for sequencing to verify correctness of sequences.

2.9.4 Insertion of *GFP* within the CDS of *AtTLP3*

AtTLP3Δ116-406 was PCR amplified using pGEM-T-*AtTLP3* as template and Phusion DNA polymerase (Finnzymes). Used primers added 5' and 3' terminal *Sal*I restriction sites (for primer sequences see Table 2.6). Sequences for two alanine residues were inserted between the 3' terminal restriction site and *AtTLP3Δ116-406* to generate a short linker between the protein and *GFP* in the resulting vector. Vector pam-MCS-35S::*GFP-AtTLP3Δ1-115* was opened by *Sal*I restriction. Subsequently, the PCR fragment and vector were gel purified. For ligation, DNA fragments and vector were incubated overnight at 4°C using T4 DNA ligase (Fermentas). The ligation reaction was used for transformation of competent *E. coli* DH5α cells. Bacteria were spread on LB plates containing 100 mg/ml ampicillin. Bacterial clones were tested in colony PCR. For this, a gene specific forward primer for *AtTLP3Δ116-406* (Table 2.6) was used in combination with primer GFP5'rev2 (5'- GTTGGCCATGGAACAGGTAG-3'). This resulted in clones only bearing a plasmid with *AtTLP3Δ116-406* inserted in the right direction. Positive clones were used for DNA minipreparation (Pure Yield Miniprep Kit, Promega) and plasmids were sent for sequencing to verify correctness of sequences.

2.9.5 Transient transformation of plant cells

Plasmid DNA was introduced into single leaf epidermal cells using a particle inflow gun (Schweizer et al., 1999). 312.5 ng tungsten particles (1.1 µm Bio-Rad) coated with 1 µg test plasmid and 0.5 µg control plasmid were delivered per shot. For *Arabidopsis thaliana*, leaves from 4-5-week-old soil grown plants were detached and put in petri dishes (Greiner Bio-One; Ø: 5 cm) containing 1% (w/v) agar-agar (Roth) in water. For *Nicotiana benthamiana*, leaves of 4-6-week-old plants were cut off, bisected and put into petri dishes (Greiner Bio-One; Ø: 9 cm) containing wet filter paper. Onions (*Allium cepa*) were acquired from a local greengrocer. Scale leaves were cut into pieces of about 4 cm^2 and put outside down into petri dishes (Greiner Bio-One; Ø: 5 cm) containing wet filter paper. Petri dishes were sealed with parafilm and kept in the dark. Confocal images were taken 16-26 h after bombardment on a TCS SP2 microscope (Leica). GFP was excited with a 488 nm laser line and detected at 505-540 nm. The marker proteins mCherry, pm-rk, and pt-rk (Nelson et al., 2007) were excited with a 543 nm laser line and detected at 620-660 nm.

Table 2.6: Primers used for generation of GFP fusion constructs

Construct	Forward Primer 5' - 3'	Reverse Primer 5' - 3'
GFP-AtTLP3Δ1-115 aa	GCGGCCGCTCCGGGTCCTAGAGGATCAC	CCCGGGTCATTCACATGCTATCTTGGTGTC
AtTLP3Δ116-406 aa-GFP	GTCGACATGTCCTTCAAGAGTCTCATTCA	GCGGCCGCCTGTTTGAGGGAGATAGGAAAAGT
$AtTLP3_{Prom}$::*AtTLP3Δ116-406 aa-GFP*	GGCGCGCCCCATTAAAGCGGCGAAAGTG	CTCGAGGGCTCTGAATTCTAACTAATAACGA
AtTLP3Δ50-406 aa-GFP	GTCGACATGTCCTTCAAGAGTCTCATTCA	GCGGCCGCCTGCTTGAAAGCATCAACAGG
AtTLP3Δ2-49, Δ116-406 aa-GFP	GTCGACATGAGCTGCTGGGCTAGTATG	GCGGCCGCGCTAGAAAGCTCAGGAACTCTG
AtTLP3Δ2-10, Δ116-406 aa-GFP	GTCGACATGAGAGGAGAGCTTG	GCGGCCGCCTGTTTGAGGGAGATAGGAAAAGT
AtTLP3Δ2-20, Δ116-406 aa-GFP	GTCGACATGGGATTCGATGTCAGATTCG	GCGGCCGCCTGCTTGAAAGCATCAACAGG
AtTLP3Δ2-39, Δ116-406 aa-GFP	GTCGACATGACTTCTGTTCCTGTTGATGCTTT	GCGGCCGCCTGTTTGAGGGAGATAGGAAAAGT
AtTLP3Δ106-406 aa-GFP	GTCGACATGTCCTTCAAGAGTCTCATTCA	GCGGCCGCGCTAGAAAGCTCAGGAACTCTG
AtTLP3Δ86-406 aa-GFP	GTCGACATGTCCTTCAAGAGTCTCATTCA	GCGGCCGCACCAGCGCAAGAAACAAC
AtTLP3Δ76-406 aa-GFP	GTCGACATGTCCTTCAAGAGTCTCATTCA	GCGGCCGCCGGCCAAGTGTCTTCGG
AtTLP3Δ66-406 aa-GFP	GTCGACATGTCCTTCAAGAGTCTCATTCA	GCGGCCGCCATAAGAACATCTCTCAGGAGCT
AtTLP2Δ112-394 aa-GFP	GTCGACCATGTCTTTGAAAAGCATCCTTCG	AGCGGCCGCCTGTTTCAATGAGATTGGAAAAGTG
GFP-AtTLP2Δ1-111 aa	GCGGCCGCTCCGGGGCCTCGAGAC	CCCGGGTTACCCTTCACATGCCG
AtTLP7Δ108-379 aa-GFP	TCAGTCGACATGCCTTTGTCACGGTC	ATGCGGCCGCCAATTTGAGGCAAGAAGGGAAAG
GFP-AtTLP7Δ1-107 aa	GCGGCCGCTCCAGGTCCTAGAGACTTTTCTA	CCCGGGTCACTCGCAGGCAAGT
AtTLP8Δ150-397aa-GFP	ATTGTCGACATGGCTGGTTCGAGAAAAGT	ATGCGGCCGCAGGTAGTGTCTTGCACAACAAAG
GFP-AtTLP8Δ1-149 aa	GCGGCCGCATTGGATGTGGGAAGATGCAC	CCCGGGTCAAACAGTACAACAAAGCTTGGAA
AtTLP10Δ123-445 aa-GFP	GTCGACATGTCGTTTCGAGGCATTGT	ATGCGGCCGCCTGTTTGAGGGAAACAGGGAAAG
GFP-AtTLPΔ1-122 aa	GCGGCCGCTCCAGGGCCTCGTGATG	CCCGGGCTATTCACAAGCAAGCTTGGTGT
GFP-HvTLP12Δ1-123 aa	GCGGCCGCTCCAGGACCTCGAGATGG	CCCGGGTCATTCACACGCCAGCTT
FL AtTLP3-GFP	GTCGACATGTCCTTCAAGAGTCTCATTCA	GTCGACTGCTGCCTGTTTGAGGGAGATAGGAAAAGT

2.9.6 Cytological analyses

For microscopy, *Arabidopsis* leaves were placed on glass slides in a bathing solution (2 mM KCl, 1 mM $CaCl_2$, 1 mM $MgCl_2$, 50 mM mannitol, and 2.5 mM MES/NaOH buffer, pH 5.7) (Hafke et al., 2005) to simulate apoplastic conditions and covered with a cover glass. The bathing solution contained no mannitol in experiments involving NaCl. *Nicotiana benthamiana* leaves were cut to fit on glass slides and embedded in water. The onion scaled leaves were cut into smaller pieces to fit on glass slides and the epidermis was peeled off. For microscopy, epidermal peels were covered with water containing 0.002% (v/v) Tween20. Further chemicals were added as indicated. For experiments involving U73122 (Merck), leaves were placed for 3 h in either bathing solution (mock) or bathing solution containing 10 µM U73122. Then mock treated leaves were placed in bathing solution containing either 0.4 M mannitol or 20 mM H_2O_2 (Merck). Inhibitor treated leaves were placed in the same solutions additionally containing 10 µM U73122.

2.10 Image processing

Images were processed using Adobe Photoshop 3.0.

3. Results

3.1 AtTLPs are required for normal colonization of *Arabidopsis* by *P. indica* but show no altered immune responses

A reverse genetic approach was chosen to investigate functions of AtTLPs. Therefore, in a first step, colonization/resistance of T-DNA insertion lines of *AtTLP* genes by/to several fungi was compared to wild-type plants. In addition, mutant lines were subjected to assays testing immune responses elicited by different stimuli.

3.1.1 T-DNA insertion lines with reduced transcription of *AtTLP* genes

'The Arabidopsis Information Resource' (TAIR) database was used to identify homo- or heterozygous *Arabidopsis* lines featuring a T-DNA insertion within one of the 11 *AtTLP* genes (Lai et al., 2004) possibly causing knock-outs or strong knock-downs of the respective genes. Such lines have proven to be extremely valuable for the investigation of gene functions (e.g. Alonso and Ecker, 2006). *AtTLP4* has previously been suggested to be a pseudo-gene (Lai et al., 2004) and was therefore excluded from the analysis. For all other genes, seeds for one to two independent transgenic lines were obtained from the Nottingham *Arabidopsis* Stock Centre. Since mutant lines with the T-DNA inserted in an exon were not available for all genes, such with an insertion in introns, the 5'UTR and promoter regions were chosen alternatively (see Table 2.1 for more information). A T-DNA insertion does not automatically guarantee reduced expression of a certain gene and might in some cases even lead to overexpression (Ülker et al., 2008). Thus, expression levels of the respective *AtTLP* transcript in mutant lines were compared to those in wild-type plants by semi-quantitative PCR using gene specific primers (Table 2.3). In this analysis only line *attlp6-1*, which features a T-DNA insertion within the promoter sequence, did not show reduced transcription when compared to wild-type plants (Figure 3.1). Hence, this line was not used in further experiments and no mutant line for *AtTLP6* was available for this study. Eight knock-out lines (showing no transcript) could be identified (*attlp2-1*, *attlp3-1*, *attlp5-1*, *attlp5-2*, *attlp10-1*, *attlp10-2*, *attlp11-1*, *attlp11-2*). In addition, five lines were found to have a strong reduction in transcript levels (*attlp1-1*, *attlp2-2*, *attlp3-2*, *attlp7-1*, *attlp8-1*, *attlp8-2*) (Figure 3.1). *attlp9-1* and *attlp9-2* have already been characterized as knock-out and knock-down lines, respectively, by Lai et al. (2004) and were thus not tested again in this study. The

experiments provided one to two lines with reduced expression for each *AtTLP* gene (except *AtTLP4* and *AtTLP6*) for further characterization. From an evolutionary point of view, except for systematic clade B (*AtTLP4*) all clades were hence covered by at least one transgenic line (Figure 3.3 A; Yang et al., 2008).

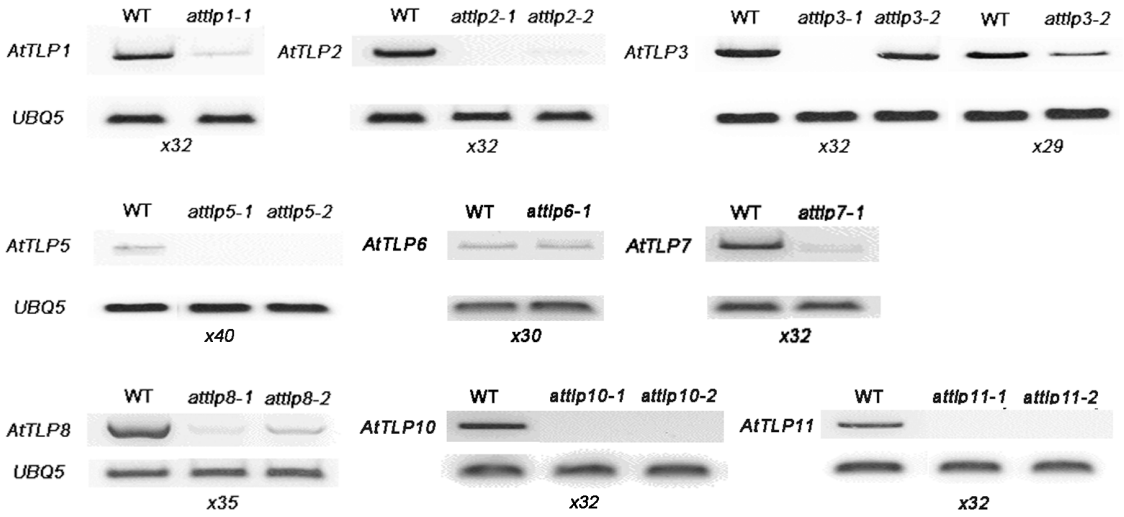

Figure 3.1: Examination of *AtTLP* transcript levels in *attlp* mutant lines. Total RNA extracted from aseptically grown three-week-old mutant and wild-type (WT) *Arabidopsis* plants was used to generate cDNA. Semi-quantitative PCR was performed to estimate respective *AtTLP* transcript levels in *attlp* mutant lines and compare them to levels in WT plants. *AtUBI5*-specific primers were included as control. DNA was separated on agarose gels and pictures were acquired using a digital camera. Numbers of PCR cycles are given below each gel image.

3.1.2 Colonization of *attlp* mutant lines by *P. indica*

In a recent study, the mutualistic basidiomycete *P. indica* was shown to induce expression of a *TLP* gene in barley roots (*HvTLP*) during colonization in microarray experiments seven days after inoculation (dai) (Schäfer et al., 2009). Sequence comparison revealed that the HvTLP protein was related to OsTLP3 and therefore similar to members of clade A1 (Yang et al., 2008). Further studies indicated that *P. indica* colonizes *Arabidopsis* roots in a similar way like barley (Deshmukh et al., 2006; Schäfer et al., 2009; Jacobs et al., 2011; Zuccaro et al., 2011). It was therefore investigated if TLPs play a role in the interaction between *Arabidopsis* roots and the mutualist. Expression of selected *AtTLP* genes in *P. indica* inoculated *Arabidopsis Col*-0 plants was examined at one, three and seven dai covering pre-penetration, biotrophic and cell-death associated colonization phases of the fungus (Jacobs et al., 2011). No primer pairs with sufficient

efficiency for qRT-PCR were found for genes *AtTLP1* and *AtTLP6* and expression of these genes could thus not be analyzed. In contrast to the results obtained for barley roots, none of the tested *AtTLPs*, including *AtTLP5* and *AtTLP10* as members of clade A1, showed differential expression in response to *P. indica* in comparison mock treated plants (Figure 3.2).

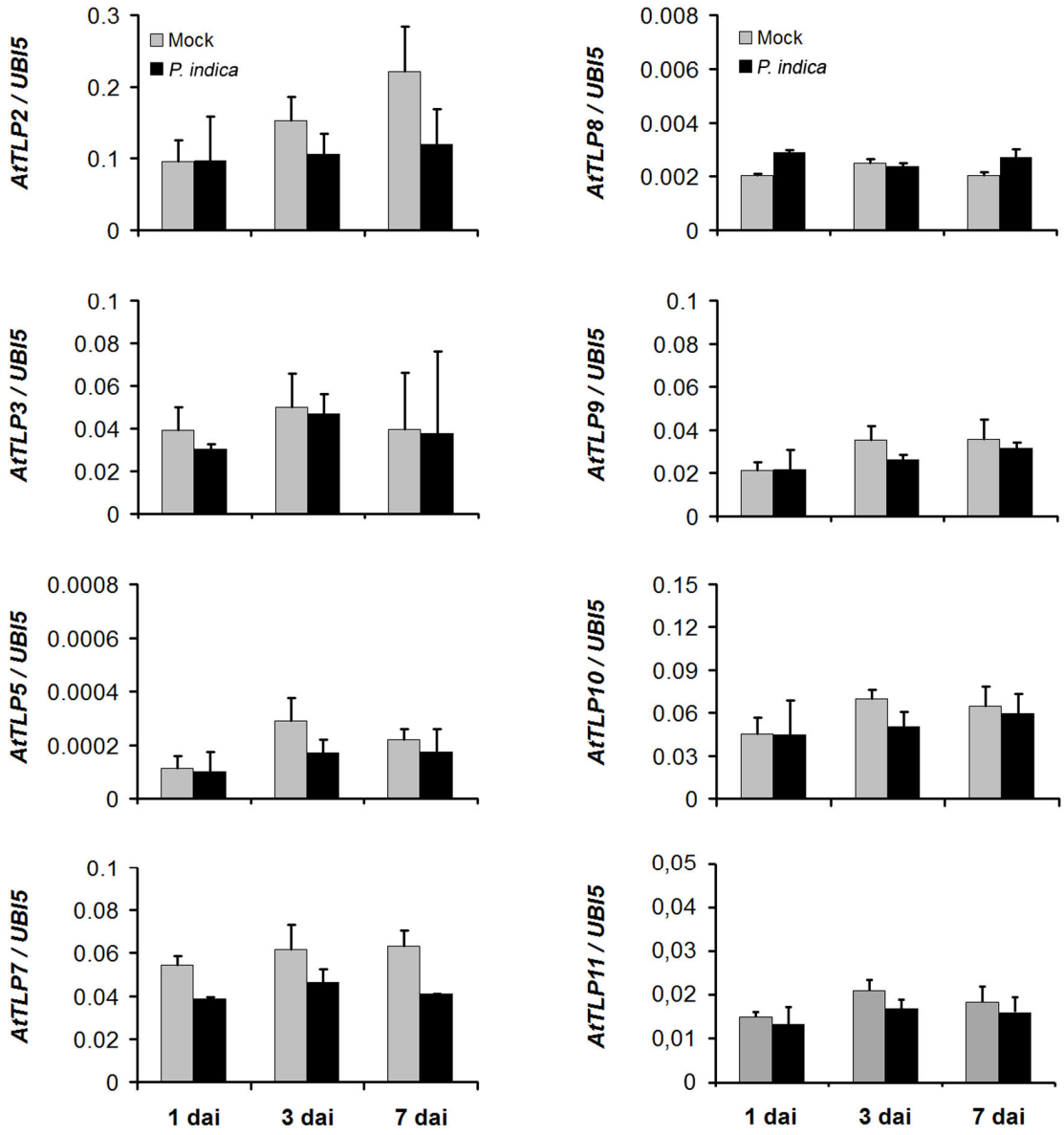

Figure 3.2: Expression analysis of *AtTLPs* after *P. indica* or mock inoculation. Three-week-old *Arabidopsis* plants (*Col*-0) were mock treated or inoculated with *P. indica*. Roots were harvested at 1, 3 and 7 dai. Total RNA was extracted and used to generate cDNA for qRT-PCR with primers specific for individual *AtTLP* genes. Expression values were calculated by the $2^{-\Delta Ct}$ method by relating Ct values of candidate genes to those of the housekeeping gene *AtUbiquitin5 (AtUBI5)*. Data are means of at least two independent experiments. Error bars indicate standard deviation

Since regulation of transcription cannot give a final answer to the participation of a protein in a host-microbe interaction, colonization of *attlp* lines by *P. indica* was investigated. For this, three-week-old *Arabidopsis* wild-type and mutant plants were inoculated with fungal spore suspension. Quantification of fungal biomass was performed at three and seven dai via qRT-PCR using genomic DNA isolated from colonized roots and plant (*AtUBI5*) and fungal (*ITS*) specific primers. All tested mutant lines showed a significantly reduced amount of fungal DNA at three dai when compared to wild-type, indicating a reduced colonization of mutant plants by the fungus (Figure 3.3 A). In contrast, no different colonization was observed at seven dai, except for lines *attlp3-2*, *attlp5-2* and *attlp11-2* where still significantly less fungal DNA was detected. As these results might hint to a better colonization of mutant lines at later stages, a more detailed study was undertaken choosing line *attlp5-1*. Experiments were carried out as described above but colonization was determined at three, five, seven and nine dai (Figure 3.3 B). Whereas a significantly reduced fungal biomass was observed at three dai, colonization levels in *attlp5-1* plants reached wild-type levels at five dai and no difference could be observed at seven and nine dai.

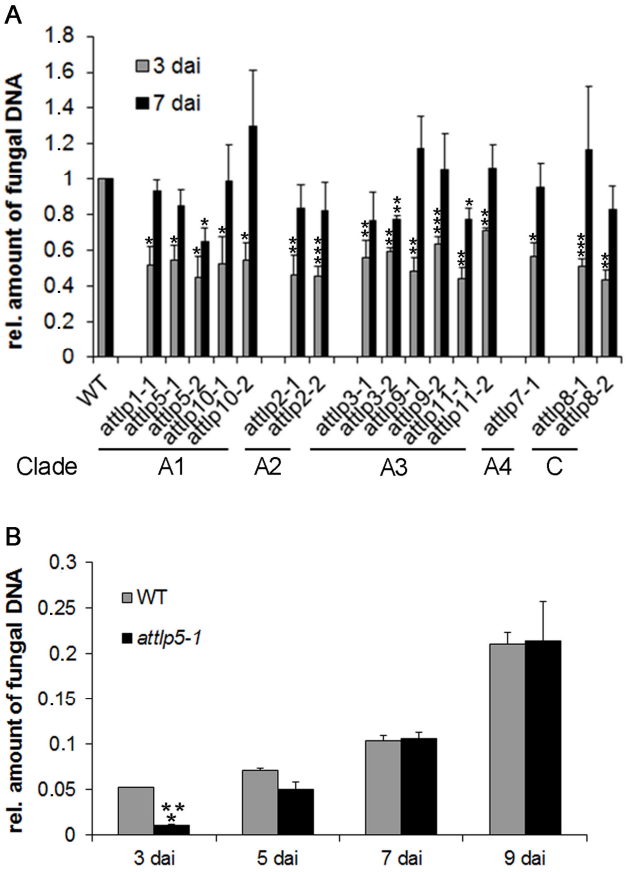

Figure 3.3: Delayed colonization of *attlp* mutant lines by *P. indica*. Three-week-old *Arabidopsis* mutant or WT (*Col*-0) plants were inoculated with *P. indica*. (A) Root samples were harvested during biotrophic (3 dai) or cell-death associated colonization (7 dai). Clades specify the systematic placement of respective *AtTLP* genes following Yang et al. (2008). Colonization in WT plants was set to one to better compare results from different experiments. Data are means of at least three independent biological experiments with bars indicating standard errors. (B) Additional time points were chosen for a more detailed analysis of colonization in *attlp5-1* plants. Genomic DNA was extracted and the amount of fungal biomass was calculated by qRT-PCR using plant and fungal specific primers. 200 plants were analyzed per mutant or WT and per time point in each experiment. Average data of three technical replicates within one biological experiment is presented. The experiment was performed twice with similar results. Bars represent standard errors. Asterisks indicate significance at $P < 0.05$ (*), 0.01 (**), 0.001 (***) as analyzed by Student's *t*-test.

3.1.3 Unaltered immune responses of *attlp* lines

Delayed colonization of mutant lines by *P. indica* might be caused by a generally enhanced immune signaling, making the plants more resistant to the fungus. In addition, *P. indica* suppresses several immune responses in colonized plants (Jacobs et al., 2011). This ability might be impaired in *attlp* plants. To test this hypothesis, *attlp* mutant and wild-type *Arabidopsis* seedlings were either mock treated or inoculated with *P. indica* and five days later half of the mock or *P. indica* treated plants were exposed to the bacterial peptide flg22 or mock treated. Plant fresh weight was determined ten days after treatment. Flg22 represents a peptide consisting of 22 amino acids of the most conserved domain at the N-terminus of the bacterial protein flagellin. It was shown to act as a MAMP in plants, inducing several immune responses. Amongst the effects caused by flg22 is a reduction in seedling growth, which results in reduced fresh weight (Felix et al., 1999; Gómez-Gómez et al., 1999). *P. indica* is able to abolish this effect in colonized *Arabidopsis* plants (Jacobs et al., 2011). All tested *attlp* lines were as sensitive to the bacterial peptide as wild-type plants (Figure 3.4 A). This observation was also made for lines *attlp3-1* and *attlp5-1* when exposed to elf18 (Figure 3.4 B), another MAMP comprising the 18 most N-terminal amino acids of bacterial elongation factor Tu (Kunze et al., 2004; Zipfel et al., 2006). Moreover, *P. indica* was able to rescue the flg22 induced growth inhibition in mutant plants as reported for wild-type plants (Figure 3.4 A).

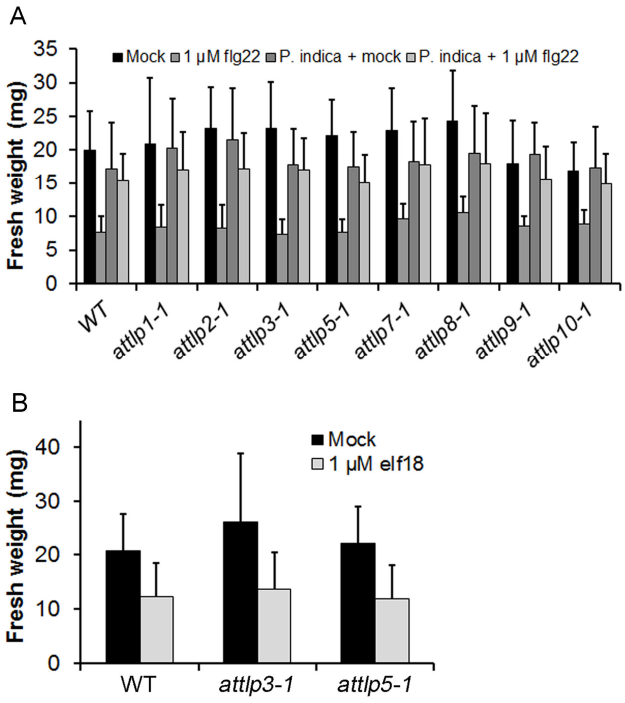

Figure 3.4: MAMP-triggered seedling growth inhibition. (A) 10-12 day old *Arabidopsis* plants were mock treated or inoculated with *P. indica* and after five days transferred to liquid medium containing no (mock) or 1 µM of the bacterial peptide flg22. Fresh weight was determined 10 days after treatment. Data are means (± SE) of two independent experiments with at least 10 plants per line and treatment. (B) Three-week-old *Arabidopsis* plants were transferred to petri dishes containing liquid medium supplemented with either 0 µM (mock) or 1 µM of the bacterial peptide elf18. Fresh weight was determined 9 days after treatment. Data represent means (± SD) of two independent experiments with at least 10 plants per line and treatment.

As a further test, expression of several marker genes for plant immunity (*CBP60G*, *WRKKY29*, *VSP2*, *OXI1*, *MYB51*) and abiotic stress (*ZAT12*, *At5G10695*, *DREB2A*) was assayed by qRT-PCT in *P. indica* inoculated wild-type and *attlp3-1* plants. No enhanced expression of the genes was observed in the mutant as compared to wild-type plants.

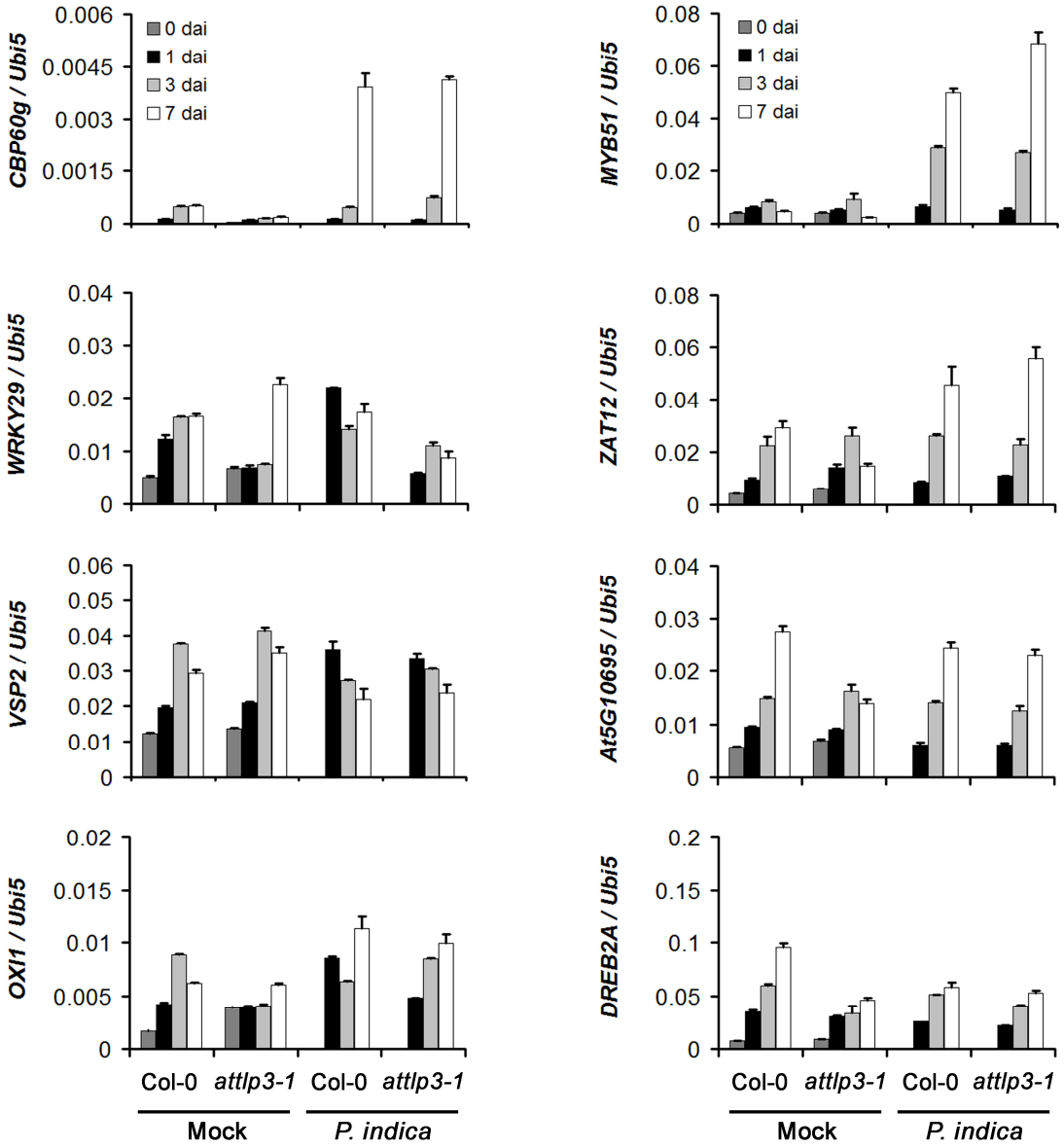

Figure 3.5: Expression analysis of marker genes for plant immunity and abiotic stress in *P. indica* colonized *Col*-0 and *attlp3-1* plants. Three-week-old *Arabidopsis* plants were inoculated with *P. indica* or mock treated. Roots were harvested at 0, 1, 3 and 7 dai. Total RNA was extracted and used for generation of cDNA. qRT-PCR was performed with gene specific primers for immunity-related (*CBP60g*, *WRKY29*, *VSP2*, *OXI1*, *MYB51*) and abiotic stress (*ZAT12*, *AT5G10695*, *DREB2A*) marker genes. Expression values were calculated by the $2^{-\Delta Ct}$ method by relating Ct values of candidate genes to those of the housekeeping gene *AtUBI5*. Standard errors are from three technical replicates of one biological experiment. Experiments were repeated at least twice with similar results.

3.1.4 Resistance to several pathogens is not affected by lack of *TLPs*

To see, if resistance to microorganisms is generally altered in plants lacking one of the *AtTLP* genes, susceptibility of selected mutant lines to two fungal and one oomycete pathogen was assayed. No altered resistance was observed for lines *attlp2-1*, *-3-1*, *-5-1* and *-8-1* to the necrotrophic leaf pathogen *Botrytis cinerea*, for lines *attlp2-1*, *-3-1*, *-5-1* and *-9-1* to the hemi-biotrophic root pathogen *Phytophtora parasitica* and for lines *attlp3-1*, *-3-2* and *-5-2* to the biotrophic leaf pathogen *Erysiphe cruciferarum*, when compared to wild-type.

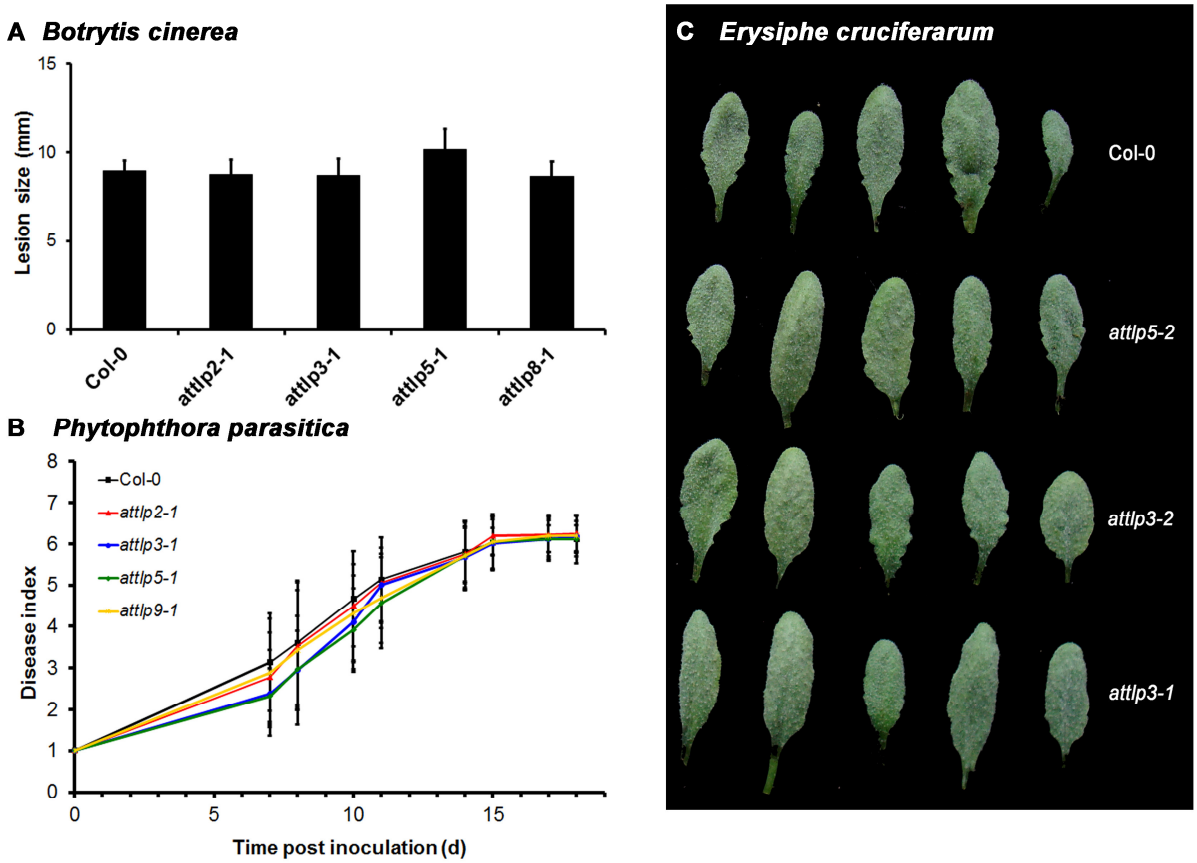

Figure 3.6: Unaltered susceptibility of selected *attlp* lines to different pathogens. (A) Lesion size at 4 dai on detached leaves of *Col*-0, *attlp2-1*, *-3-1*, *-5-1*, *-8-1* plants inoculated with *Botrytis cinerea* spore suspension. Data are means (± SE) from at least ten plants per line of one biological experiment. The experiment was conducted three times with similar results. (B) Roots of *Col*-0, *attlp2-1, -3-1, -5-1* and *-9-1* were inoculated with *Phytophthora parasitica* and disease indices were determined at 7, 8, 10, 11, 14, 15, 17, and 18 dai. Differences in disease indices between *Col*-0 and mutants were statistically insignificant. Bars represent standard deviations from one biological. The experiment was repeated two times with similar results. (C) Leaves of *Col*-0, *attlp3-1, -3-2* and *-5-2* were inoculated with *Erysiphe cruciferarum*. Images present leaves overgrown with the fungus at 11 dai. The experiment was repeated two times with similar results.

Taken together, the results of this chapter indicate that AtTLPs are needed for normal colonization of *Arabidopsis* roots by *P. indica*, although seemingly not differentially expressed during colonization. Furthermore, no evidence was found for a generally increased activity of immune signaling in *attlp* lines or an involvement of AtTLPs in resistance to pathogens.

3.2 Subcellular localization of plant TLPs

3.2.1 Conserved 3D protein structure of AtTLP3

Structural biology can help to answer biological questions at an early state of investigation and 3D homology modeling has become a powerful tool in resolving the structure of proteins when the crystallographic structure of a related protein is available (e.g. Hrmova and Fincher, 2001; Bateman et al., 2009). This is the case for the Tubby domain of mouse (Mm) TUBBY which has been resolved by Boggon et al. (1999) (PDB-ID 1C8Z) as was done for the human (Hs) Tub protein isoform a (PDB-ID 1S31). Both served as templates to determine the structure of AtTLP3 as a first member of *Arabidopsis* TLPs (Figure 3.7 B). The protein shows about 35% amino acid conservation to the mammalian proteins (Figure 3.7 A). A 3D alignment of AtTLP3 with the structures of Mm and HsTub revealed that despite the relatively low conservation in amino acids the *Arabidopsis* protein may feature a conserved position and orientation of α-helices and β-sheets in the Tubby domain (Figure 3.7 C). However, some secondary structures and the N-terminal F-box were unique to the plant protein (Figure 3.7 B, C, D). Importantly, an overlay of the 3D structure of the Tubby domain of AtTLP3 with that of Mm and HsTub bound to the PIP_2 headgroup analog L-alpha-glycerophospho-D-myo-inositol-4,5-bis-phosphate (IBS) showed an overlay of amino acid positions of the PIP_2 binding cavity in AtTLP3 (Figure 3.7 D,E). The most obvious differences here were the replacement of R363 and P204 / T205 in MmTUBBY by N233 and G346 / V347, respectively, in AtTLP3. R363 was shown to be involved in PIP_2 binding (Santagata et al., 2001). The differences in the latter two amino acids resulted in a change of the run of the backbone of the binding site. Nevertheless, the overall structure of the binding site was highly conserved and, R330 / K332 the two most important amino acids for PIP_2 binding in mice (Santagata et al., 2001), were found in a conserved position in AtTLP3 (R187 / K189). DNA binding capability was demonstrated for some mammalian and plant TLPs (Boggon et al., 1999; Lai et al., 2004; Cai et al. 2008; Wardhan et al., 2012). Interestingly, when comparing the surface charges of the predicted DNA binding groove, AtTLP3 did not show the strong overall positive

charge of the mammalian TLPs (Figure 3.7 F, G). Additionally, the grove was smaller in the model for AtTLP3 than in the mammalian proteins.

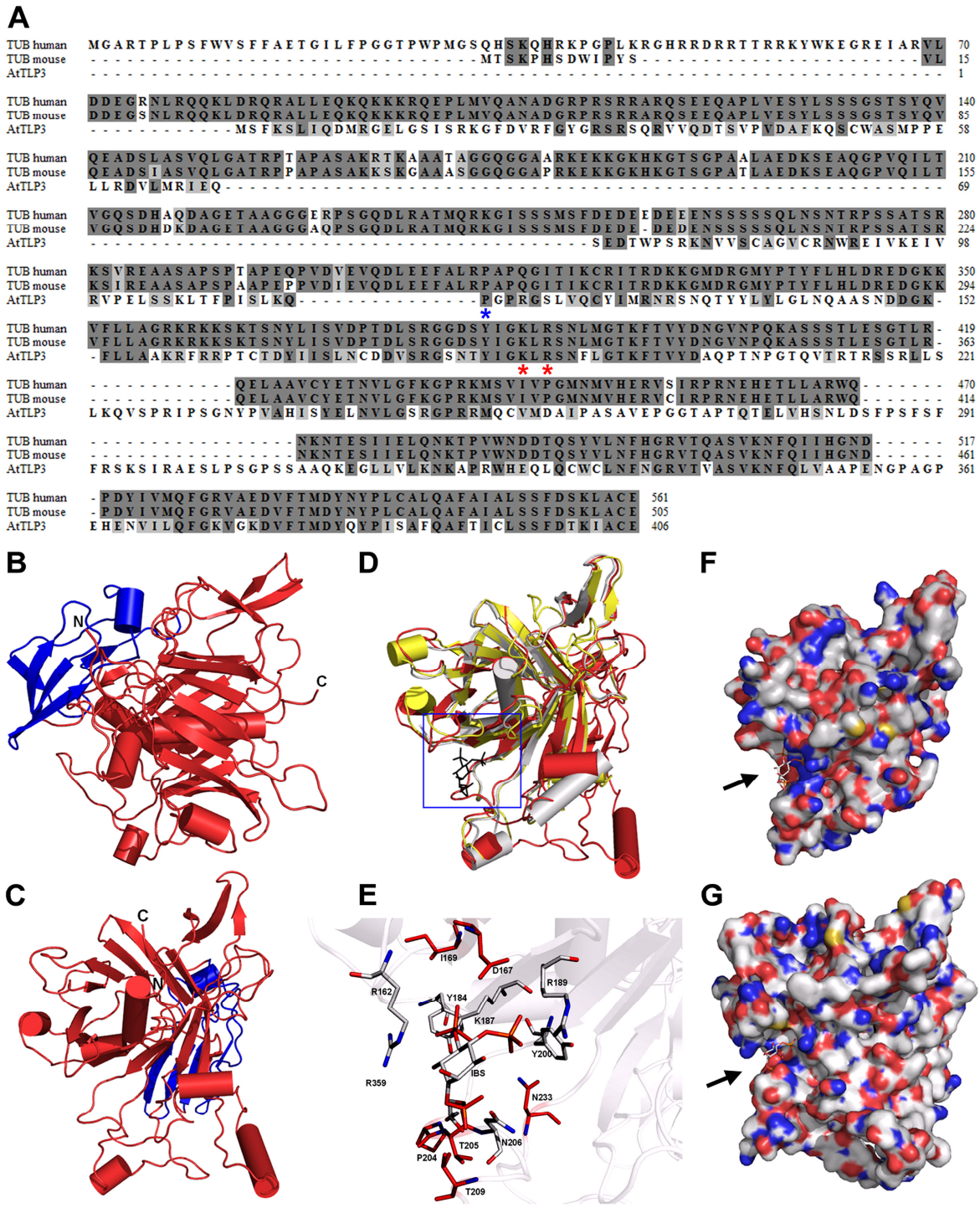

Figure 3.7: Comparison of sequence and 3D structure of AtTLP3 with the human and mouse TUBBY protein. (A) Sequence alignment for human (Acc. 19923167) and mouse TUBBY (TUB) protein (Acc. 11230782) with AtTLP3 (Acc. 30690823). The alignment was created using ClustalW (Larkin et al., 2007). Identical and similar amino acids are shaded in dark grey and light grey, respectively. The two amino acids which are required for PIP_2-binding (Santagata et al., 2001) are indicated (red asterisks underneath the respective amino acids). The blue asterisk underneath the respective amino acids indicates the start of the Tubby domain. (B, C) 3D homology model of AtTLP3 showing the F-box domain (blue) and Tubby domain (red). N and C-terminus are labeled. (D) Superposition of the structural model of AtTLP3 (red) with the crystal structure of the human TUBBY protein (PDB-ID: 1S31) (yellow) and the crystal structure of mouse TUBBY protein (grey) bound to IBS (black, blue frame). (E) Magnification of the frame in D shows the highly conserved inositol lipid-binding domain of AtTLP3. A comparison of AtTLP3, mouse and human TUBBY proteins was done. The PIP_2 headgroup analog L-α-glycerophospho-D-myoinositol 4,5-bisphosphate (IBS) was used to show conservation of binding sites. Amino acid residues, which are similar in type and position (conformation) in all three proteins are coloured in grey. Amino acids that are specific for the AtTLP3 protein are marked in red. (F, G) Surface representation of mouse TUBBY protein binding IBS (F) and structural model of AtTLP3 (G) binding to IBS. Arrows indicate IBS binding site. The groove of highly positive charge (blue regions) is more significant in the mouse protein, and the dimension of the groove differs in the AtTLP3 structural model.

3.2.2 Truncated versions of AtTLP3 localize to the plasma membrane and plastids in *Arabidopsis*

Transient transformation of plant cells via particle bombardment offers a fast and simple tool to study the subcellular localization dynamics of proteins in various plant species including *Arabidopsis* (reviewed in e.g. Panstruga, 2004; Mathur, 2007; Okumoto et al., 2012). It was therefore decided to choose this biolistic approach to investigate the intracellular localization of AtTLPs. Unfortunately, transient expression of GFP-tagged full-length versions of AtTLP1, AtTLP2, AtTLP3 and AtTLP7 in *Arabidopsis* leaf epidermal cells under control of a 35S promoter did not result in detection of GFP. The same was observed for a full-length version of AtTLP3 when N-terminally fused to the red fluorescent protein mCherry. In leaves transformed with mCherry and AtTLP-GFP variants, many cells with red but no green fluorescence were found. Since no autofluorescence was observed (indicator of cell death), this suggested instability of AtTLP-GFP constructs rather than toxicity.

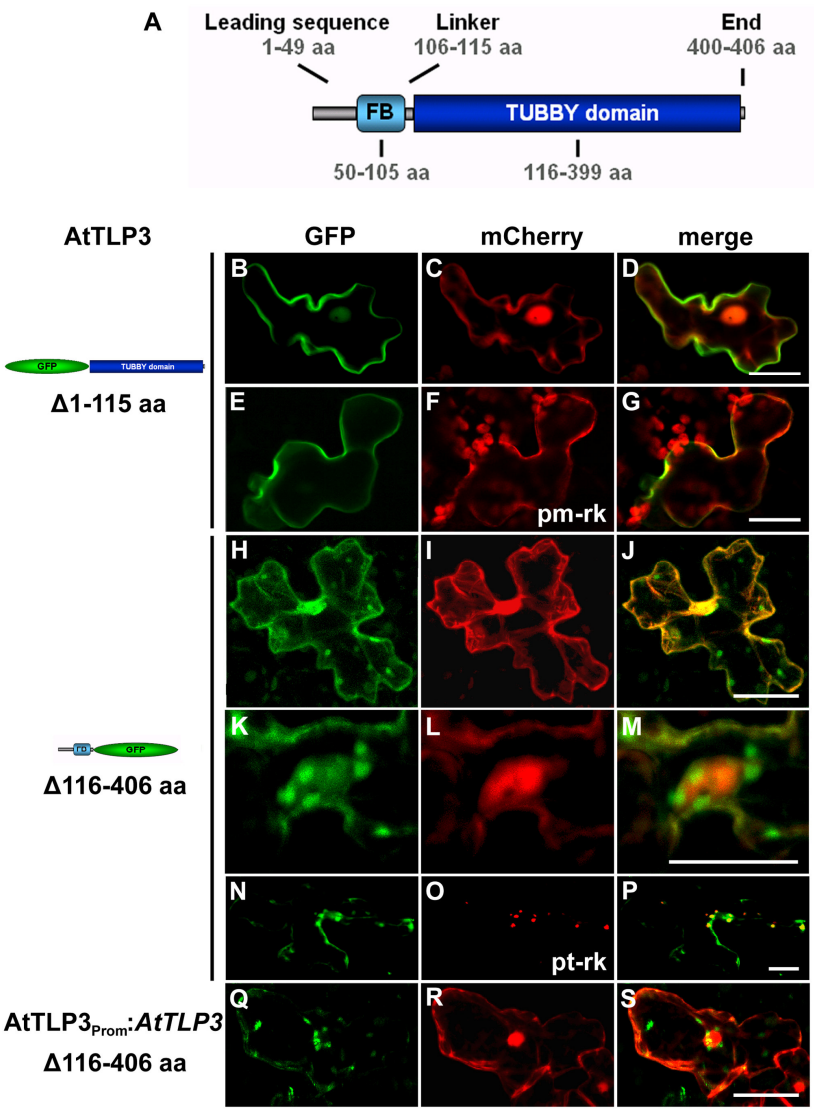

Figure 3.8: Subcellular localization of the Tubby domain and N-terminal region of AtTLP3 in *Arabidopsis* leaf epidermal cells. (A) Domain organization of AtTLP3. Figures indicate amino acid (aa) positions and length of protein segments. The F-box (FB) and Tubby domains are depicted in light and dark blue, respectively. (B-S) Single *Arabidopsis* leaf epidermal cells were transformed using a biolistic approach. Respective AtTLP constructs used for transformation are outlined on the left. Cells were co-transformed with truncated versions of AtTLP3 tagged with GFP under the control of a CaMV35S promoter (B, E, H, K, N) or the native promoter of AtTLP3 (Q) and the red fluorescent marker protein mCherry (C, I, L, R), which locates to the cytoplasm and nucleus. As additional marker proteins, pm-rk (F; plasma membrane) and pt-rk (O; plastids) were used (Nelson et al., 2007). Corresponding merged images are shown on the right to indicate subcellular localization of GFP fusions (D, G, J, M, P, S). Yellow colour indicates co-localization of the GFP construct with the respective red marker protein. (B-D) Localization of the AtTLP3 Tubby domain (GFP-CT-AtTLP3) at the edge of the cell. (E-G) GFP-CT-AtTLP3 co-localizes with the plasma membrane marker pm-rk. (H-J) Nucleo-cytosolic and plastidial localization of the N-terminal part of AtTLP3 (NT-AtTLP3-GFP). (K-M) Close up look on plastids and nucleus in a cell expressing AtTLP3-NT-GFP and mCherry. (N-P) Confirmation of plastidial localization of AtTLP3-NT-GFP with the plastidial marker pt-rk. (Q-S) Cells expressing AtTLP3-NT-GFP under the control of the native AtTLP3 promoter. Green fluorescence can be seen in the plastids, the nucleus and the cytosol. Pictures were taken at 16-26 h after particle bombardment with a CLSM. Experiments were performed three times with similar results. Bars = 20 µm.

In mammals, GFP-tagged truncated versions of MmTUBBY comprising either the N-terminal (all sequences in front of the Tubby domain) or C-terminal (Tubby domain) part of the protein were detected in the nucleus and at the plasma membrane, respectively (Santagata et al., 2001). Furthermore, fluorescence was observed when the first 60 amino acids of AtTLP7 and AtTLP9 were fused to GFP and transiently expressed in *Arabidopsis* cell cultures (Carrie et al., 2009).

Therefore, GFP-tagged truncated versions of AtTLP3 were generated and expressed in *Arabidopsis* leaf epidermal cells (Figure 3.8). AtTLP3 consists of a short leading sequence (amino acids (aa) 1-49), an F-box domain (aa 50-105), a linker sequence (aa 106-115), the Tubby domain (aa 116-400) and a short end sequence (aa 401-406), as predicted by SMART (Schultz et al., 1998; Letunic et al., 2012) (Figure 3.8 A). Truncated versions were either composed of the whole N-terminal part (NT) excluding the Tubby domain (NT-AtTLP3-GFP) or the C-terminal part (CT) comprising the Tubby domain plus end sequence (GFP-CT-AtTLP3). Cells were usually co-transformed with the nuclear and cytosolic marker protein mCherry to better assess localization of the GFP construct and to monitor the success of transformation. Positions of TLP3 variants within the cell were verified by co-expression with an appropriate subcellular marker protein. Fluorescence from CT-AtTLP3 accumulated at the edge of transformed cells. In some cells a weak fluorescence was also observed in the cytosol and nucleus (Figure 3.8 B-D). Co-transformation with the plasma membrane (PM) marker protein pm-rk (Nelson et al., 2007) confirmed PM localization of the GFP construct. In contrast, when expressing the N-terminal part of AtTLP3, fluorescence was detected in the cytosol, the nucleus and in plastids (Figure 3.8 H-M). Plastidial localization was confirmed using the plastidial marker protein pt-rk (N-P) (Nelson et al., 2007). To reduce probability of artifacts in plastidial localization due to strong overexpression, cells were also transformed with NT-AtTLP3-GFP under control of the native AtTLP3 promoter. The fluorescence pattern was the same as in cells using the 35S promoter, though much weaker (Figure 3.8 Q-S).

3.2.3 In-depth study of plastidial localization of NT-AtTLP3

In silico analyses using ChloroP did not reveal a chloroplast targeting peptide (cTP) at the N-terminus of AtTLP3 but gave a score of 0.496, which is just below the 0.5 cutoff indicative for cTPs (Emanuelsson et al., 1999), suggesting that a cTP is yet present in the N-terminal region. To examine if this is the case and which part of the sequence is responsible for plastid import, a series of truncated versions of the N-terminal part of AtTLP3 was generated, tagged with a C-terminal GFP and used for biolistic transformation of *Arabidopsis* cells. All constructs lacked the C-terminal part of the protein (aa 116-406). Neither the leading sequence (Figure 3.9 A-C) nor the F-box domain (Figure 3.9 D-F) were sufficient for import into plastids, which is demonstrated by cytosolic and nuclear localization of both constructs. In addition, subsequent deletion of the first 10 (Figure 3.9 G-I), 20 (Figure 3.9 J-L) and 39 (Figure 3.9 M-O) amino acids did not affect

plastidial localization, indicating that these are not necessary for transport into plastids. Also, truncated versions lacking either the linker sequence (Figure 3.9 P-R) or the linker sequence and the 20 C-terminal amino acids of the F-box (Figure 3.9 S-U), were still imported into plastids. In contrast, removing the last 30 (Figure 3.9 V-X) or 40 (Figure 3.9 y-AA) amino acids of the F-box (aa 50-106; Figure 3.8 A) together with the linker sequence abolished plastidial localization. Thus, a sequence stretch comprising a part of the leading sequence and the F-box seems to be necessary for import of NT-AtTLP3-GFP into plastids.

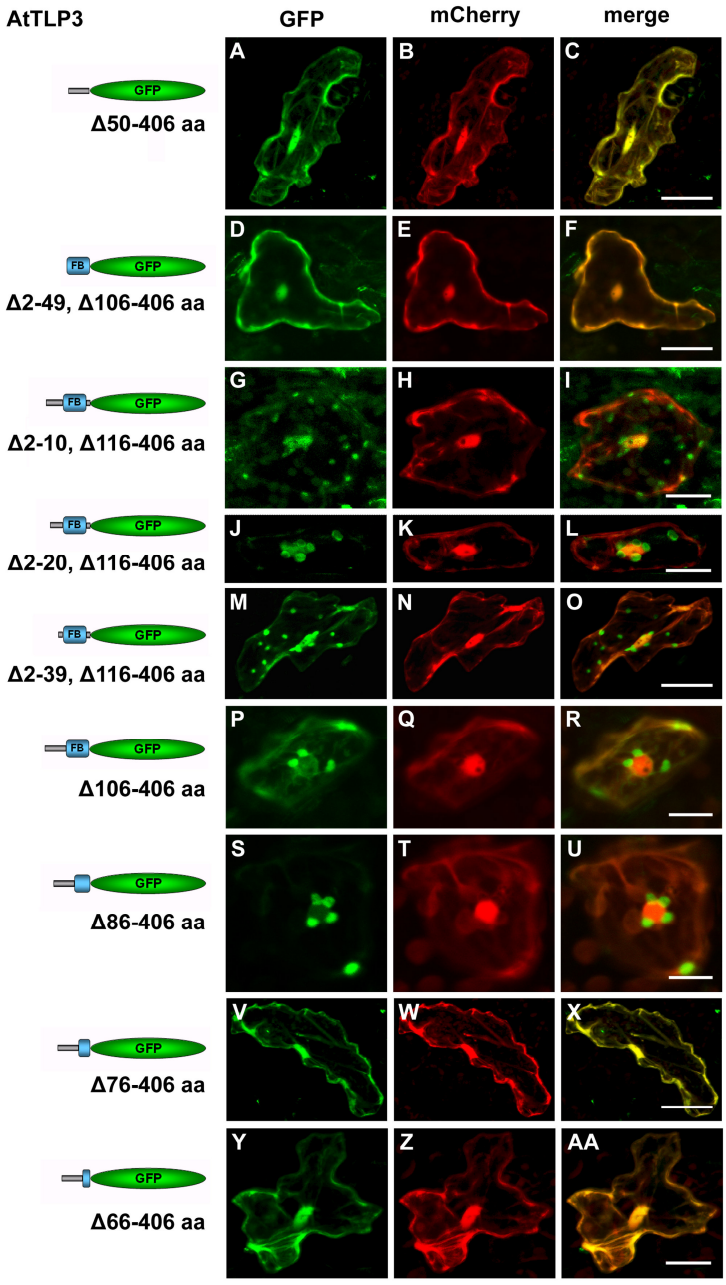

Figure 3.9: Subcellular localization of *AtTLP3-NT-GFP* deletion variants. (A, D, G, J, M, P, S, V, Y) Confocal images of *Arabidopsis* cells co-transformed via particle bombardment with deletion variants of the N-terminal region of AtTLP3 fused to C-terminal GFP and (B, E, H, K, N, Q, T, W, Z) the nucleo-cytosolic marker mCherry. All GFP constructs lack the C-terminus of AtTLP3 (Δ116-406 aa). The linker region (106-115 aa) is either included (G, J, M) or not (A, D, P, S, V, Y). Constructs used for transformation are outlined on the left. (C, F, I, L, O, R, U, X, AA) Merged images are shown to indicate localization of the deletion constructs. (A-C) Nuclear and cytosolic localization of the GFP-tagged AtTLP3 leading sequence (Δ50-406) and (D-F) F-box domain (Δ2-50, Δ106-406). (G-U) Nucleo-cytosolic and plastidial localization of deletion variants lacking different sets of amino acids (G-I) (Δ2-10, Δ116-406), (J-L) (Δ2-20, Δ116-406), (M-O) (Δ2-39, Δ116-406), (P-R) (Δ106-406) and (S-U) (Δ86-406). (V-X) Nucleo-cytosolic localization of GFP-fusion constructs lacking amino acids (Δ76-406) and (Y-AA) (Δ66-406). Experiments were performed three times with similar results. Bars = 20 µm.

3.2.4 Subcellular localization of selected other AtTLPs

In silico studies using the subcellular localization prediction program WoLF PSort (Horton et al., 2007) predicted chloroplast targeting for the N-terminal parts of seven out of ten tested AtTLPs (Table 3.1). AtTLP2 was predicted to be located in the cytosol, followed by chloroplast localization, while mitochondrial targeting was predicted for AtTLP7, which is in line with *in silico* data generated by Schwacke et al. (2007). Nevertheless, mitochondrial localization of AtTLP7 was experimentally excluded (Carrie et al., 2009). A sole nuclear localization was predicted for AtTLP8. In addition, an amino acid sequence alignment was used to look for a possible PIP_2 binding capacity in the Tubby domains of AtTLPs belonging to other systematic clades than A3 (Figure 3.2 A). This showed a conservation of AtTLP3 R187 / K189, corresponding to the presumably most important amino acids for PIP_2 binding in mammalian TLPs, in AtTLP2, -7 and -10. A serine and threonine occurred at that position in AtTLP8, making PIP_2 binding of this protein unlikely (Figure 3.10 A).

To examine the subcellular localization of these proteins, N- and C-terminal deletion variants of AtTLP2, -7, -8 and -10 similar to those for AtTLP3 were generated and used for biolistic transformation of *Arabidopsis* leaves (Figure 3.10 B). NT-GFP versions of AtTLP2, -7 and -10 were detected in the cytosol, nucleus and plastids (Figure 3.10 B-G; K-M), while GFP-CT constructs of these proteins were found at the PM (Figure 3.10 N-S; W-Y). There might though be differences in the localization dynamics between these AtTLP proteins. For example, CT-AtTLP2 did often show a significant fluorescence in the cytosol and nucleus, which was not observed for CT-TLP7 or CT-10. Further studies will be necessary to investigate the reason for this. N- and C-terminal versions of AtTLP8 showed a sole nucleo-cytosolic localization (Figure 3.10 H-J; T-V).

Table 3.1: Predicted subcellular localization of AtTLPs based on their N-terminal sequences using WoLF PSORT

Name	AGI	Amino acids	WoLF PSORT
AtTLP1	AT1G76900	1-120	Chloroplast (7.0), cytosol (3.0), nucleus (2.0), mitochondrion (1.0)
AtTLP2	AT2G18280	1-111	Cytosol (6.0), chloroplast (5.0), nucleus (2.0)
AtTLP3	AT2G47900	1-115	Chloroplast (12.0), cytosol (1.0)
AtTLP5	AT1G43640	1-118	Chloroplast (9.0), cytosol (3.0), plasma membrane (1.0)
AtTLP6	AT1G47270	1-132	Chloroplast (7.0), cytosol/nucleus (3.0), nucleus (2.5), cytosol (2.5), extracellular (1.0)
AtTLP7	AT1G53320	1-107	Mitochondrion (6.0), nucleus (3.5), cytosol/nucleus (2.5), chloroplast (2.0), extracellular (2.0)
AtTLP8	AT1G16070	1-149	Nucleus (13)
AtTLP9	AT3G06380	1-97	Chloroplast (7), mitochondrion (7)
AtTLP10	AT1G25280	1-122	Chloroplast (10), nucleus (4)
AtTLP11	AT5G18680	1-103	Chloroplast (7.5), chloroplast/mitochondrion (6.0), mitochondrion (3.5), cytosol (2.0)

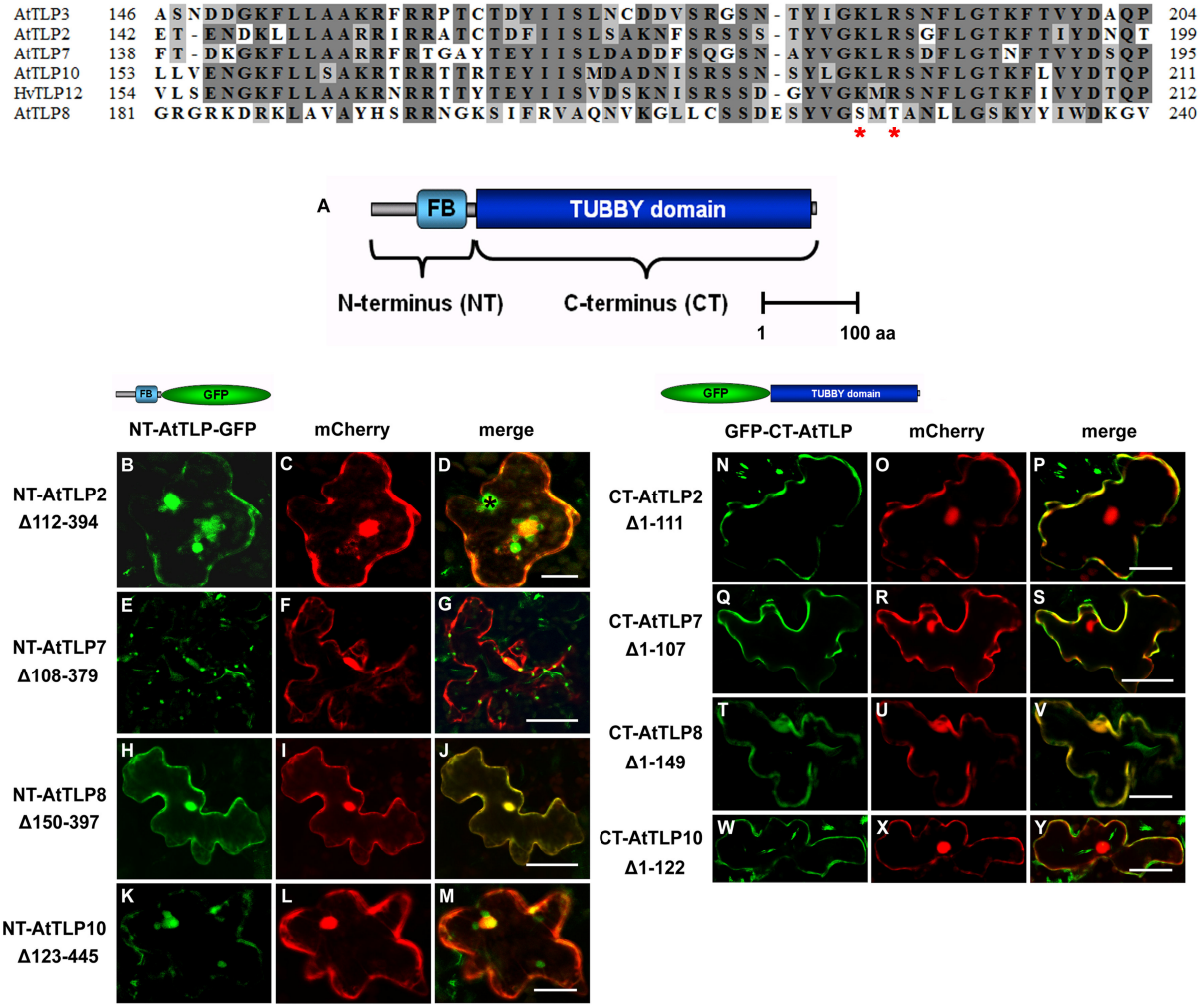

Figure 3.10: Subcellular localization of GFP-tagged truncated versions of selected AtTLPs. (Top panel) Amino acid sequence alignment for different AtTLPs and a barley TLP (HvTLP12). Shown is a part of the Tubby domain of the proteins. The two amino acids most essential for PIP_2 binding are marked with red asterisks (Santagata et al., 2001). Similar and identical amino acids are shaded light and dark grey, respectively. Numbers on the left and right site indicate position of the amino acids within the proteins. The alignment was created using ClustalW (Larkin et al., 2007). (A) Principal domain organization of AtTLPs except for AtTLP8, which does not carry an F-box domain. The F-box (FB) at the N-terminus (NT) and Tubby domain at the C-terminus (CT) are depicted in light and dark blue, respectively. Scale bar indicates the length of AtTLPs in amino acids (aa). (B-Y) Single *Arabidopsis* leaf epidermal cells were transformed using a particle inflow gun. Cells were co-transformed with either NT-AtTLP-GFP or GFP-CT-AtTLP fusion constructs under control of a CaMV35S promoter and the nucleo-cytosolic marker mCherry. Corresponding merged images are shown on the right to indicate subcellular localization of the proteins. AtTLP constructs used for transformation are drafted on the left of each image series. (B-D) Nucleo-cytosolic and plastidial localization of NT-AtTLP2-GFP(Δ112-394). (E-G) Nucleo-cytosolic and plastidial localization of NT-AtTLP7-GFP(Δ108-379). (H-J) Nucleo-cytosolic localization of NT-AtTLP8-GFP(Δ150-397). (K-M) Nucleo-cytosolic and plastidial localization of NT-AtTLP10-GFP(Δ123-445). (N-P) PM localization of GFP-CT-AtTLP2*(*Δ1-111). (Q-S) PM localization of GFP-CT-AtTLP7(Δ1-107). (T-V) Nucleo-cytosolic localization of GFP-CT-AtTLP8(Δ1-149). (W-Y) PM localization of GFP-CT-AtTLP10(Δ1-122). Pictures were taken at 16-26 h after particle bombardment with a CLSM. Experiments were performed three times with similar results. Bars = 20 µm.

3.2.5 PM localization of plant Tubby domains is not restricted to *Arabidopsis*

As PIP_2 is a common component of membranes, proteins binding to this phosphoinositide might show a conserved PM localization across different species. Santagata et al. (2001) demonstrated PM targeting of the Tubby domain of MmTUBBY in yeast, but using the same yeast two hybrid system, AtTLP2 was not directed to the PM in another study (Lai et al., 2012). To see if AtTLP3 attachment to the PM is at least conserved in plants, the GFP-CT-AtTLP3 construct was used to transform leaf epidermal cells of onion (Figure 3.11 A-C) and *Nicotiana benthamiana* (Figure 3.11 D-F) via a ballistic approach. In both plant species green fluorescence of the fusion protein was observed at the PM. Furthermore, the GFP-tagged Tubby domain of barley (Hv) TLP12, designated for its similarity to rice TLP12, was localized at the PM when transiently expressed in *Arabidopsis* leaf epidermal cells (Figure 3.11 G-I).

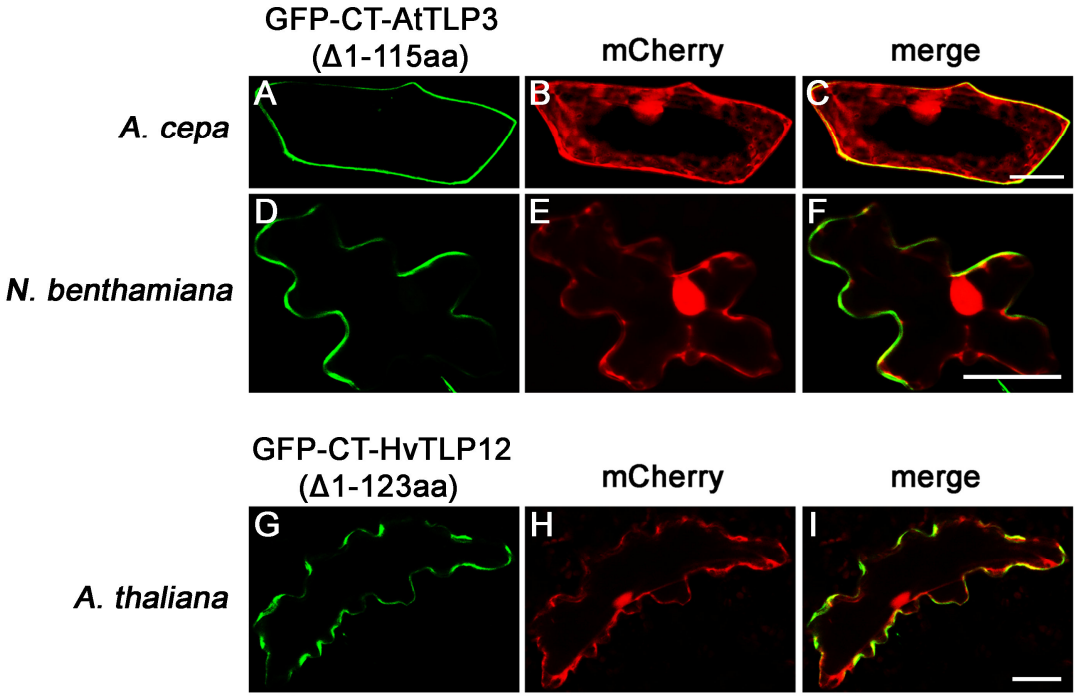

Figure 3.11: Conserved PM localization of Tubby domains in other plant species. (A, D, G) Single epidermal cells were transformed with a plant Tubby domain fused to N-terminal GFP and (B, E, H) nucleo-cytosolic marker mCherry, using a biolistic approach. (C, F, I) Merged images are shown on the right to indicate subcellular localization of proteins. Yellow colour indicates co-localization of red and green fluorescent proteins. (A-C) The GFP-tagged Tubby domain (GFP-CT-AtTLP3(Δ1-115aa) from AtTLP3 is localized at the PM in an epidermal cell of an *Allium cepa* scale leaf and (D-F) a leaf epidermal cell of *Nicotiana benthamiana*. (G-I) The GFP-tagged Tubby domain of barley TLP12 (GFP-CT-HvTLP12(Δ1-123aa) localizes to the PM when expressed in *Arabidopsis* leaf epidermal cells. Experiments were performed three times with similar results. Bars = 20 µm.

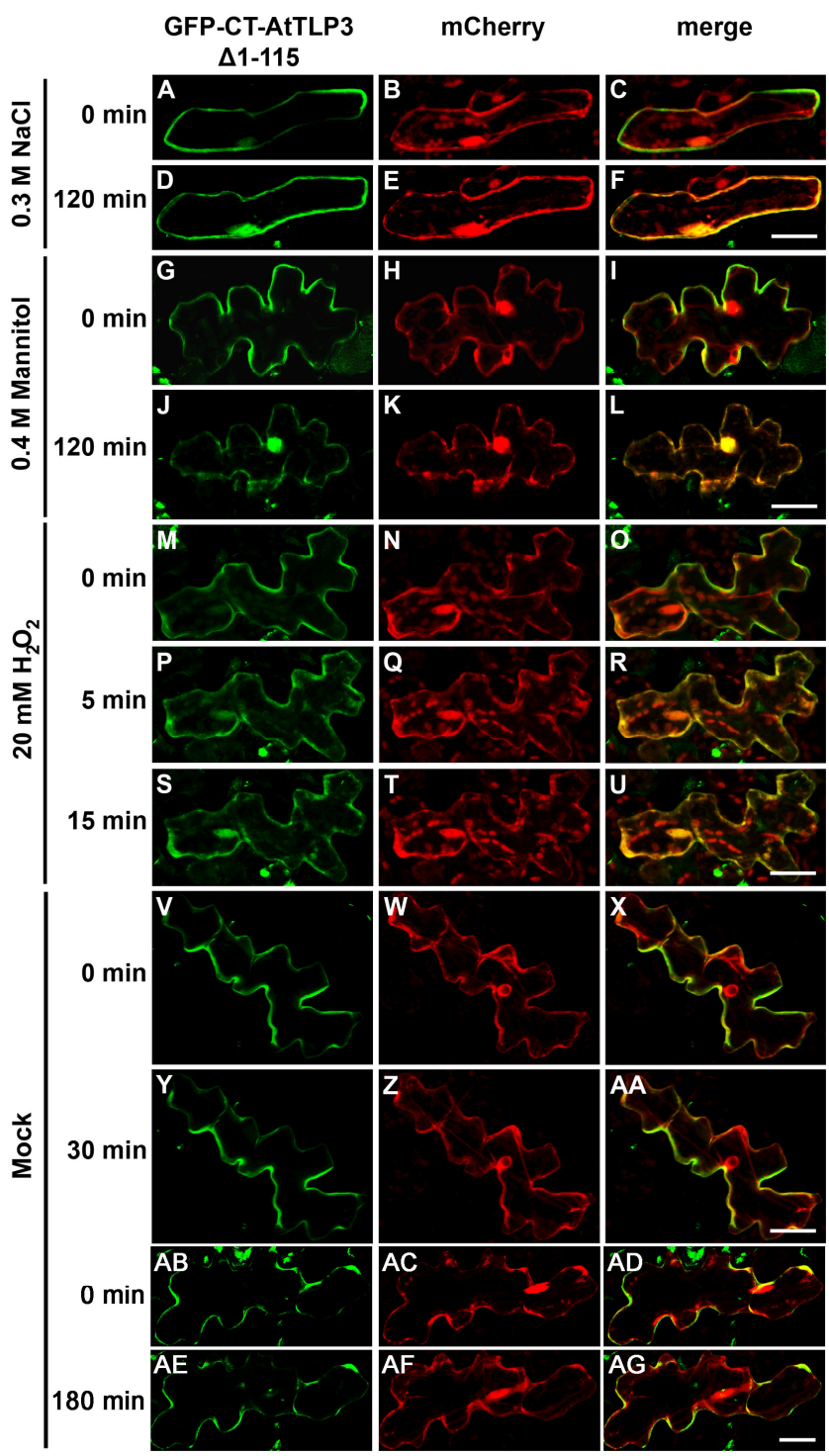

Figure 3.12: Salt, drought and oxidative stress elicited re-localization of the Tubby domain of AtTLP3. (A, D, G, J, M, P, S, V, Y, AB, AE) Particle bombardment was employed to transform *Arabidopsis* leaf epidermal cells with the Tubby domain of AtTLP3 (GFP-CT-AtTLP3(Δ1-115) and (B, E, H, K, N, Q, T, W, Z, AC, AF) the nucleo-cytosolic marker protein mCherry. (C, F, I, L, O, R, U, X, AA, AD, AG) Merged images are shown on the right. Yellow colour shows co-localization of green and red fluorescent proteins. Microscopy was performed 16-26 h after transformation using a CLSM. Leaves were placed on a glass slide in a bathing solution simulating apoplastic conditions (Mock) (Hafke et al., 2005). (A-U) For treatments, the bathing solution was supplemented to 0.3 M NaCl (A-F), 0.4 M mannitol (G-L) or 20 mM H_2O_2 (M-U). (A, G, M, V-AG) Under control conditions GFP-CT-AtTLP3 was located at the PM of transformed cells. (A-F) Within 2 h after addition of 0.3 M NaCl or (G-L) 0.4 M mannitol, green fluorescence could only be detected in the cytosol and nucleus and no longer at the PM, indicating re-localization of GFP-CT-AtTLP3. (M-U) Upon H_2O_2 treatment translocation of the protein to the nucleus and cytosol was observed within 5 min with a full re-localization within 15 min. (V-AA) No re-localization was observed in mock treated leaf cells after 30 min or (AB-AG) after 180 min. Experiments were performed three times with similar results. Pictures at 0 min were taken directly before respective treatment. Bars = 20 µm.

3.2.6 The Tubby domain of AtTLP3 is released from the PM in response to salt, drought and oxidative stress

The MmTUBBY protein is released from the PM in response to the activation of G-protein coupled receptors (Santagata et al., 2001), which is thought to activate TUBBY signaling (Santagata et al., 2001). Several conditions were therefore tested to investigate if the Tubby domain of AtTLP3 can also be released from the PM. Application of hormones (jasmonate, abscisic acid, salicylic acid, indole-3-acetic acid (auxin), brassinolide and gibberellic acid) to transformed *Arabidopsis* leaves did not result in a detectable change in localization (data not shown). In contrast, when exposing the leaves to salt stress (0.3 M NaCl) (Figure 3.12 A-F) and mannitol-induced drought stress (0.4 M mannitol) (Figure 3.12 G-L), within 2 h after application green fluorescence was no longer detected at the PM but in the cytosol and nucleus as seen by the yellow colour in the merged picture. This indicates to a re-localization of the protein. Mock treatments with bathing solution simulating apoplastic conditions (Hafke et al., 2005) did not cause translocation (Figure 3.12 AB-AG). An even faster dislodgment from the PM occurred though, when 20 mM H_2O_2 was added to the bathing solution. Here re-localization could be observed as soon as five minutes after treatment (Figure 3.12 M-R) and in most cases complete translocation happened within 15 min (Figure 3.12 S-U). Again PM detachment was not seen in mock treated cells (Figure 3.12 V-AA).

3.2.7 PM attachment of the AtTLP3 Tubby domain requires amino acids K187 and R189 and re-localization depends on phospholipase C activity

A change of amino acids R330 / K332 to alanine in MmTUBBY completely abolished its ability to bind phosphoinositides (Santagata et al., 2001). Following this, the corresponding amino acids R187 / K189 in the Tubby domain of AtTLP3 were mutated to alanine. No PM localization could be observed when this GFP-tagged construct was transiently expressed in *Arabidopsis* leaf cells. Instead overlay of green fluorescence with that of the red marker protein mCherry indicated a nucleo-cytosolic localization (Figure 3.13 D-F).

Proteins of the phospholipase C family are responsible for hydrolizing PIP_2 thereby generating inositol 1,4,5-trisphosphate and diacylglycerol (for reviews see e.g. Meijer and Munnik, 2003; Heilmann, 2009). In mammals, phospholipase-C β is required to release TUBBY from the PM (Santagata et al., 2001), as was demonstrated by pre-incubating cells with the phospholipase C inhibitor U73122, which blocked PM detachment of the protein. U73122 is also widely used as

PLC inhibitor in plants (e.g. Pingret et al., 1998; Dodd et al., 2007). Pre-incubation of *Arabidopsis* leaves transformed with GFP-CT-AtTLP3 with U73122 abolished re-localization of the protein in mannitol (Figure 3.13 M-R) and H_2O_2 (Figure 3.13 S-AA) treated leaves.

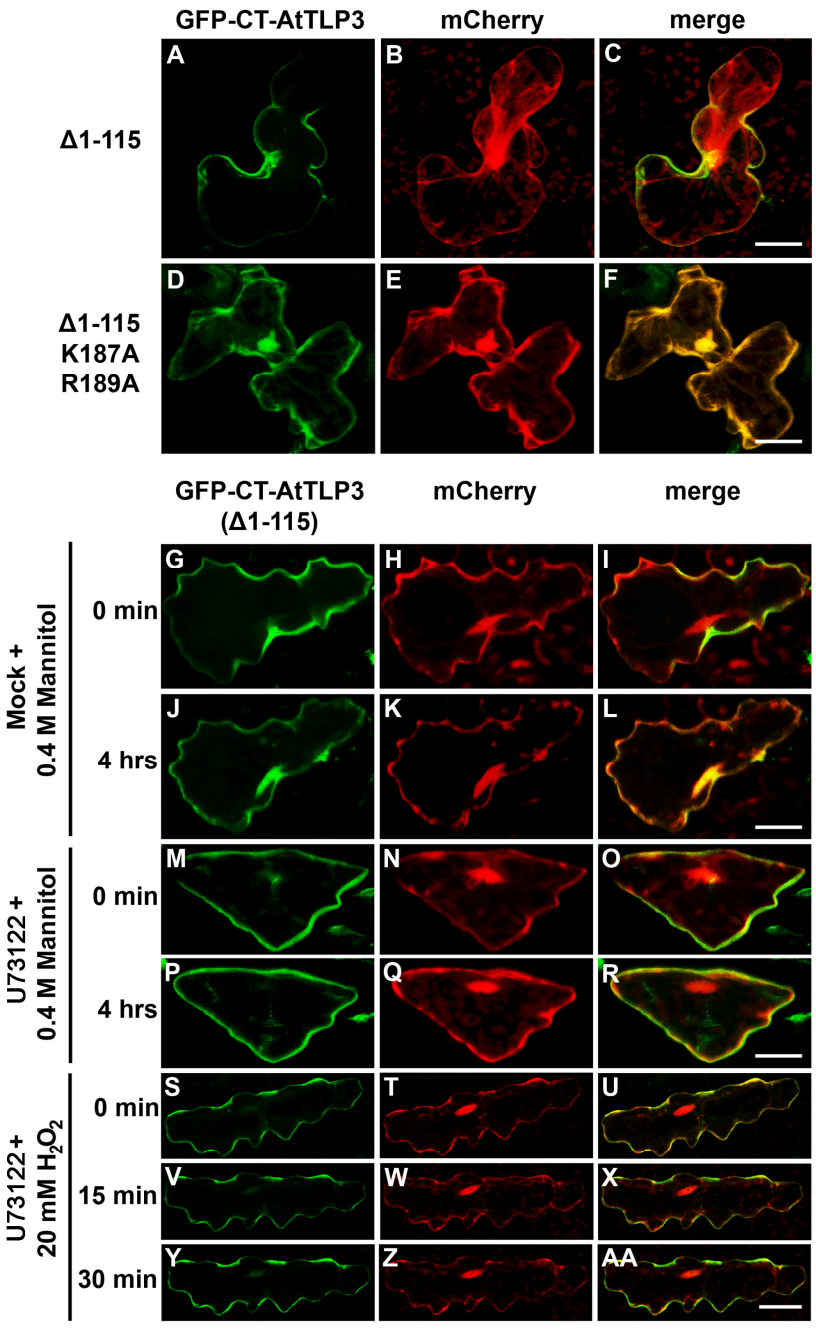

Figure 3.13: PM attachment of GFP-CT-AtTLP3 depends on amino acids K187 and R189 and phospholipase C activity is required for re-localization. (A, G, J, M, P, S, V, Y) Individual *Arabidopsis* leaf epidermal cells were co-transformed with either GFP-CT-AtTLP3(Δ1-115) or (D) GFP-CT-AtTLP3(Δ1-115) K187A, R189A and (B, E, H, K, N, Q, T, W, Z) nucleo-cytosolic marker mCherry. (C, F, I, L, O, R, U, X, AA) Yellow colour indicates co-localization of green and red fluorescent proteins in merged images. Deletion and changes of amino acids in constructs used for transformation are outlined on the left. (A-C) GFP-CT-AtTLP3 displayed PM localization in transformed cells. (D-F) A version of GFP-CT-AtTLP3 where amino acids K187 and R189 were changed to alanine showed nuclear and cytosolic localization. (G-L) Exposure of cells transformed with GFP-CT-AtTLP3(Δ1-115) and mCherry to 0.4 M mannitol for 4 h led to dislodgement of the TLP construct from the PM. (M-R) Translocation of GFP-CT-AtTLP3(Δ1-115) in response to mannitol and (S-AA) to 20 mM H_2O_2 was blocked by pretreatment with 10 µM of the phospholipase C inhibitor U73122 for 3 h. Experiments were performed three times with similar results. Pictures at 0 min were taken directly before respective treatment. Bars = 20 µm.

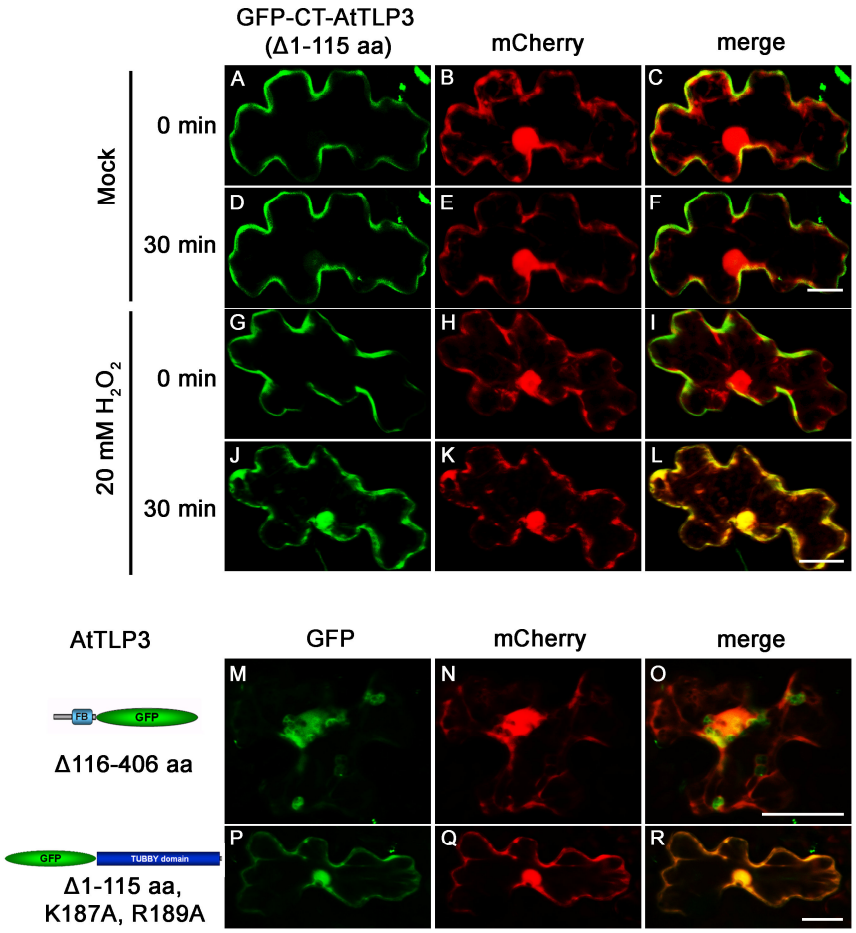

Figure 3.14: Conserved localization of AtTLP-GFP deletion variants in *N. benthamiana*. (A, D, G, J, M, P) *N. benthamiana* leaf epidermal cells were transiently co-transformed with different GFP-tagged truncated versions of AtTLP3 and (B, E, H, K, N, Q) the nuclear and cytosolic marker protein mCherry, using a biolistic method. (C, F, I, L, O, R) Merged images are shown on the right and yellow colour indicates co-localization of green and red fluorescent proteins. Constructs used for trans-formation are drafted on the left. (A-C) The Tubby domain of AtTLP3 (GFP-CT-AtTLP3Δ1-115aa) is located at the PM right after placing the leaf segment in water on a glass slide and (D-F) also 30 min later (mock). (G-I) PM localization of GFP-CT-AtTLP3 before treatment with H_2O_2. (J-L) Nucleo-cytosolic localization of GFP-CT-AtTLP3 30 min after application of 20 mM H_2O_2. (M-O) Nucleo-cytosolic and plastidial localization of the N-terminal part of AtTLP3 including the F-box domain. (P-R) Nuclear and cytosolic localization of GFP-CT-AtTLP3Δ1-115aa with amino acids K187 and R189 changed to alanine. Experiments were repeated three times with similar results. Bars = 20 µm.

3.2.8 Subcellular localization dynamics of truncated AtTLP3 versions are conserved in *Nicotiana benthamiana*

N. benthamiana is widely used in studies concerning subcellular localization of proteins (e.g. Dufresne et al., 2008; Link et al., 2011). However, heterologous expression of proteins c result in deviating behavior of proteins compared to their native system. Because of the conserved localization of GFP-CT-AtTLP3 in *N. benthamiana* (Fig. 3.11), the subcellular localization dynamics of truncated AtTLP3-GFP versions were investigated in this model organism as well (Figure 3.14). As in *Arabidopsis*, exposure of leaf segments to 20 mM H_2O_2 caused dislodgement of the Tubby domain of AtTLP3 from the PM and accumulation in the cytosol and nucleus (Figure 3.14 G-L). No detachment was observed when leaves were kept in water as control

(Figure 3.14 A-F). In addition, conserved localization as compared to *Arabidopsis* was observed for two other truncated protein versions tested. NT-AtTLP3-GFP was found in the cytosol, nucleus and plastids (Figure 3.14 M-O), while GFP-CT-AtTLP3 K187A / R189A accumulated in the cytosol and nucleus (Figure 3.14 P-R). Together, these results indicate that *N. benthamiana* might serve as a model to study subcellular localization of AtTLPs.

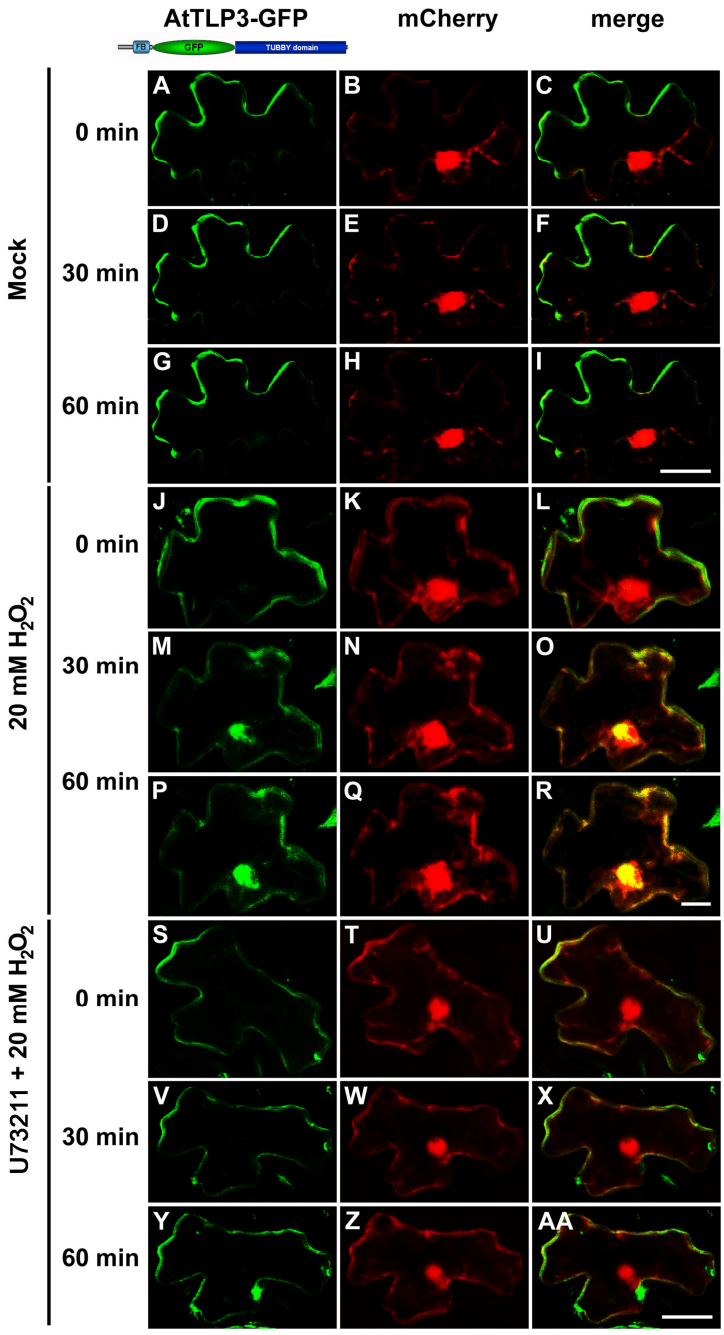

Figure 3.15: Plasma membrane localization and translocation of full-length (FL) AtTLP3-GFP in *N. benthamiana*. (A, D, G, J, M, P, S, V, Y) Co-transformation of single *N. benthamiana* leaf epidermal cells with AtTLP3-GFP and (B, E, H, K, N, Q, T, W, Z) the nuclear and cytosolic marker protein mCherry by particle bombardment-mediated gene transfer. (C, F, I, L, O, R, U, X, AA) Merged images are shown on the right and yellow colour shows co-localization of green and red fluorescent proteins. (A-C) Plasma membrane localization of FL-AtTLP3 protein with a GFP cloned in frame between the linker sequence and the Tubby domain. (A-I) Placement of leaf sections in water does not change PM localization of FL-AtTLP3-GFP. (J-L) PM localization of FL-AtTLP3-GFP before treatment with H_2O_2. (M-O) Nucleo-cytosolic localization of FL-AtTLP3-GFP after exposure to H_2O_2 for 30 min and (P-R) 60 min. (S-AA) PM dislodgement of FL-AtTLP3-GFP in response to 20 mM H_2O_2 is blocked by pretreatment with 10 µM of the phospholipase C inhibitor U73122 for 3 h. (S-U) PM localization of FL-AtTLP3-GFP after exposure to U73122 but before application of H_2O_2. (V-X) PM localization of FL-AtTLP3-GFP 30 min and (Y-AA) 60 min after treatment with H_2O_2. Experiments were performed three times with similar results. Bars = 20 µm.

3.2.9 Subcellular localization of full-length (FL) AtTLP3-GFP in *N. benthamiana*

Different to *Arabidopsis*, fluorescence was detected for a full-length version of AtTLP3 with a GFP inserted between the linker sequence and the Tubby domain, when transiently expressed in *N. benthamiana* leaf epidermal cells. As observed for the Tubby domain, the full-length version was localized at the PM and dislodgement occurred in response to 20 mM H_2O_2 (Figure 3.15 J-R). PM detachment was inhibited by pretreatment of leaf segments with phospholipase C inhibitor U73122 (Figure 3.15 S-AA), while re-localization still took place when exposing leaf segments to 20 mM H_2O_2 after keeping them in water for 3 h (not shown).

3.3 Histochemical analyses of AtTLP Promoter:*GUS* lines

Lai et al. (2004) studied the organ specific expression of all *TLP* genes in *Arabidopsis*. Roots, rosette leaves, lateral stems, flower clusters and green siliques were harvested from 42-day-old plants and expression was studied employing semi-quantitative RT-PCR. All *AtTLPs* except *AtTLP4*, *AtTLP5* and *AtTLP8* were found to be expressed ubiquitiously. While this gives an important first indication to the expression of *AtTLPs*, further studies might be required to better understand the functions of these proteins. Therefore, the promoter activity of two *AtTLP* genes using plants transformed with the *β-glucuronidase* (GUS) gene driven by the native promoter of either *AtTLP3* or *AtTLP5* was investigated. For this purpose, T2 transgenic plants were analyzed for GUS activity at several developmental stages (Figure 3.16 and Figure 3.17). Stained *Arabidopsis Col*-0 plants of the same age did not show any blue colour (not shown). For each *AtTLP* gene highly similar results were obtained from two independent transgenic lines.

In young seedlings, *AtTLP3*-related GUS staining was present in cotyledons and the vascular system of the hypocotyl and root (Figure 3.16). The expression pattern in the vasculature of roots did not change in nine- and 18-day-old plants, whereas GUS staining could additionally be detected in lateral root primordia and around the tip of some roots. Expression was also seen in rosette leaves of 4-6-week-old plants and flowers, whereas no GUS staining was detected in mature siliques.

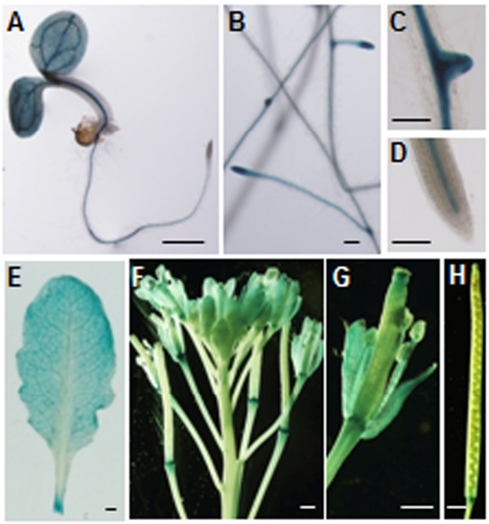

Figure 3.16: Histochemical GUS-analysis of AtTLP3 Promoter:*GUS* transgenic plants. (A-H) Organ and tissue specific expression of *AtTLP3* in AtTLP3$_{Prom}$:*GUS* plants. (A) 4-day-old seedling, (B-D) roots of 18 day-old plants, (E) rosette leaf, (F) anthotaxy, (G) single flower with some sepals and petals removed, (H) mature silique. Bars: 1 mm in A, E - H; 0.1 mm in B - D. Highly similar results were obtained from two independent transgenic lines.

GUS staining in young AtTLP5$_{Prom}$:*GUS* seedlings showed promoter activity in the root vasculature and cotyledons (Figure 3.17). In contrast to AtTLP3$_{Prom}$:*GUS* seedlings, promoter activity of *AtTLP5* was not restricted to the vasculature in hypocotyls. This expression pattern was conserved in nine- and 18-day-old plants. In addition, GUS staining was observed at the tip of some roots. Nevertheless, the stained area was more restricted than in AtTLP3$_{Prom}$:*GUS* plants, mainly localizing in the middle of the root tip. No staining was observed in lateral root primordia. Staining was also detected in rosette leaves of young (not shown) and 4-6-week-old plants. Here staining was often not uniform (Figure 7.1). *AtTLP5* promoter activity was also seen in flowers and, to some extent, in mature siliques (Figure 3.17).

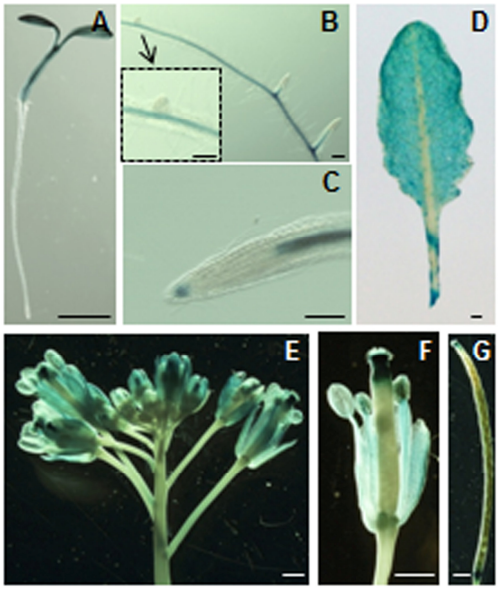

Figure 3.17: Histochemical GUS-analysis of AtTLP5 Promoter:*GUS* transgenic plants. Organ and tissue specific expression of *AtTLP5* in AtTLP5$_{Prom}$:*GUS* plants. (A) 4-day-old seedling, (B-C) roots of 18-day-old plants. The insert in (B) shows a higher magnification of a lateral root primordium. (D) rosette leaf, (E) anthotaxy, (F) single flower with some sepals and petals removed, (G) mature silique. Bars: 1 mm in A, D - G; 0.1 mm in B - C. Highly similar results were obtained from two independent transgenic lines.

3.4 Abiotic and oxidative stress assays

The results from the subcellular localization studies suggested a role of AtTLP3 in salt, drought and oxidative stress signaling. Therefore, effects caused by these stresses in selected *attlp* lines were assayed and expression of *AtTLP3* in response to H_2O_2 was analyzed.

3.4.1 Tolerance of *attlp* lines to abiotic stress

The impact of drought (100 mM mannitol) and salt (10, 100 mM NaCl) stress on root elongation in wild-type and *attlp3-1* plants was investigated by transferring plants of the same size to petri dishes containing solid medium supplemented with indicated concentrations of mannitol and NaCl. Both treatments caused a reduction in root growth, which was similar in wild-type and mutant plants (Figure 3.18 A and B). To test for effects of oxidative stress, leaf discs from wild-type, *attlp3-1* and *attlp3-2* plants were exposed to different concentrations of H_2O_2. Conductivity of the surrounding solution was recorded to determine cell-death elicited ion leakage of plant cells. No differences were observed in the reaction of wild-type and mutant plants (Figure 3.18 C).

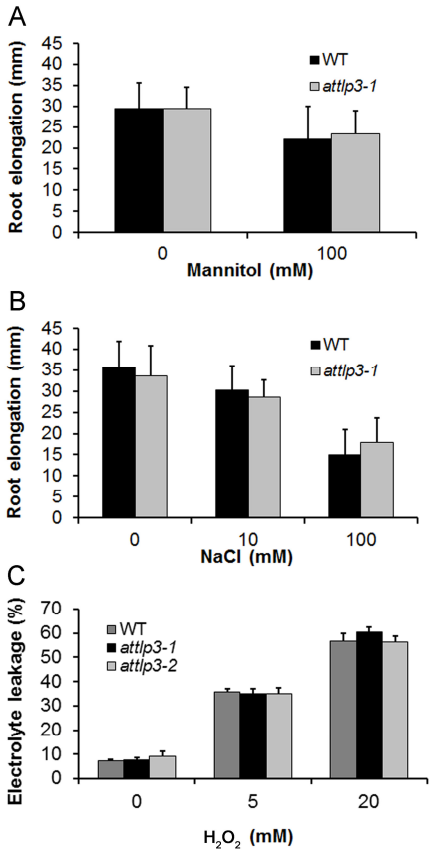

Figure 3.18: Impact of salt, drought and oxidative stress on *attlp3* lines. (A, B) Root growth in wild-type (*Col*-0) and *attlp3-1* seedlings under non-stress, drought stress (100 mM mannitol) and salt stress (10 and 100 mM NaCl) conditions. After aseptic growth for 8 days on minimal medium in vertically placed squared petri dishes, plants of similar size were transferred to new plates containing indicated concentrations of mannitol and NaCl. Root elongation was determined 6 days after relocation. Data are means (± SD) from at least 40 plants measured in two independent experiments. (C) Effect of oxidative stress (H_2O_2) on viability of wild-type (*Col*-0) and *attlp3* cells. Leaf discs from 4-5-week-old soil grown plants were exposed to different concentrations of H_2O_2 in water. Conductivity of the solutions was determined 48 hours after treatment (hat) before and after boiling the samples to determine relative electrolyte leakage. Values are means (± SD) from three technical replicates each comprising 15 leaf discs per line and treatment. The experiment was performed twice with similar results.

AtTLPs constitute a family of 11 genes in *Arabidopsis* (Lai et al., 2004). Experiments so far suggested that at least several, if not all, *AtTLPs* might participate in similar signaling pathways as reaction to certain environmental stresses. Therefore, while altered phenotypes were obtained in some assays using single knockout and knockdown lines (Figure 3.3 and Lai et *al.*, 2004) others might be masked by functional redundancy. Hence it could be necessary to investigate *Arabidopsis* lines with defects in more than one *TLP* gene. Three pairs of paralogous genes have been shown to exist within the *TLP* family in *Arabidopsis* (*AtTLP1* and *AtTLP5, AtTLP2* and *AtTLP6*, *AtTLP9* and *AtTLP11*), marking the most related genes (Yang et al., 2008). For no line with reduced transcript levels for *AtTLP6* was available, double knockout lines *attlp1/5* and *attlp9/11* were generated by crossing plants of respective single mutant lines. T3 double mutant plants were exposed to H_2O_2 together with respective azygous T3 plants as wild-type and effects on root growth were determined. Wild-type and double mutants showed similar reduction in root growth in response to the oxidative stress treatment (Figure 3.19).

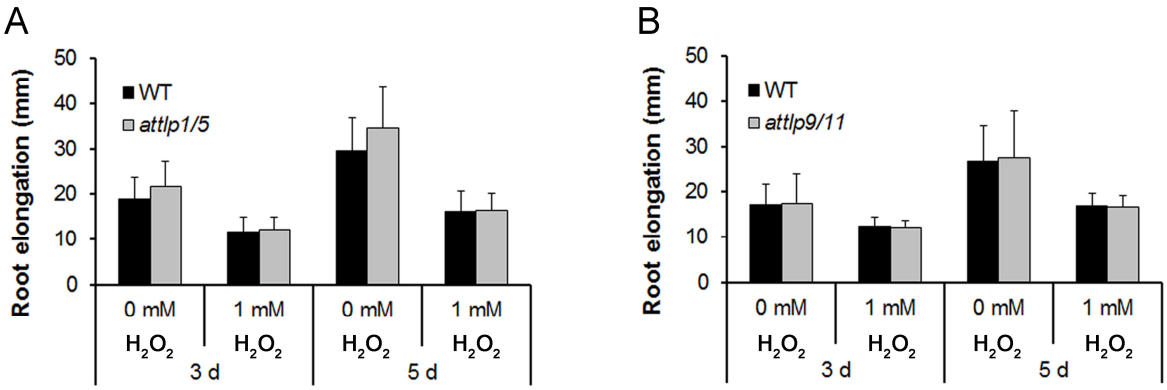

Figure 3.19: Effect of oxidative stress on root growth of *attlp* double mutants. Azygous T3 plants (WT) and *attlp* double mutant plants *attlp1/5* (A) and *attlp9/11* (B) were aseptically grown in vertically placed squared petri dishes for eight days on minimal medium. Thereafter, plants of similar size were relocated to new plates containing indicated concentrations of H_2O_2. Root elongation was recorded at 3 days after the transfer and onwards. Data are means (± SD) of at least 15 plants from one biological experiment. The experiment was performed twice with similar results.

3.4.2 Differential transcription of *AtTLP3* in response to H_2O_2

To study the expression of *AtTLP3* in response to oxidative stress, *Col*-0 plants were either grown under normal conditions or exposed to 1 or 10 mM H_2O_2. Total RNA was extracted from whole plants at 0, 1, 5 and 24 hours after treatment (hat) and generated cDNA was used in qRT-PCR. Interestingly, expression of *AtTLP3* was down regulated at 1 hat in response to 10 mM H_2O_2, but when plants were treated with 1 mM H_2O_2 down regulation occurred at 24 hat indicating some dose dependent effect (Figure 3.20).

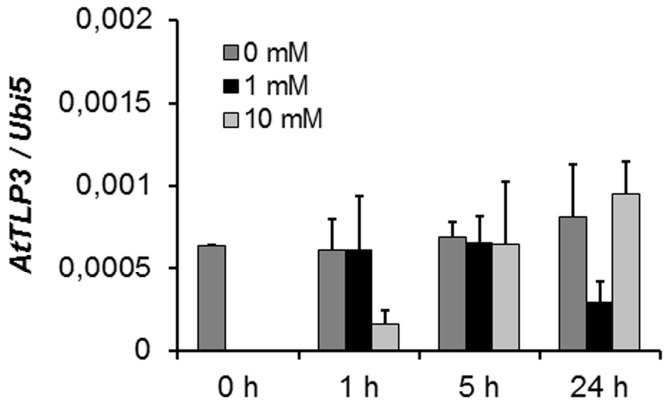

Figure 3.20: *AtTLP3* is differentially regulated in response to oxidative stress. Expression analysis of *AtTLP3* by qRT-PCR after application of H_2O_2. 8-day-old aseptically grown *Arabidopsis Col*-0 plants were transferred to liquid minimal medium. After further three days H_2O_2 was added to indicated concentrations. At 0, 1, 5 and 24 hat whole plants were harvested. Total RNA was extracted from 30-40 plants per line, treatment and time point and used for cDNA generation. qRT-PCR was performed with *AtTLP3* gene specific primers. Expression values were calculated by the $2^{-\Delta Ct}$ method by relating Ct values of candidate genes to those of the housekeeping gene *AtUBI5*. Data are means (± SD) of three independent experiments.

Together, no altered phenotypes in response to mannitol-induced drought stress, salt stress and oxidative stress could be observed in several single and two double mutant lines during the experiments described in this chapter. Nevertheless, expression of *AtTLP3* was differentially regulated in response to oxidative stress.

4. Discussion

Tubby-like proteins (TLPs) constitute a conserved gene family with members present in all eukaryotic kingdoms except most fungi (e.g. Riechmann et al., 2000; Liu, 2008; Lai et al., 2012). In mammals, they exert pivotal physiological functions as demonstrated by severe disease syndromes caused by mutations in some of the proteins (for reviews see Ikeda et al., 2002; Carroll et al., 2004; Lai et al., 2012; Mukhopadhyay and Jackson, 2011). No such serious effects have been observed so far for mutant plants lacking single *TLP* genes (Lai et al., 2004). This might at least in part be explained by a greater functional redundancy in plants compared to mammalian organisms originating from an expansion of the gene family (Lai et al., 2004; Liu, 2008; Yang et al., 2008; Lai et al., 2012). Nevertheless, first studies over the last eight years reported possible functions of plant TLPs in e.g. salt and drought stress responses and reaction to phytopathogenic bacteria (Lai et al., 2004; Ko et al., 2006; Cai et al., 2008; Kou et al., 2009; Wardhan et al., 2012). As all three of these topics are major concerns in agriculture, detailed knowledge about this relatively unknown gene family should be generated to estimate and possibly exploit their benefits for development of crop plants with improved stress tolerance. A recent study about the effect of overexpression of a *TLP* from *Cicer arietanum* (Ca) in tobacco yielded very promising first results in that respect (Wardhan et al., 2012). In the present study *Arabidopsis thaliana* (At) *TLP* T-DNA insertion lines were employed to search for new mutant phenotypes caused by the lack of these proteins to gain further insight into their function. In addition, a detailed research on the subcellular localization of AtTLP proteins was performed by confocal laser scanning microscopy (CLSM) on GFP-tagged fusion proteins. AtTLP3 was chosen as representative member of the family and subjected to more detailed studies. For example, the effect of several abiotic stresses and hormones on the position of AtTLP3 within the cell was closely examined.

4.1 Investigating the role of AtTLPs in biotic interactions

4.1.1 AtTLPs as possible compatibility factors during early colonization of *Arabidopsis* roots by the mutualistic fungus *Piriformospora indica*

Working with *P. indica* and seeing that transcription of a *TLP* was induced in barley roots after inoculation with the fungus (Schäfer et al., 2009), it was investigated if these proteins might play a role in the interaction of *Arabidopsis* roots with the mutualist. *P. indica* colonization had been shown to be similar in *Arabidopsis* and barley before (Deshmukh et al., 2006; Schäfer et al., 2009; Jacobs et al., 2011; Zuccaro et al., 2011) and the dicotyledonous model plant was chosen over the crop plant because of its greater availability of genetic tools. In contrast to barley, the results obtained for *Arabidopsis* did not show an enhanced transcription of tested *AtTLP* genes in response to the fungus at one, three and seven day/s after inoculation (dai) (Figure 3.2). Nevertheless, lower amounts of fungal DNA were detected in *attlp* lines as compared to wild-type plants, demonstrating a reduced colonization of mutant plants (Figure 3.3 A). In most lines this was observed at three dai, whereas at seven dai most mutants contained wild-type levels of fungal DNA. This might be indicative for enhanced fungal growth during the cell-death dependent colonization phase and increased colonization of mutant plants at later time points. A similar pattern of colonization has been observed in other mutants before (Jacobs et al., 2011). For example, an *Arabidopsis* DELLA-quintuple mutant displayed reduced colonization by *P. indica* at three dai, but was better colonized by the fungus as wild-type plants at seven dai (Jacobs et al., 2011). The five DELLA proteins in *Arabidopsis* act as repressors in gibberellic acid (GA) signaling. GA causes their degradation, which alleviates repression and leads to expression of GA responsive genes (reviewed e.g. in Sun, 2008; Schwechheimer and Willige, 2009). It was suggested that reduced colonization by *P. indica* is related to increased SA signaling in the quintuple-mutant as was seen by enhanced expression of the salicylic acid (SA) marker gene *CBP60g* in mutant plants inoculated with the mutualist (Jacobs et al. 2011). This is in line with a report showing that GA modulates the SA / ethylene (ET) / jasmonic acid (JA) network to influence immune responses (Navarro et al., 2008). On the other side, the increased colonization during cell-death dependent colonization was ascribed to a cell-death inhibiting function of DELLA proteins (Achard et al., 2008; Jacobs et al., 2011). Therefore, to obtain further information on *P. indica* colonization of *tlp* mutants, a more detailed analysis was performed using line *attlp5-1*. Here it could clearly be demonstrated that *P. indica* displayed a delayed colonization in the mutant, with significantly reduced amounts of fungal DNA only observed at

three dai whereas wild-type levels were reached at five dai (Figure 3.3 B). No further change in colonization was detected at later time points. Thus, fungal growth in *attlp* mutant lines is only hampered at early stages in the interaction, but not at later phases where the fungus relies on plant cell-death to colonize the plant properly (Deshmukh et al., 2006; Jacobs et al., 2011; Qiang et al., 2012b).

As TLPs from rice have been implicated to function in response to biotic stress (Cai et al., 2008; Kou et al., 2009), an explanation for the observed delayed colonization in *attlp* lines would be an enhanced immune response in these lines. MAMP-triggered immunity (MTI) was reported to be involved in the regulation of *P. indica* colonization. Pretreatment of plants with the bacterial MAMP flg22 led to a reduced colonization, while mutants defective in SA signaling displayed higher amounts of fungal DNA than wild-type plants (Jacobs et al., 2011). Furthermore, *P. indica* was shown to suppress a wide array of immune responses in its hosts. For example MAMP-induced root oxidative burst, defense gene expression (e.g. *WRKY29*, *OXI1*, *MYB51*, *CBP60g*) and seedling growth inhibition was not observed in *P. indica* colonized wild-type *Arabidopsis* plants (Jacobs et al., 2011). Thus, reduced colonization of *attlp* lines might also be caused by failed immune suppression by the fungus. This phenomenon was observed in the *Arabidopsis pub22/23/24* triple mutant (Jacobs et al., 2011). PUB22, PUB23 and PUB24 are three closely related *U-box* ubiquitin E3 ligases (Azevedo et al., 2001) and have been shown to act as negative regulators of MTI. Although immune responses were not activated under non-stress conditions, the triple mutant showed increased immune reactions when challenged with different MAMPs and displayed higher resistance to pathogens (Trujillo et al., 2008). Reduced colonization was also found for the JA signaling mutant *jin1-1* and in *jar1-1* compromised in JA signaling and biosynthesis, respectively. As in wild-type plants the expression of the JA marker gene *VSP2* was induced by *P. indica*, it was suggested that the fungus uses JA signaling to suppress SA mediated responses (Jacobs et al., 2011). While flg22 still caused growth inhibition in both mutants when inoculated with *P. indica*, the fungus was not able to inhibit the root oxidative burst and elicited a stronger induction of *CBP60g* and *MYB51* in *jin1-1* than in wild-type plants (Jacobs et al., 2011). *MYB51* encodes a protein involved in the biosynthesis of anti-microbial glucosinolates (Clay et al., 2009). To test for these hypotheses, seedlings of *attlp* lines were exposed to bacterial MAMPs but no significant differences in fresh weight were found between wild-type and *attlp* mutant plants in *P. indica* colonized or non-colonized plants (Figure 3.4). To test for further immune reactions, transcription of several immune marker genes was investigated in *P. indica* colonized

or mock treated wild-type and *attlp3-1* plants (Figure 3.5). To cover different immune pathways, marker genes for MTI (*WRKY29*; Asai et al., 2002), oxidative stress (*OXI1*; Rentel et al., 2004; Torres et al., 2005), SA (*CBP60g*; Wang et al., 2009) and JA induced expression (*VSP2*; Koornneef and Pieterse, 2008) were assayed by qRT-PCR. Furthermore, expression of *MYB51* was investigated. As described before (Jacobs et al., 2011), *P. indica* induced transcription of *CBP60g* and *MYB51* at seven dai, but no higher expression levels were detected in mutant plants when compared to wild-type for any tested gene.

Plant responses to biotic and abiotic stresses have been shown to involve the expression of different but overlapping sets of genes and there is evidence for ample crosstalk between the different stress signaling pathways (reviewed e.g. in Fujita et al., 2006; Pieterse et al., 2009). A role of special interest comes to reactive oxygen species (ROS) like hydrogen peroxide (H_2O_2), which seem to be a crosspoint of interactions between the various pathways, though the exact mode of action of these small molecules in these processes remains elusive (Fujita et al., 2006). For example, a mutation in the *Arabidopsis* transcription factor *Botrytis susceptible 1* (*BOS1*) led to decreased tolerance to high salt conditions, oxidative stress and increased susceptibility to the necrotrophic fungal pathogen *Botrytis cinerea* (Mengiste et al., 2003). As TLPs have been implicated to act in salt and drought stress responses the possibility of altered abiotic stress signaling, potentially influencing colonization in *attlp* mutants by *P. indica* was assessed. Therefore, transcription of selected key marker genes for abiotic stresses was assayed in *P. indica* inoculated and mock treated *attlp3-1* and wild-type plants (Figure 3.5). *DREB2A* and *At5g10695*, encoding for a transcription factor and a HSP70 protein, respectively, were previously reported to be induced by cold, drought, heat and oxidative stress (Quan et al., 2008). In addition, the transcription factor ZAT12 is one of a few proteins whose expression responds similarly to a great variety of environmental stresses, including high salt, ROS and fungal infection (Davletova et al., 2005; Quan et al., 2008). Consistently, it was moderately induced by *P. indica* in this study. Again, no altered expression of stress marker genes was detected in mutants compared to wild-type plants. In summary, no hints were found for increased immune or altered abiotic stress reactions in tested *attlp* mutant plants concerning *P. indica* colonization. Therefore, AtTLPs might constitute compatibility factors required by *P. indica* for normal colonization of roots at an early stage of the interaction.

4.1.2 AtTLPs do not generally affect plant resistance to pathogens

Pathogenic microorganisms can be coarsely divided into two groups depending on their lifestyles (Glazebrook, 2005). Biotrophic organisms like the oomycete *Hyaloperonospora arabidopsidis* and fungal mildews like *Blumeria graminis* do not kill host cells but gain their nutrients from living tissue. Effector triggered immunity (ETI) was shown to be an important defense mechanism against this type of pathogens since the hypersensitive response (HR), a type of immunity-related programmed cell-death, deprives the microorganisms of their nutrients. Immune responses are mediated by SA, JA and ET while we just begin to understand the participation of other hormones (reviewed e.g. in Glazebrook, 2005; Eichmann and Hückelhoven, 2007; Coates and Beynon, 2010; Pieterse et al., 2012). As SA and ET/JA signaling have been shown to suppress each other, induction of the latter is thought to disturb resistance to biotrophs (Glazebrook, 2005; Pieterse et al., 2009). In contrast, necrotrophic pathogens like the fungi *Botrytis cinerea* and *Sclerotinia sclerotiorum* actively kill host cells to feed from the dead material (Bolton et al., 2006; Williamson et al., 2007). ETI is predicted to play, if any, only a minor role. Instead, resistance is mediated by ET and JA and to some extend also by SA. In summary, the view that SA is responsible for resistance against biotrophs, while plants protect themselves against necrotrophs via ET/JA signaling still holds true, although it is a bit to simplified as interactions between plants and pathogens have been shown to be more complex (e.g. Glazebrook, 2005; Pieterse et al., 2009). In addition, many pathogens like the soil-borne fungus *Fusarium oxysporum* do not strictly fit into one of the categories often infecting their hosts as biotrophic organisms for some time followed by a necrotrophic phase. These microorganisms are therefore designated as hemi-biotrophs (Glazebrook, 2005; Thatcher et al., 2009; Horbach et al., 2011).

To explore, whether AtTLPs generally influence the interaction with microorganisms, mutant plants were challenged with pathogens featuring different lifestyles (Figure 3.6). No altered resistance was detected in *attlp* lines to the necrotrophic and biotrophic fungal pathogens *Botrytis cinerea* (Figure 3.6 A) and *Erysiphe cruciferarum* (Figure 3.6 C), respectively. *B. cinerea* can infect a broad spectrum of over 200 mainly dicotyledoneous but also some monocotylenodeous plant species (Williamson et al., 2007). Strain B05.10 employed in this study is able to rapidly degrade *Arabidopsis* tissue. In contrast to this, the ecto-parasitic powdery mildew *E. cruciferarum* has a more narrow host range mainly infecting cruciferous plants (Adam et al., 1999). Powdery mildews grow mainly on the plant surface only infecting epidermal cells from

which they acquire nutrients (e.g. Eichmann and Hückelhoven, 2008). In addition, as the interaction with both of these pathogens was restricted to leaves but *P. indica* only colonizes plant roots, *Phytophothora parasitica* was included in the studies as well to explore the possibility of organ specific resistance (Figure 3.6 B). This soil-borne hemi-biotrophic oomycete has a wide host range, infecting roots of plants from about 60 different plant species including *Arabidopsis* (Attard et al., 2008). Detected colonization and disease symptoms were similar on wild-type and mutant plants infected with *B. cinerea, E. cruciferarum* and *P. parasitica*. These results indicate that AtTLPs might not be involved in resistance to these fungal and oomycete pathogens in general. This is consistent to the above discussed results that *attlp* lines showed no signs of altered immune responses and a further hint that AtTLPs might specifically be needed in the mutualistic *Arabidopsis* - *P. indica* interaction.

4.2 Structural features of AtTLP3 and their implications for protein functions

The resolution of the crystallographic structure of the mouse (Mm) TUBBY protein (Boggon et al., 1999; Santagata et al., 2001) brought new insights into the role of the protein in the cell. The C-terminal hydrophobic α-helix was precluded to be a transmembrane domain as had been suggested before (Nishina et al., 1998; Boggon et al., 1999). A DNA as well as a poly-phosphoinositide (PPI) binding site was identified (Boggon et al., 1999; Santagata et al., 2001). And overall, especially the structure of the C-terminal Tubby domain got the trademark of a new protein family, which was shown to exist in a multitude of eukaryotic organisms (Boggon et al., 1999; Liu, 2008; Lai et al., 2012; Mukhopadhyay and Jackson, 2011). Thus, like in many other cases, knowledge of the protein structure greatly enhanced research in this field.

So far, comparisons of Tubby domains from the plant and mammalian kingdoms were restricted to amino acid sequence alignments (e.g. Santagata et al., 2001; Lai et al., 2004; Liu, 2008). It was especially noted, that there is a divergence between plant and animal TLPs concerning amino acids N310 / R363 (MmTUBBY) which participate in phosphatidylinositol 4,5-bisphophate (PIP_2) binding (Santagata et al., 2001). It was proposed that plant TLPs might not be able to bind the PPI (Lai et al., 2012). In contrast, the 3D homology model of AtTLP3 generated in this study showed a remarkable structural conservation of the Tubby domain and also of the PIP_2 binding cavity when compared to mouse and human (Hs) TUBBY (Figure 3.7). As expected from sequence alignments, MmTUBBY amino acids K330 / R332 were conserved in AtTLP3 (K187 / R189). These amino acids were demonstrated to be most essential for PIP_2 binding where K330

is thought to coordinate between the 4-, and 5-position phosphates of the inositol ring and R332 to stabilize the 4-position phosphate (Santagata et al., 2001). Instead of R363 in MmTUBBY, AtTLP3 carries an asparagine at that position (N233), though the 3D model does not suggest an effect in the interaction with IBS and PIP_2 binding sites. Whilst Santagata et al. (2001) showed abrogation of plasma membrane (PM) localization in a mutant MmTUBBY protein where R363 was replaced by an alanine, they predicted that this amino acid is responsible for binding to 3'-phosphorylated PPIs. MmTUBBY only bound PPIs phosphorylated at two adjacent positions of the inositol ring (Santagata et al., 2001). Thus, R363 should be important for binding of phosphatidylinositol 3,4-bisphophate and phosphatidylinositol 3,4,5-trisphosphate. Both PPIs do not seem to occur in plants (Munnik and Vermeer, 2010). It is therefore tempting to speculate that amino acids corresponding to MmTUBBY R363 are not involved in PPI attachment in plants and the released evolutionary pressure enabled its mutation.

As noted before, TLPs have been suggested to act as regulators of transcription and several possess the ability to bind to double-stranded DNA (Boggon et al., 1999; Santagata et al., 2001; Cai et al., 2008; Gaudinier et al., 2011; Wardhan et al., 2012). But until now no gene targets have been identified and only the N-terminal domains of MmTUBBY and TLP1 were able to induce transcription of a marker gene when fused to the DNA binding domain of GAL4 (Boggon et al., 1999), while this was not the case for AtTLP9 (Lai et al., 2004) and CaTLP1 (Wardhan et al., 2012). Therefore, wether TLPs actually function as transcription factors has yet to be demonstrated. DNA attachment was suggested to take place in a positively charged groove with appropriate dimensions to bind the macromolecule running along the β-barrel of the Tubby domain (Boggon et al., 1999; Santagata et al., 2001). Interestingly, in the AtTLP3 structural model this groove is much smaller than in Mm and HsTUBBY and lacks the strong positive charge (Figure 3.7 F-G). It seems therefore unlikely that AtTLP3 is able to bind double-stranded DNA.

In addition to the Tubby domain, AtTLP3, like many other plant TLPs and in contrast to mammalian ones, features an F-box domain in its N-terminal region (Gagne et al., 2002; Lai et al., 2004; Yang et al., 2008; Lai et al., 2012). The F-box is a degenerated protein motif of about 40-60 amino acids at the N-terminus of proteins, which can be found across all kingdoms (e.g. Kipreos and Pagano, 2000; Gagne et al., 2002). With about 700 members in *Arabidopsis* (Gagne et al., 2002) and rice (Jain et al., 2007) this protein superfamily is greatly expanded in plants compared to other organisms. The genomes of *Saccharomyces cerevisiae*, *Caenorhabditis*

elegans, *Drosophila*, and humans only contain 11, 326, 22 and 38 F-box proteins (FBPs), respectively (Kipreos and Pagano, 2000). The enlargement suggests a fundamental role for FBPs in plant development and physiology. Indeed FBPs have been shown to participate in different processes in plants. In *Arabidopsis*, they act for example as receptors for the plant hormones auxin (TIR1) (Dharmasiri et al., 2005) and JA (COI1) (Yan et al., 2009) and are involved in the regulation of responses to GA (Gomi et al., 2004; Ueguchi-Tanaka et al., 2005) and ET (Guo and Ecker, 2003; Potuschak et al., 2003; Gagne et al., 2004). The best studied and probably most common way by which these proteins exert their functions, is as part of SCF E3 ligases in ubiquitin mediated degradation of proteins. Within the complex, the FBP is bound to a SKP1-like protein via its F-box and to the substrate protein with a second C-terminal protein-protein interaction domain. By this FBPs confer substrate specificity to the SCF complex (reviews e.g. Lechner et al., 2006; Spartz and Gray, 2008; Yee and Goring, 2009). Despite the focus on this process, recent research revealed roles of FBPs independently from SCF complexes (Kipreos and Pagano, 2000; Hermand, 2006). For instance, the mammalian FBP MoKA interacts with the transcription factor KLF7 via its F-box, which leads to increased transcriptional activation. It was demonstrated that this did not involve degradation of KLF7 (Smaldone et al., 2004; Smaldone and Ramirez, 2006). In addition, there are examples where FBPs interact with SKP1 without being part of an SCF complex (Hermand, 2006). The yeast FBP RCY1 interacts with SKP1 in recycling of the SNARE protein SNC1 back to the PM. This action does not involve formation of an SCF complex (Wiederkehr et al., 2000; Galan et al., 2001). AtTLP9 and 10 have been shown to interact with *Arabidopsis* SKP-1 like protein 1 (ASK1) in yeast-two-hybrid assays (Risseeuw et al., 2003; Lai et al., 2004) and were suggested to possibly be part of SCF complexes and to be involved in protein degradation (Lai et al., 2004). Nevertheless, no such complex containing a plant TLP has been identified till now nor was a role in protein degradation demonstrated. In addition, unlike most other FBPs shown to be part of an SCF complex, TLPs lack a C-terminal protein-protein interaction domain, instead featuring the Tubby domain. It might therefore be that plant TLPs act independently of SCF complexes in ways not yet identified.

4.3 Subcellular localization of selected plant TLPs

Eukaryotic cells are subdivided into several different compartments, each possessing its own unique equipment of proteins and tasks (Lunn, 2007). The function of a protein is therefore closely linked to its subcellular localization. The discovery of the *Aequorea victoria* green fluorescent protein (GFP) and its adaptation for scientific purposes was a hallmark in cell biology. Since then a great variety of GFP derivatives and other fluorescent proteins (FPs) have been developed equipping researchers with a host of tools for different applications. FPs are used for example to study protein-protein interactions, expression profiles, developmental processes, dynamics of small molecules like Ca^{2+} and of course the subcellular localization of proteins. (reviews see e.g. Panstruga, 2004; Mathur, 2007; Mano et al., 2009; Okumoto et al., 2012). For this purpose the FP is fused in frame at either the C- or the N-terminus or inserted in the middle of a protein of interest and is either stably or transiently expressed in target tissues or cells. In addition, fusing only a part of the protein, e.g. specific domains, or versions with single amino acid exchanges to a FP can yield insights into function of specific protein parts (e.g. Santagata et al., 2001; Link et al., 2011). One major advantage of this approach is that cells can be observed *in vivo* under fluorescence microscopes under non- or only slightly invasive conditions, avoiding fixation or staining artifacts. The cytosol and nucleus can be considered as default localization of GFP and its derivatives in plants in these experiments. But whole sets of marker proteins targeted to a specific organelle or position within the cell have been developed, which in some cases have led to the identification of till then unknown cell compartments (e.g. Nelson et al., 2007; Mathur, 2007; Geldner et al., 2009). To achieve targeting to a specific cell location, a FP is usually fused to a protein with established localization. These markers also serve as control to identify the position of proteins with unknown localization. Biolistic transformation methods for expression of proteins provide a fast and efficient tool that theoretically has no restriction concerning plant species (e.g. Finer et al., 1999; Schweizer et al., 1999).

In mammals, several studies have been performed to elucidate the subcellular localization of TLP family members (e.g. Boggon et al., 1999; He et al., 2000; Santagata et al., 2001; Norman et al., 2009). The mouse TUBBY protein for example localized to the plasma membrane in transfected cells via its PIP_2 binding site. From there it is translocated to the nucleus in response to G protein activation (Santagata et al., 2001), giving hints to the signaling pathways the protein might be involved in. In plants, a GFP-tagged rice TLP was found in the nuclei of onion epidermal cells (Cai et al., 2008) and a YFP fusion of a chickpea TLP accumulated in the root apoplastic space

when expressed in *Arabidopsis* (Wardhan et al., 2012). To date, no detailed study has been performed on the localization of *Arabidopsis* TLPs.

4.3.1 Studies on truncated N-terminal AtTLP versions revealed nucleo-cytosolic and plastidial localizations

No green fluorescence could be detected, when full-length AtTLP GFP-fusions were transiently expressed in *Arabidopsis* leaf epidermal cells. This might suggest that CaMV35S promoter driven overexpression led to silencing of the gene constructs. Another possible explanation is cell -death caused by overexpression of the proteins. Nevertheless, an increased number of cells displaying autofluorescence was not observed in cells co-transformed with mCherry, making this alternative unlikely. However, instability has been reported for many FBPs (Nibau et al., 2011). In addition, fluorescence for a full-length AtTLP3 version with a GFP inserted between the linker sequence and the Tubby domain was observed in *N. benthamiana* (Figure 3.15). Therefore, it is more likely that the proteins were degraded by specific proteases in *Arabidopsis*. Nevertheless, as it was desired to study subcellular localization of AtTLPs in their native system, truncated versions coupled to GFP were generated and used for transient expression. First, localization of the AtTLP3 sequence N-terminal to the Tubby domain composed of a leading sequence (aa 1-49), an F-box domain (aa 50-105) and a short linker sequence (aa 106-115) was investigated (Figure 3.8 K-P). When observing leaves under a CLSM, green fluorescence was detected in the nucleus, the cytosol and plastids.

In the signaling model for MmTUBBY and HsTLP3 the proteins are sequestered at the plasma membrane via their C-terminal Tubby domain. After dislodgement in response to G protein activation TUBBY is directed by two N-terminal nuclear localization signals (NLS) towards the nucleus, where it is thought to regulate transcription. The same was suggested for HsTLP3. Consistent with this, fusion constructs using the N-terminal half of both proteins connected to GFP were detected primarily in the nucleus. The same was observed for a full-length version of TUBBY coupled to GFP after detachment from the PM (Santagata et al., 2001). In contrast to this, no nuclear localization signals were predicted *in silico* for AtTLP3 (cNLS Mapper, available at http//nls-mapper.iab.keio.ac.jp/), as well as for AtTLP7 and -9 (Schwacke et al., 2007). Since in the present study fluorescence from NT-AtTLP3-GFP was clearly detected in the cytosol and plastids in addition to the nucleus, at least the presence of a highly efficient NLS in the N-terminus of AtTLP3 can be ruled out.

Nuclear pore complexes are the gates to the nucleus (reviewed e.g. in Wente and Rout, 2010). It was shown, that molecules with a molecular weight of about 40 kDa can pass them relatively free (Feldherr and Akin, 1997; Keminer and Peters, 1999) and even a protein with a molecular weight of about 73 kDa was found in the nucleus without possessing a NLS (Haasen et al., 1999). This is why small proteins like GFP (about 27 kDa) or mCherry (about 29 kDa) can be seen inside the nucleus in addition to the cytosol where they are synthesized although they do not feature a NLS. The same might be true for NT-AtTLP3-GFP with a predicted molecular weight of about 40 kDa. Therefore, the presence of a NLS in AtTLP3 seems very unlikely while nuclear localization is not. Thus it is possible that *Arabidopsis* TLPs locate to the nucleus without a NLS, but wether nuclear localization has functional importance for AtTLP signaling remains to be shown.

The subcellular localization prediction program WoLF PSORT (Horton et al., 2007) suggested plastidial targeting for several AtTLPs including AtTLP3 (Table 3.1). But as especially the observed plastid targeting of NT-AtTLP3-GFP might be the result of strong overexpression due to the 35S promoter, the localization experiments were repeated using the endogenous AtTLP3 promoter instead (Figure 3.8 Q-S). However, no change in the pattern of localization was detected. Thus, plastidial import of NT-AtTLP3-GFP is unlikely to be caused by strong overexpression. The best studied and presumably most common way of plastidial import is directed by highly variable peptide sequences at the N-terminus of proteins ranging from 45 to over 100 amino acids (aa), which are designated as chloroplast targeting peptides (cTPs). They have been shown to be both necessary and sufficient for directing proteins into plastids and during the import process the nascent protein is cleaved at the cTP (reviewed e.g. in Bruce, 2000; Soll and Schleiff, 2004). The 49 amino acid leading sequence of AtTLP3 might be a good candidate to contain a cTP. Whereas a ChloroP (Emanuelsson et al., 1999) analysis of the N-terminal sequence of AtTLP3 did not directly result in the prediction of a cTP, the yielded score of 0.496 was just below the threshold of 0.5 for such sequences. Given the observed localization and the prediction from WoLF PSORT this indicates the presence of a cTP in AtTLP3. However, a detailed study on GFP-fused to sequentially truncated versions of the AtTLP3 N-terminal part revealed that the first 39 amino acids were dispensable for plastidial localization as were amino acids 86-115 (Figure 3.9). This results suggest that a part of the leading sequence (aa 40-49) and the N-terminal half of the F-box (aa 50-85) were necessary for import of truncated versions into plastids. Further evidence for this observation came from a study on the localization of N-terminal parts of AtTLP2, -7, -8 and -10 (Figure 3.10 B-M). GFP fusion constructs of AtTLP2, -7

and -10 showed a plastidial and nucleo-cytosolic localization like AtTLP3. It was not investigated further, which sequences were responsible for plastidial import of these constructs. But another study found solely nucleo-cytosolic localization for the first 60 amino acids of AtTLP7 when fused to GFP, suggesting that the localization for at least this protein might be similar to AtTLP3 (Carrie et al., 2009). The N-terminal part of AtTLP8 was the only one not to be localized in plastids but was detected in the nucleus and cytosol (Figure 3.10 K-M). AtTLP8 differs from other AtTLPs. For example, AtTLP8 is the only AtTLP without an F-box domain (Lai et al., 2004). Localization of AtTLP8 is thus in line with the observation that a part of the F-box domain is necessary for plastidial import of AtTLP3. Nevertheless, a canonical import of NT-AtTLP3 into plastids seems unlikely. So far no F-box has been described as part of a cTP. In recent years other import pathways for plastids have been discovered including possibilities for entry of natively folded mature proteins, for example via the ER (e.g. Villarejo et al., 2005; Nanjo et al., 2006). But since no hints for ER targeting were found for AtTLPs this pathway can be excluded. Link et al. (2011) found some truncated versions of the *potato leaf roll virus* movement protein 17 targeted to plastids when fused to GFP and expressed in *Nicotiana benthamiana*. The responsible amino acids were not located in the N-terminal part of the protein and no import into plastids was detected for full-length versions of the protein. If targeting to plastids had *in vivo* functions was not determined. Similarly, no signs of plastidial localization were observed in this study for a full-length AtTLP3 protein connected to GFP in *N. benthamiana*. As NT-AtTLP3-GFP was still detected in *N. benthamiana* plastids the failed translocation of the full-length version is unlikely the result of a lack of additional proteins (e. g. HSPs), which might be necessary for plastidial import (Soll and Schleiff, 2004). More likely, the significantly increased size of the FL-AtTLP3-GFP variant blocked the import. The molecular weight for FL-AtTLP3-GFP is about 73 kDa and that for NT-AtTLP3-GFP only about 41 kDa (predicted by: The sequence manipulation site; Stothard, 2000). The predicted molecular weight for native AtTLP3 is about 45 kDa and therefore more similar to NT-AtTLP3-GFP. Taking together, whether the detected plastid targeting of NT-AtTLPs has a functional role *in vivo* remains to be shown. Further research, at best involving immuno-localization, will be required to finally clarify the target compartment of AtTLP3 and other AtTLPs. Nevertheless, the results shown here give first important indications towards possible sites of action of AtTLPs within the cell.

4.3.2 Plasma membrane localization of AtTLP3 is most likely mediated by PIP_2 binding

The GFP-tagged Tubby domain of AtTLP3 (GFP-CT-AtTLP3) was detected at the PM when observed under a CLSM (Figure 3.8 B-G). Plant cells use a variety of processes to target proteins to the PM. In a first classification, these proteins can be discerned as either integrated or peripheral membrane proteins. As their name says, integrated proteins are an integral part of a membrane. This is achieved by a transmembrane domain. But the proteins usually also feature domains, which protrude into the cytoplasm or the extracellular space.

Integration as origin for PM localization of AtTLP3 seemed unlikely since the protein translocated into the cell interior in response to certain stimuli. Though considering only this point, the possibility of protein cleavage could not be ruled out, releasing only a part of AtTLP3 into the cytosol. This was demonstrated for example for AtbZIP17, which was shown to be integrated into the ER membrane via a transmembrane domain. Upon salt stress the protein is cleaved and an N-terminal fragment translocates to the nucleus (Liu et al., 2007). Nevertheless, the 3D structure of AtTLP3 excluded a transmembrane domain (Figure 3.7). In addition, no TLP protein was so far reported to be membrane integrated. Thus, an integration of AtTLP3 into the PM can be most probably precluded.

In contrast to integrated membrane proteins, membrane-associated proteins are usually soluble in a hydrophilic surrounding and only anchored to a membrane, for example by addition of a lipid modification (*N*-myristoylation, prenylation, S-acylation) (reviewed e.g. in Sorek et al., 2009). As a further possibility, proteins themselves have been shown to bind to membrane components. For example, several protein domains confer binding to phosphorylated phosphoinositides (Meijer and Munnik, 2003; Lemmon, 2004). One such protein is the PLCδ1 enzyme, which is attached to the PM by its pleckstrin homology (PH) domain. As this domain was shown to specifically bind PIP_2 but also soluble IP3, it has been used as an *in vivo* biosensor, mainly in animals, enabling researchers to study cellular dynamics of the PPI and IP3 (Ferguson et al., 1995; Lemmon et al., 1995; Stauffer et al., 1998; Várnai and Balla, 1998; Várnai and Balla, 2006). PIP_2 binding as cause of PM localization has also been demonstrated for MmTUBBY and HsTLP3 (Santagata et al., 2001). In addition, the 3D homology model of AtTLP3 revealed a conserved binding cavity for this PPI (Figure 3.7 D-E). Therefore PIP_2 binding as origin of AtTLP3 PM localization seemed likely. PIP_2 is a common element of membranes in all eukaryotic organisms. Santagata et al. (2001) reasoned that a protein binding this PPI should also be located at the PM in other organisms. Indeed, PM targeting was demonstrated for MmTUBBY in yeast (Santagata et al.,

2001). Therefore, the Tubby domain of AtTLP3 should also display PM localization in other plant species than *Arabidopsis*. In fact, expressing the AtTLP3 construct in onion and *N. benthamiana* cells revealed a conserved position of the protein within the cell, indicating an attachment to a general membrane component (Figure 3.11 A-F). In contrast to *Arabidopsis*, in *N. benthamiana* also a full-length version of AtTLP3 fused to GFP was detectable which also localized to the PM (Figure 3.15). PIP_2 exists in much lower amounts in plants than in animals (reviewed e.g in Munnik et al 1998; Meijer and Munnik, 2003). In a study investigating the use of the $PH_{PLC\delta1}$ domain fused to YFP as a biosensor for PIP_2 in plants, Van Leeuwen et al. (2007) found a mainly cytosolic localization of the reporter protein in stably transformed tobacco BY-2 cells and *Arabidopsis* plants. Only after exposing the BY-2 cells to salt stress, an increase in PM localization was reported for a few minutes. It was thus concluded that $PH_{PLC\delta1}$ constitutes an applicable biosensor for PIP_2 in plants, but that levels of the PPI in membranes are too low to cause a distinct PM localization like seen in mammals. As AtTLP3 was detected mainly at the PM, though often showing relatively weak fluorescence, this might speak against a specific PIP_2 binding. Nevertheless, other studies using $PH_{PLC\delta1}$ as biosensor produced somewhat different results than obtained by Van Leeuwen et al. (2007). Tang et al. (2007), for example observed a more distinct PM localization of a $PH_{PLC\delta1}$-GFP construct in stably transformed *Arabidopsis* plants. Furthermore, fluorescent $PH_{PLC\delta1}$ reporters were detected mainly at the tip membrane of growing pollen tubes (Kost et al., 1999; Dowd et al., 2006; Helling et al., 2006). Interestingly, in non-growing pollen tubes the reporter adopted a more uniform localization across the PM (Dowd et al., 2006; Helling et al., 2006). Similar results were obtained for *Arabidopsis* root hairs (Vincent et al., 2005). Taken together, the distinct fluorescence from AtTLP3 at the PM is in line with several other studies employing a fluorescent PIP_2 biosensor in plants, though a higher proportion of the $PH_{PLC\delta1}$ domain was generally detected in the cytosol as compared to AtTLP3. Differences between the Tubby and $PH_{PLC\delta1}$ domains have been reported elsewhere (Nelson et al., 2008; Quinn et al., 2008; Szentpetery et al., 2009). In fact, soluble IP3 has been demonstrated to dislodge the latter from the PM (Hirose et al., 1999; Nash et al., 2001). In human HEK293-AT1 cells, a much higher fraction of the $PH_{PLC\delta1}$ was found in the cytosol compared to the Tubby domain of MmTUBBY when fused to GFP. Indeed, a higher affinity for PIP_2 was found for the Tubby domain when compared to $PH_{PLC\delta1}$ (Szentpetery et al., 2009). Also, in contrast to $PH_{PLC\delta1}$ no binding affinity for IP3 was observed for the Tubby domain (Santagata et al., 2001; Quinn et al., 2008; Nelson et al., 2008; Szentpetery et al., 2009). As AtTLP3 seems to adopt a more

distinct PM localization than reported for $PH_{PLC\delta1}$ in plants, the above described properties for the mammalian Tubby domain might also be true for the plant TLP. Nevertheless, as stated in section 3.2.4, a higher proportion of the Tubby domain of AtTLP2 was observed in the cytosol of many cells. This might reflect differences in PPI affinity existing between the various plant TLPs.

It is important to note, that these points do not question the lower abundance of PIP_2 in plant membranes as compared to mammals (reviewed e.g. in Munnik et al., 1998; Meijer and Munnik, 2003). In an interesting experiment, Szentpetery et al. (2009) expressed the Tubby domain of MmTUBBY and the $PH_{PLC\delta1}$ domain fused to a fluorescent protein either separately or together in human HEK293-AT1 cells. As both domains bind to PIP_2, binding competition had been expected in the cells co-transformed with both constructs. In contrast, no such competition could be detected and it was proposed that cells increase their PIP_2 concentration in response to higher levels of PIP_2 binding proteins. Therefore qualitative statements as to the actual levels of PIP_2 in cells might not be possible by the use of fluorescent biosensors.

To further substantiate these observations, two amino acids in the Tubby domain of AtTLP3 (K187 / R189) were mutated to alanine. The corresponding amino acids in MmTUBBY (K330 / R332) have been shown to be essential for PIP_2 binding (Santagata et al., 2001). Single mutations to alanine abrogated PM localization of a GFP-tagged version in transfected cells and a recombinant protein with alanine in both positions lost its capacity to bind PPIs in lipid blot experiments (Santagata et al., 2001). Consistent with this, the GFP-CT-AtTLP3 (K187A / R189A) fusion protein was only observed in the cytosol and nucleus of transformed cells (Figure 3.13 D-F). A further and very strong point for the assumption, that AtTLP3 binds PIP_2 is presented by results obtained from experiments using U73122. This aminosteroid has been characterized as an inhibitor of PLC activity in animals (Smith et al., 1990) and was shown to be active in plants as well (Pingret et al., 1998). Plant PLC enzymes hydrolize the phosphoinositides PIP_2 and phosphatidylinositol 4-phosphate (PI4P) (Melin et al., 1987; Munnik and Vermeer, 2010). As available information only indicate TLP binding to PPIs phosphorylated at two adjacent positions of the inositol ring (Santagata et al., 2001), PI4P binding of AtTLP3 seems unlikely.

K187 and R189 of AtTLP3 are conserved in several plant TLPs (Lai et al., 2004 and Figure 3.10), indicating that these proteins might also bind PIP_2. As a first step to elucidate this question, localization of GFP-tagged Tubby domains from different plant TLPs was investigated in *Arabidopsis* leaf epidermal cells (Figure 3.10). In fact, the Tubby domains of AtTLP2, -7 and -10

were found at the PM. In addition the Tubby domain of HvTLP12, named for its homology to OsTLP12 (Yang et al., 2008), was also targeted to the PM in *Arabidopsis*, indicating a more widespread occurrence of PIP_2 binding in plant TLPs. Considering the affiliation of the tested truncated proteins to their systematic clades within the plant TLPs it becomes obvious that each of the clades A1-A4 (Yang et al., 2008) is represented by at least one protein targeted to the PM. Thus, PM localization was not restricted to a specific clade during evolution. It might though be possible that some of the other TLPs from these clades display a different localization pattern. For example, in AtTLP5 the arginine corresponding to R189 of AtTLP3 is replaced by a lysine (Lai et al., 2004). Although both are positively charged amino acids, an influence on localization cannot be precluded. For example, a change in the Tubby domain from MmTUBBY R332 to the positively charged amino acid histidine presumably reduced its affinity to PIP_2 (Quinn et al., 2008). In contrast to the other TLPs, the Tubby domain of AtTLP8 was found only in the nucleus and cytosol (Figure 3.10 T-V). AtTLP8 is more distantly related to other TLPs and belongs systematically to clade C where it constitutes the only TLP from *Arabidopsis* (Yang et al., 2008). A striking difference of AtTLP8 as compared to other AtTLPs is its lack of an F-box domain. Alterations are also observed in the Tubby domain as it features a serine and a threonine in the PIP_2 binding cavity instead of lysine and arginine in the other investigated proteins (Lai et al., 2004 and Figure 3.10). The localization of AtTLP8 therefore fits to the hypothesis that PIP_2 binding strongly relies on these both positively charged amino acids. In summary, a PM localization for the Tubby domains of several plant TLPs could be demonstrated. In addition, results from several experiments with AtTLP3 strongly suggest that this originates from a capability to bind the poly-phosphoinositide PIP_2.

4.4 AtTLP3: A new player in abiotic stress signaling?

In mouse Neuro-2A cells GFP-coupled MmTUBBY re-located from the PM into the nucleus after exposure to the neurotransmitter acetylcholine (Santagata et al., 2001). The protein had been shown to bind DNA and its N-terminal part was determined to activate transcription (Boggon et al., 1999). It was therefore suggested that release from the PM in response to the external stimulus activated TUBBY signaling (Santagata et al., 2001). In a similar way GFP-MmTUBBY translocated from the PM into the cytosol in human SH-SY5Y neuroblastoma cells treated with the synthetic acetylcholine derivate metacholine (Nelson et al., 2008). Furthermore, HsTLP3 also displayed a dual PM and nuclear localization when expressed in Neuro-2A cells (Santagata et al.,

2001). Thus, sequestration of TLP proteins at the PM and signaling activation by PM dislodgement in response to external stimuli seems to be a more common feature of this protein family. This scheme might though not be true for all TLPs as some mammalian ones have, at least until now, not been detected at the PM (e.g. Li et al., 2001; Mukhopadhyay et al., 2010). But as AtTLP3 in the present study displayed a distinct PM localization, it might be the case for this plant protein.

As some plant TLPs have already been implicated to act in ABA and salt/drought stress responses (Lai et al., 2004; Ko et al., 2006; Wardhan et al., 2012), it was at hand to test these conditions as possible re-localization trigger for AtTLP3. Nevertheless, in contrast to first expectations no PM detachment occurred in response to ABA and also to several other phytohormones (jasmonate, abscisic acid, salicylic acid, indole-3-acetic acid (auxin), brassinolide and gibberellic acid). It should be noted though, that under the applied assay conditions only robust changes in re-localization could be detected. It can therefore not be ruled out that at least some of the applied hormones elicited a minor amount of translocation. Under natural conditions this might be enough to activate downstream responses. However, when exposing transformed leaves to NaCl or mannitol, the GFP-tagged Tubby domain of AtTLP3 was detected in the cytosol and nucleus within 2 h (Figure 3.12). It is widely accepted that exposure of plants to salt and drought stress is often accompanied by an increase in H_2O_2 (e.g. Mittler et al., 2004; Parida and Das, 2005; Quan et al., 2008). Application of this reactive oxygen species (ROS) to transformed leaves elicited a fast dislodgement of the Tubby domain of AtTLP3 from the PM in *Arabidopsis* (Figure 3.12) as well as re-localization of full-length AtTLP3 in *N. benthamiana* (Figure 3.15). It might therefore be possible that a burst in H_2O_2 also triggered re-localization during treatment with NaCl and mannitol. Importantly, PM detachment was blocked by pretreatment of transformed leaves with PLC inhibitor U73122 (Figure 3.13). This shows that the observed translocation of AtTLP3 is not an unspecific incident caused by membrane damage originating from the applied stress. Instead, it is a specific signaling event depending on the activation of a PLC enzyme, similar to the re-localization described for MmTUBBY (Santagata et al., 2001).

ROS, from which H_2O_2 is just the best studied so far, fulfill roles in a variety of processes ranging from plant defense to growth regulation. In addition, ROS play crucial roles in adaptation to abiotic stresses. For example, overexpression of the ROS detoxifying enzymes ascorbate peroxidase and superoxide dismutase in tobacco yielded plants more tolerant to oxidative, salt

and drought stress (Badawi et al., 2004a; Badawi et al., 2004b). Similar observations were made with tobacco plants overexpressing CaTLP1 (Wardhan et al., 2012). A major compartment for the generation of H_2O_2 within the cell are chloroplasts. To adapt to changes in H_2O_2 levels, molecules in the chloroplast, therefore, have influence on gene expression of the plastome as well as in the nucleus (e.g. Pfannschmidt, 2003). Another important side of H_2O_2 production is at the cell wall. The best described mechanism for its generation here concerns PM located NADPH oxidases, which reduce oxygen to generate superoxide radicals. These are rapidly converted to H_2O_2 (Simon-Plas et al., 2002; Torres et al., 2002). As H_2O_2 is involved in such a host of signaling pathways it is still uncertain how specificity is achieved. A spatio-temporal regulation similar to calcium was suggested as one possibility to gain this specificity (Mittler et al., 2011). However, it is known that PLC enzymes are activated in response to H_2O_2 (e.g. Legendre et al., 1993; Mittler et al., 2004). Thus, the observation that AtTLP3 is released from the PM after H_2O_2 in a PLC dependent manner complies with previous knowledge. It is therefore tempting to speculate that after the cell senses H_2O_2 at the PM, AtTLP3 is released in a PLC dependent manner and translocates to plastids and/or the nucleus to act in ROS signaling.

Though the presented results indicate that AtTLP3 may act in salt/drought and oxidative stress signaling, no altered responses to these stresses were detected in *attlp3* mutant lines (Figure 3.18). This might origin from functional redundancy of AtTLPs, especially as other plant TLPs have been suggested to act in these stress response pathways as well (Ko et al., 2006; Cai et al., 2012). It might therefore be necessary to study the effect of abiotic stresses on mutant plants lacking more than one *TLP* gene. At the moment it is not known, which AtTLPs might act redundantly. Thus in a first attempt, it was aimed to generate double knockout lines for the most related *TLP* genes in *Arabidopsis* as they may conduct conserved functions. Three paralogous gene pairs were identified within the *AtTLP* family (*AtTLP1* and -*5*; *AtTLP2* and -*6*; *AtTLP9* and -*11*; Yang et al., 2008), with *AtTLP3* belonging to the same clade as *AtTLP9* and -*11*. However, exposure of *attlp1/5* and *attlp9/11* double mutant plants to H_2O_2 did not reveal altered effects on cell-death when compared to wild-type plants (Figure 3.19). Even so, as only one assay was performed till now employing the double mutant lines, more sophisticated experiments should follow. In addition, triple mutants should be generated to investigate plants lacking a complete systematic clade.

Support for this strategy is given by qRT-PCR analyses, which revealed transcriptional downregulation of *AtTLP3* in *Arabidopsis Col*-0 plants exposed to H_2O_2 (Figure 3.20). The

particular time point and seemingly dose dependent manner of transcriptional regulation of *AtTLP3* after H_2O_2 treatment suggest a specific regulation of the protein in response to the stress. In summary, while no altered phenotypes could be observed in tested *tlp* mutant lines when exposed to salt, drought and oxidative stress, the specific differential transcription of *AtTLP3* in response to H_2O_2 and detachment of the protein from the PM in response to salt, mannitol and H_2O_2 indicate a participation of AtTLP3 in plant responses to these stresses.

4.5 *AtTLP3* and -*5* displayed tissue specific expression patterns

Up to now the promoter activity of plant *TLP*s have not been examined at a tissue level. Several studies (Lai et al., 2004; Cai et al., 2008; Yang et al, 2008) investigated the transcription of *TLP*s in *Arabidopsis* and rice plants, choosing a PCR based approach and extraction of RNA from several organs like roots, rosette leaves and flowers. Of all 14 *OsTLP*s only three were not expressed in all organs (Yang et al, 2008). In *Arabidopsis*, an organ specific expression was detected only for *AtTLP5* and -*8*, which lack expression in stems and rosette leaves. *AtTLP4* did not yield a PCR product (Lai et al., 2004). Histochemical GUS-staining in two AtTLP-Promoter:*GUS* lines yielded a more differentiated view on promoter activity of *AtTLP3* and -*5* (Figure 3.16 and Figure 3.17). Compliant with the observations made by Lai et al. (2004), *AtTLP3* was found to be expressed in all plant organs. In cotyledons, transcription was highest in the vascular tissue. For rosette leaves the results were supported by the observations made using the endogenous promoter of *AtTLP3* to express NT-AtTLP3-GFP, where the promoter was found active in *Arabidopsis* leaf epidermal cells (Figure 3.8 Q-S). In contrast to this, transcription was more restricted in the hypocotyl and the root system. Here, GUS-staining was mainly detected in the vascular tissue. In addition, promoter activity was found in lateral root primordia and around the root tip of some roots, especially younger ones. It might therefore be that AtTLP3 plays a role in the generation of lateral roots. Contrary to Lai et al. (2004) who did not detect *AtTLP5* expression in rosette leaves, promoter activity was clearly found in AtTLP5-Promoter:*GUS* lines in rosette leaves (Figure 3.17 and Figure 7.1). As Lai et al. (2004) investigated expression on the mRNA level while the present study examined promoter activity this might indicate to a rapid degradation of *AtTLP5* mRNA. On the other hand, uniform *AtTLP5* promoter activity was not detected in all rosette leaves used. Many leaves showed a more uneven pattern or no GUS-staining at all (Figure 7.1). This might indicate to a developmental dependence of *AtTLP5* transcription in leaves. There were also differences in *AtTLP5* promoter activity when compared

to *AtTLP3*. In the hypocotyl *AtTLP5* transcription was not restricted to the vasculature. In addition, while *AtTLP5* transcription was detected mainly in the vasculature in roots like *AtTLP3*, no promoter activity was found in lateral root primordia. In root tips *AtTLP5* transcription was more restricted than *AtTLP3* promoter activity, supposedly to the cells of the root apical meristem. Therefore, there may be specific roles of *AtTLP*s in some cell types, while in others they may show functional redundancy.

However, these studies did not deliver a hint to why roots of *attlp* lines displayed a delayed colonization by *P. indica*. The fungus colonizes mainly the root epidermis and cortex of *Arabidopsis* and was not detected in meristematic regions (Jacobs et al., 2011). Therefore root cells expressing *AtTLP3* and *-5* do not seem to get into contact with the fungus, suggesting an indirect role of *AtTLP*s in the interaction with the mutualist. Nevertheless, as all experiments were carried out without *P. indica*, it is possible that the transcription patterns change in the presence of the fungus. It would therefore be interesting to investigate AtTLP-Promoter:*GUS* lines inoculated with *P. indica*.

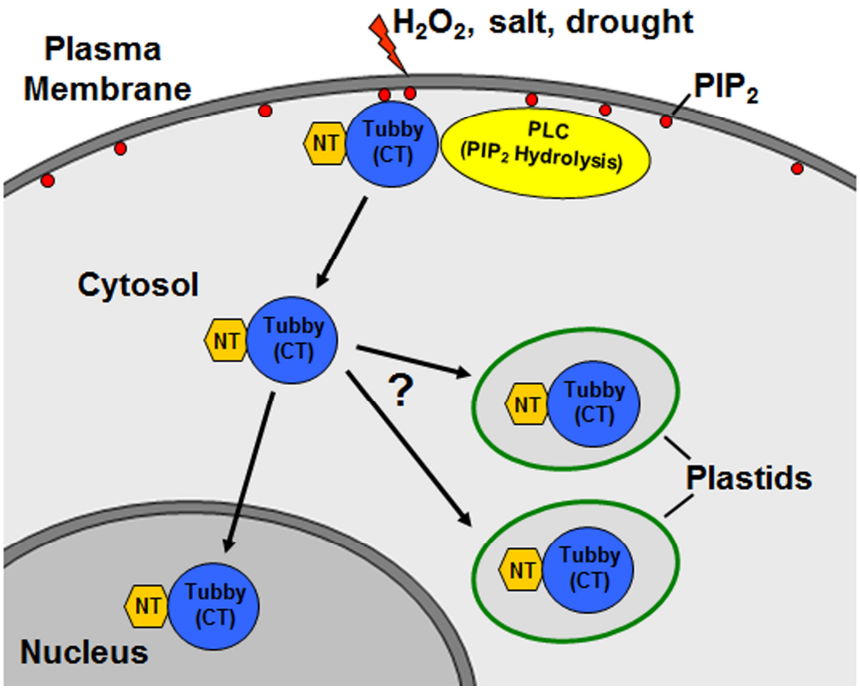

Figure 4.1: Proposed schematic model for signaling through AtTLP3. AtTLP3 is attached to the plasma membrane (PM) via binding to PIP_2. Hydrogen peroxide (H_2O_2), salt and mannitol-induced drought stress cause a PLC mediated release of AtTLP3 from the PM to the cytosol and presumably the nucleus. The N-terminal part was also detected in plastids though it is not yet clear if this takes place *in vivo* with the native protein. CT: C-terminal part of AtTLP3 including the Tubby domain; NT: N-terminal part of AtTLP3; PIP_2: Phosphatidylinositol 4,5-bisphosphate; PLC: Phospholipase C.

4.6 Conclusions

The present study aimed to get new insights into the role of TLPs, a protein family which has attracted scientific attention in animals but is scarcely investigated in plants. A general role for AtTLPs in the early interaction of *Arabidopsis thaliana* roots with the mutualistic fungus *P. indica* could be demonstrated, as a delayed colonization by the fungus was detected in *attlp* mutant lines. Several assays did not reveal an enhanced immune response in tested *attlp* lines, nor a generally altered resistance to pathogens. Hence, AtTLPs might constitute compatibility factors needed by *P. indica* to colonize *Arabidopsis* in a proper way. Alternatively, they could perform a more indirect role in the interaction as might be inferred from the cell specific transcription pattern of two *AtTLP* genes, which is restricted to root regions which are not colonized by the fungus.

In addition, a detailed analysis on subcellular localization of AtTLPs was performed. From this, a preliminary model for AtTLP3 signaling was developed based on the one proposed by Santagata et al. (2001) for MmTUBBY. Under non-stress conditions AtTLP3 is sequestered at the PM. Several distinct evidences indicate that this localization is most likely caused by the ability of AtTLP3 to bind the membrane phospholipid PIP_2. Certain environmental stresses triggered the release of AtTLP3 from the PM. This presumably activates its signaling like suggested for MmTUBBY, though no evidences have been found for this so far. The PM detachment was shown to be dependent on PLC activity. In the current study, salt and mannitol-induced drought stress could be identified to elicit the translocation. A direct re-localization was also observed in response to H_2O_2. As an increase of this reactive oxygen species accompanies salt and drought stress it might be responsible for the observed protein translocation in response to the other stresses. First indications for subcellular localization AtTLP3 is directed after dislodgment from the PM can be drawn from this study. Targets of AtTLP3 might be located in the cytosol or the nucleus. Additionally, the possibility of plastid targeting was identified, as seen with N-terminal AtTLP3 variants fused to GFP.

5. Summary/Zusammenfassung

5.1 Summary

TUBBY and Tubby-like proteins (TLPs) have first been described in mice, where mutations in respective genes lead to severe disease phenotypes. Mouse TUBBY was shown to be targeted to the plasma membrane (PM) in transfected cells by specific phosphatidylinositol 4,5-bisphosphate (PIP_2) binding. Several neuro-transmitters elicited dislodgement of TUBBY from the PM in a phospholipase C (PLC) dependent manner, which led to a translocation of the protein into the nucleus. There, it was suggested to function as transcriptional regulator. Mammalian TLPs have also been implicated to work in vesicular trafficking, insulin signaling and as extracellular bridging molecules in phagocytosis.

Since their first description, *TLPs* have been detected in the genomes of a multitude of eukaryotic organisms, including plants. The conservation throughout so many species suggests fundamental biological functions. In higher plants, 11 TLPs were identified in the model species *Arabidopsis thaliana* where AtTLP9 was implicated to act in abscisic acid signaling. In addition, results from other plant species suggest roles for TLPs in biotic interactions and abiotic stress signaling.

In this study, a delayed colonization of *attlp* mutant lines by the mutualistic fungus *Piriformospora indica* was observed. As no increased immune reactions were detected in the mutant lines, AtTLPs might constitute compatibility factors needed by *P. indica* in the early interaction with *Arabidopsis* roots. Further studies were carried out to investigate the subcellular localization of plant TLPs. GFP-tagged AtTLP3 was detected at the PM in cells transiently over-expressing the protein. The obtained results suggest a conservation of the PIP_2 binding capacity as origin of AtTLP3 PM targeting. Moreover, H_2O_2 triggered a specific, PLC dependent re-localization of the protein, possibly activating further downstream responses. In contrast to mouse TUBBY, a plastidial and nucleo-cytosolic localization was observed for the N-terminal part of AtTLP3. It is tempting to speculate that AtTLP3 translates rises in H_2O_2 levels into intracellular signaling.

Taken together, this study shed further light on this relatively unexplored gene family in *Arabidopsis*, supporting the proposed roles of *TLP*s in abiotic and biotic stress signaling. In addition, the response of AtTLP3 to H_2O_2 provides an interesting new direction for further research on plant TLPs.

5.2 Zusammenfassung

TUBBY und die verwandten Tubby-like Proteine (TLPs) wurden zuerst in Mäusen (Mus musculus) beschrieben, wo Mutationen in den entsprechenden Genen schwere Krankheitssyndrome hervorrufen. MmTUBBY wurde der Plasmamembran (PM) nachgewiesen. Als Ursprung für diese Lokalisation wurde eine spezifische Interaktion des Proteins mit Phosphatidylinositol 4,5-biphosphat (PIP_2) in der Membran identifiziert. Applikation verschiedener Neurotransmitter führte zu einer Phospholipase C (PLC) abhängigen Freisetzung des Proteins von der PM und zur Akkumulation im Zellkern, wo es möglicherweise an der Genregulation beteiligt ist. Weitere Funktionen von TLPs in Säugetieren wurden in der Regulation von vesikulärem Transport, der Phagocytose und im Insulin Signalweg beschrieben.

*TLP*s wurden in den Genomen einer Vielzahl eukaryotischer Organismen identifiziert, was auf essentielle Funktionen dieser Proteinfamilie hindeutet. 11 TLPs wurden in der Modellpflanze *Arabidopsis thaliana* beschrieben, wo AtTLP9 eine Rolle in der Signaltransduktion von Abscisinsäure zu spielen scheint. Ergebnisse aus anderen Pflanzen deuten auf Funktionen pflanzlicher TLPs in biotischen Interaktionen und in der Reaktion auf abiotischen Stress hin.

In der vorliegenden Studie konnte eine verspätete Besiedlung von *attlp* Mutantenlinien durch den mutualistischen Pilz *Piriformospora indica* gezeigt werden. Da keine erhöhten Immunreaktionen in den Mutanten nachgewiesen wurden, könnten AtTLPs als Kompatibilitätsfaktoren dienen, die von *P. indica* in der frühen Interaktion mit Wurzeln von *Arabidopsis* benötigt werden. Weitere Experimente dienten der Untersuchung der subzellulären Lokalisation pflanzlicher TLPs. GFP-gekoppeltes AtTLP3 wurde nach transienter Überexpression an der PM von Zellen beobachtet. Die erhaltenen Ergebnisse deuten auf eine Konservierung der PIP_2 Interaktion als Ursprung für die beobachtete Lokalisation hin. Zugabe von H_2O_2 führte zu einer spezifischen PLC abhängigen Freisetzung des Proteins von der PM. Im Gegensatz zu MmTUBBY, wurde der N-terminale Bereich von AtTLP3 in Plastiden, dem Cytosol und dem Zellkern detektiert. Es bleibt zu untersuchen, ob AtTLP3 Anstiege in H_2O_2 Konzentrationen in intrazelluläre Signale umwandelt.

Zusammengenommen liefert die vorliegende Studie neue Erkenntnisse über diese bis jetzt nur wenig in Pflanzen beschriebene Proteinfamilie in *Arabidopsis*. Die erhaltenen Ergebnisse unterstützen die Annahme, dass TLPs an Reaktionen auf biotischen und abiotischen Stress beteiligt sind. Zusätzlich liefert die Relokalisation von AtTLP3 als Antwort auf H_2O_2 einen interessanten neuen Ansatz zur Erforschung pflanzlicher TLPs.

6. References

Abramoff MD, Magalhaes PJ, Ram SJ (2004) Image Processing with ImageJ. Biophotonics International **11:** 36-42

Abramovitch RB, Anderson JC, Martin GB (2006) Bacterial elicitation and evasion of plant innate immunity. Nat Rev Mol Cell Biol **7:** 601-611

Achard P, Renou J-P, Berthomé R, Harberd NP, Genschik P (2008) Plant DELLAs Restrain Growth and Promote Survival of Adversity by Reducing the Levels of Reactive Oxygen Species. Current Biology **18:** 656-660

Adam L, Ellwood S, Wilson I, Saenz G, Xiao S, Oliver RP, Turner JG, Somerville S (1999) Comparison of Erysiphe cichoracearum and E. cruciferarum and a survey of 360 Arabidopsis thaliana accessions for resistance to these two powdery mildew pathogens. Mol Plant Microbe Interact **12:** 1031-1043

Allen TR, Millar T, Berch SM, Berbee ML (2003) Culturing and direct DNA extraction find different fungi from the same ericoid mycorrhizal roots. New Phytologist **160:** 255-272

Alonso JM, Ecker JR (2006) Moving forward in reverse: genetic technologies to enable genome-wide phenomic screens in Arabidopsis. Nat Rev Genet **7:** 524-536

Amir-Moazami O, Alexia C, Charles N, Launay P, Monteiro RC, Benhamou M (2008) Phospholipid scramblase 1 modulates a selected set of IgE receptor-mediated mast cell responses through LAT-dependent pathway. J Biol Chem **283:** 25514-25523

Apel K, Hirt H (2004) Reactive oxygen species: metabolism, oxidative stress, and signal transduction. Annu Rev Plant Biol **55:** 373-399

Arnold K, Bordoli L, Kopp J, Schwede T (2006) The SWISS-MODEL workspace: a web-based environment for protein structure homology modelling. Bioinformatics **22:** 195-201

Asai T, Tena G, Plotnikova J, Willmann MR, Chiu WL, Gomez-Gomez L, Boller T, Ausubel FM, Sheen J (2002) MAP kinase signalling cascade in *Arabidopsis* innate immunity. Nature **415:** 977-983

Attard A, Gourgues M, Callemeyn-Torre N, Keller H (2010) The immediate activation of defense responses in *Arabidopsis* roots is not sufficient to prevent *Phytophthora parasitica* infection. New Phytol **187:** 449-460

Attard A, Gourgues M, Galiana E, Panabières F, Ponchet M, Keller H (2008) Strategies of attack and defense in plant–oomycete interactions, accentuated for *Phytophthora parasitica* Dastur (syn. *P. Nicotianae* Breda de Haan). J Plant Physiol **165:** 83-94

Azevedo C, Santos-Rosa MJ, Shirasu K (2001) The U-box protein family in plants. Trends Plant Sci **6:** 354-358

Badawi GH, Kawano N, Yamauchi Y, Shimada E, Sasaki R, Kubo A, Tanaka K (2004) Over-expression of ascorbate peroxidase in tobacco chloroplasts enhances the tolerance to salt stress and water deficit. Physiol Plant **121:** 231-238

Badawi GH, Yamauchi Y, Shimada E, Sasaki R, Kawano N, Tanaka K, Tanaka K (2004) Enhanced tolerance to salt stress and water deficit by overexpressing superoxide dismutase in tobacco (*Nicotiana tabacum*) chloroplasts. Plant Sci **166:** 919-928

Baltruschat H, Fodor J, Harrach BD, Niemczyk E, Barna B, Gullner G, Janeczko A, Kogel KH, Schäfer P, Schwarczinger I, Zuccaro A, Skoczowski A (2008) Salt tolerance of barley induced by the root endophyte *Piriformospora indica* is associated with a strong increase in antioxidants. New Phytol **180:** 501-510

Banerjee P, Kleyn PW, Knowles JA, Lewis CA, Ross BM, Parano E, Kovats SG, Lee JJ, Penchaszadeh GK, Ott J, Jacobson SG, Gilliam TC (1998) *TULP1* mutation in two extended Dominican kindreds with autosomal recessive retinitis pigmentosa. Nat Genet **18:** 177-179

Bateman A, Finn RD, Sims PJ, Wiedmer T, Biegert A, Söding J (2009) Phospholipid scramblases and Tubby-like proteins belong to a new superfamily of membrane tethered transcription factors. Bioinformatics **25:** 159-162

Bechtold N, Ellis J, Pelletier G (1993) *In planta Agrobacterium* mediated gene transfer by infiltration of adult *Arabidopsis thaliana* plants. C R Acad Sci III **316:** 1194-1199

Bhushan D, Pandey A, Choudhary MK, Datta A, Chakraborty S, Chakraborty N (2007) Comparative proteomics analysis of differentially expressed proteins in chickpea extracellular matrix during dehydration stress. Mol Cell Proteomics **6:** 1868-1884

Boggon TJ, Shan WS, Santagata S, Myers SC, Shapiro L (1999) Implication of tubby proteins as transcription factors by structure-based functional analysis. Science **286:** 2119-2125

Boller T, Felix G (2009) A renaissance of elicitors: perception of microbe-associated molecular patterns and danger signals by pattern-recognition receptors. Annu Rev Plant Biol **60:** 379-406

Bolton MD, Thomma BPHJ, Nelson BD (2006) *Sclerotinia sclerotiorum* (Lib.) de Bary: biology and molecular traits of a cosmopolitan pathogen. Mol Plant Pathol **7:** 1-16

Bruce BD (2000) Chloroplast transit peptides: structure, function and evolution. Trends Cell Biol **10:** 440-447

Brundrett M (2004) Diversity and classification of mycorrhizal associations. Biol Rev Camb Philos Soc **79:** 473-495

Caberoy NB, Alvarado G, Li W (2012) Tubby regulates microglial phagocytosis through MerTK. J Neuroimmunol http://dx.doi.org/10.1016/j.jneuroim.2012.07.009

Caberoy NB, Li W (2009) Unconventional secretion of tubby and tubby-like protein 1. FEBS Lett **583:** 3057-3062

Caberoy NB, Maiguel D, Kim Y, Li W (2010) Identification of tubby and tubby-like protein 1 as eat-me signals by phage display. Exp Cell Res **316:** 245-257

Caberoy NB, Zhou Y, Li W (2010) Tubby and tubby-like protein 1 are new MerTK ligands for phagocytosis. EMBO J **29:** 3898-3910

Cai M, Qiu D, Yuan T, Ding X, Li H, Duan L, Xu C, Li X, Wang S (2008) Identification of novel pathogen-responsive *cis*-elements and their binding proteins in the promoter of *OsWRKY13*, a gene regulating rice disease resistance. Plant Cell Environ **31:** 86-96

Carrie C, Kühn K, Murcha MW, Duncan O, Small ID, O'Toole N, Whelan J (2009) Approaches to defining dual-targeted proteins in *Arabidopsis*. Plant J **57:** 1128-1139

Carroll K, Gomez C, Shapiro L (2004) Tubby proteins: the plot thickens. Nat Rev Mol Cell Biol **5:** 55-63

Chen S, Songkumarn P, Liu J, Wang GL (2009) A versatile zero background T-vector system for gene cloning and functional genomics. Plant Physiol **150:** 1111-1121

Chinchilla D, Bauer Z, Regenass M, Boller T, Felix G (2006) The *Arabidopsis* receptor kinase FLS2 binds flg22 and determines the specificity of flagellin perception. Plant Cell **18:** 465-476

Chisholm ST, Coaker G, Day B, Staskawicz BJ (2006) Host-Microbe Interactions: Shaping the Evolution of the Plant Immune Response. Cell **124:** 803-814

Clay NK, Adio AM, Denoux C, Jander G, Ausubel FM (2009) Glucosinolate metabolites required for an *Arabidopsis* innate immune response. Science **323:** 95-101

Coates ME, Beynon JL (2010) *Hyaloperonospora arabidopsidis* as a pathogen model. Annu Rev Phytopathol **48:** 329-345

Coleman DL, Eicher EM (1990) Fat (*fat*) and tubby (*tub*): two autosomal recessive mutations causing obesity syndromes in the mouse. J Hered **81:** 424-427

Dangl JL, Jones JDG (2001) Plant pathogens and integrated defence responses to infection. Nature **411:** 826-833

Das A, Kamal S, Shakil NA, Sherameti I, Oelmüller R, Dua M, Tuteja N, Johri AK, Varma A (2012) The root endophyte fungus *Piriformospora indica* leads to early flowering, higher biomass and altered secondary metabolites of the medicinal plant, *Coleus forskohlii*. Plant Signal Behav **7:** 103-112

Davletova S, Schlauch K, Coutu J, Mittler R (2005) The zinc-finger protein Zat12 plays a central role in reactive oxygen and abiotic stress signaling in *Arabidopsis*. Plant Physiol **139:** 847-856

Deshmukh S, Hückelhoven R, Schäfer P, Imani J, Sharma M, Weiss M, Waller F, Kogel KH (2006) The root endophytic fungus *Piriformospora indica* requires host cell death for proliferation during mutualistic symbiosis with barley. Proc Natl Acad Sci USA **103:** 18450-18457

Deshmukh SD, Kogel KH (2007) *Piriformospora indica* protects barley from root rot caused by *Fusarium graminearum*. J Plant Dis Protect **114:** 263-268

Dharmasiri N, Dharmasiri S, Estelle M (2005) The F-box protein TIR1 is an auxin receptor. Nature **435:** 441-445

Dodd AN, Gardner MJ, Hotta CT, Hubbard KE, Dalchau N, Love J, Assie JM, Robertson FC, Jakobsen MK, Goncalves J, Sanders D, Webb AAR (2007) The *Arabidopsis* circadian clock incorporates a cADPR-based feedback loop. Science **318:** 1789-1792

Doehlemann G, Berndt P, Hahn M (2006) Different signalling pathways involving a Gα protein, cAMP and a MAP kinase control germination of *Botrytis cinerea* conidia. Mol Microbiol **59:** 821-835

Dowd PE, Coursol S, Skirpan AL, Kao TH, Gilroy S (2006) *Petunia* phospholipase C1 is involved in pollen tube growth. Plant Cell **18:** 1438-1453

Druege U, Baltruschat H, Franken P (2007) *Piriformospora indica* promotes adventitious root formation in cuttings. Sci Hortic-Amsterdam **112:** 422-426

Dufresne PJ, Thivierge K, Cotton S, Beauchemin C, Ide C, Ubalijoro E, Laliberté J-F, Fortin MG (2008) Heat shock 70 protein interaction with *Turnip mosaic virus* RNA-

dependent RNA polymerase within virus-induced membrane vesicles. Virology **374:** 217-227

Durrant WE, Dong X (2004) Systemic acquired resistance. Annu Rev Phytopathol **42:** 185-209

Eichmann R, Hückelhoven R (2008) Accommodation of powdery mildew fungi in intact plant cells. J Plant Physiol **165:** 5-18

Emanuelsson O, Nielsen H, von Heijne G (1999) ChloroP, a neural network-based method for predicting chloroplast transit peptides and their cleavage sites. Protein Sci **8:** 978-984

Fakhro A, Andrade-Linares DR, von Bargen S, Bandte M, Büttner C, Grosch R, Schwarz D, Franken P (2010) Impact of *Piriformospora indica* on tomato growth and on interaction with fungal and viral pathogens. Mycorrhiza **20:** 191-200

Feldherr CM, Akin D (1997) The location of the transport gate in the nuclear pore complex. J Cell Sci **110:** 3065-3070

Felix G, Duran JD, Volko S, Boller T (1999) Plants have a sensitive perception system for the most conserved domain of bacterial flagellin. Plant J **18:** 265-276

Ferguson KM, Lemmon MA, Schlessinger J, Sigler PB (1995) Structure of the high affinity complex of inositol trisphosphate with a phospholipase C pleckstrin homology domain. Cell **83:** 1037-1046

Finer JJ, Finer KR, Ponappa T (1999) Particle bombardment mediated transformation. Curr Top Microbiol Immunol **240:** 59-80

Fujita M, Fujita Y, Noutoshi Y, Takahashi F, Narusaka Y, Yamaguchi-Shinozaki K, Shinozaki K (2006) Crosstalk between abiotic and biotic stress responses: a current view from the points of convergence in the stress signaling networks. Curr Opin Plant Biol **9:** 436-442

Gagne JM, Downes BP, Shiu SH, Durski AM, Vierstra RD (2002) The F-box subunit of the SCF E3 complex is encoded by a diverse superfamily of genes in *Arabidopsis*. Proc Natl Acad Sci USA **99:** 11519-11524

Gagne JM, Smalle J, Gingerich DJ, Walker JM, Yoo SD, Yanagisawa S, Vierstra RD (2004) *Arabidopsis* EIN3-binding F-box 1 and 2 form ubiquitin-protein ligases that repress ethylene action and promote growth by directing EIN3 degradation. Proc Natl Acad Sci USA **101:** 6803-6808

Galan JM, Wiederkehr A, Seol JH, Haguenauer-Tsapis R, Deshaies RJ, Riezman H, Peter M (2001) Skp1p and the F-box protein Rcy1p form a non-SCF complex involved in recycling of the SNARE Snc1p in yeast. Mol Cell Biol **21:** 3105-3117

Galiana E, Rivière MP, Pagnotta S, Baudouin E, Panabières F, Gounon P, Boudier L (2005) Plant-induced cell death in the oomycete pathogen *Phytophthora parasitica*. Cell Microbiol **7:** 1365-1378

Gaudinier A, Zhang L, Reece-Hoyes JS, Taylor-Teeples M, Pu L, Liu Z, Breton G, Pruneda-Paz JL, Kim D, Kay SA, Walhout AJM, Ware D, Brady SM (2011) Enhanced Y1H assays for *Arabidopsis*. Nat Methods **8:** 1053-1055

Geldner N, Dénervaud-Tendon V, Hyman DL, Mayer U, Stierhof YD, Chory J (2009) Rapid, combinatorial analysis of membrane compartments in intact plants with a multicolor marker set. Plant J **59:** 169-178

Glazebrook J (2005) Contrasting mechanisms of defense against biotrophic and necrotrophic pathogens. Annu Rev Phytopathol **43:** 205-227

Glen M, Tommerup IC, Bougher NL, O'Brien PA (2002) Are Sebacinaceae common and widespread ectomycorrhizal associates of *Eucalyptus* species in Australian forests? Mycorrhiza **12:** 243-247

Gómez-Gómez L, Felix G, Boller T (1999) A single locus determines sensitivity to bacterial flagellin in *Arabidopsis thaliana*. Plant J **18:** 277-284

Gomi K, Sasaki A, Itoh H, Ueguchi-Tanaka M, Ashikari M, Kitano H, Matsuoka M (2004) GID2, an F-box subunit of the SCF E3 complex, specifically interacts with phosphorylated SLR1 protein and regulates the gibberellin-dependent degradation of SLR1 in rice. Plant J **37:** 626-634

Guo H, Ecker JR (2003) Plant Responses to Ethylene Gas Are Mediated by $SCF^{EBF1/EBF2}$-Dependent Proteolysis of EIN3 Transcription Factor. Cell **115:** 667-677

Haasen D, Köhler C, Neuhaus G, Merkle T (1999) Nuclear export of proteins in plants: AtXPO1 is the export receptor for leucine-rich nuclear export signals in *Arabidopsis thaliana*. Plant J **20:** 695-705

Hafke JB, van Amerongen JK, Kelling F, Furch ACU, Gaupels F, van Bel AJE (2005) Thermodynamic battle for photosynthate acquisition between sieve tubes and adjoining parenchyma in transport phloem. Plant Physiol **138:** 1527-1537

Hagstrom SA, Duyao M, North MA, Li T (1999) Retinal degeneration in *tulp1*$^{-/-}$ mice: vesicular accumulation in the interphotoreceptor matrix. Invest Ophthalmol Vis Sci **40:** 2795-2802

Hagstrom SA, North MA, Nishina PM, Berson EL, Dryja TP (1998) Recessive mutations in the gene encoding the tubby-like protein TULP1 in patients with retinitis pigmentosa. Nat Genet **18:** 174-176

He W, Ikeda S, Bronson RT, Yan G, Nishina PM, North MA, Naggert JK (2000) GFP-tagged expression and immunohistochemical studies to determine the subcellular localization of the tubby gene family members. Brain Res Mol Brain Res **81:** 109-117

Heckenlively JR, Chang B, Erway LC, Peng C, Hawes NL, Hageman GS, Roderick TH (1995) Mouse model for Usher syndrome: linkage mapping suggests homology to Usher type I reported at human chromosome 11p15. Proc Natl Acad Sci USA **92:** 11100-11104

Heilmann I (2009) Using genetic tools to understand plant phosphoinositide signalling. Trends Plant Sci **14:** 171-179

Helling D, Possart A, Cottier S, Klahre U, Kost B (2006) Pollen tube tip growth depends on plasma membrane polarization mediated by tobacco PLC3 activity and endocytic membrane recycling. Plant Cell **18:** 3519-3534

Hermand D (2006) F-box proteins: more than baits for the SCF? Cell Div **1:** 30

Hilbert M, Voll LM, Ding Y, Hofmann J, Sharma M, Zuccaro A (2012) Indole derivative production by the root endophyte *Piriformospora indica* is not required for growth promotion but for biotrophic colonization of barley roots. New Phytol 10.1111/j.1469-8137.2012.04275.x

Hirose K, Kadowaki S, Tanabe M, Takeshima H, Iino M (1999) Spatiotemporal dynamics of inositol 1,4,5-trisphosphate that underlies complex Ca^{2+} mobilization patterns. Science **284:** 1527-1530

Horbach R, Navarro-Quesada AR, Knogge W, Deising HB (2011) When and how to kill a plant cell: Infection strategies of plant pathogenic fungi. J Plant Physiol **168:** 51-62

Horton P, Park KJ, Obayashi T, Fujita N, Harada H, Adams-Collier CJ, Nakai K (2007) WoLF PSORT: protein localization predictor. Nucleic Acids Res **35:** 585-587

Hrmova M, Fincher GB (2001) Plant enzyme structure. Explaining substrate specificity and the evolution of function. Plant Physiol **125:** 54-57

Huynh TT, Thomson R, McLean CB, Lawrie AC (2009) Functional and genetic diversity of mycorrhizal fungi from single plants of *Caladenia formosa* (Orchidaceae). Ann Bot **104:** 757-765

Ikeda A, Ikeda S, Gridley T, Nishina PM, Naggert JK (2001) Neural tube defects and neuroepithelial cell death in *Tulp3* knockout mice. Hum Mol Genet **10:** 1325-1334

Ikeda A, Nishina PM, Naggert JK (2002) The tubby-like proteins, a family with roles in neuronal development and function. J Cell Sci **115:** 9-14

Ikeda S, Shiva N, Ikeda A, Smith RS, Nusinowitz S, Yan G, Lin TR, Chu S, Heckenlively JR, North MA, Naggert JK, Nishina PM, Duyao MP (2000) Retinal degeneration but not obesity is observed in null mutants of the tubby-like protein 1 gene. Hum Mol Genet **9:** 155-163

Innes RW (2004) Guarding the goods. New insights into the central alarm system of plants. Plant Physiol **135:** 695-701

Jacobs S, Zechmann B, Molitor A, Trujillo M, Petutschnig E, Lipka V, Kogel KH, Schäfer P (2011) Broad-spectrum suppression of innate immunity is required for colonization of Arabidopsis roots by the fungus *Piriformospora indica*. Plant Physiol **156:** 726-740

Jain M, Nijhawan A, Arora R, Agarwal P, Ray S, Sharma P, Kapoor S, Tyagi AK, Khurana JP (2007) F-box proteins in rice. Genome-wide analysis, classification, temporal and spatial gene expression during panicle and seed development, and regulation by light and abiotic stress. Plant Physiol **143:** 1467-1483

Jefferson RA, Kavanagh TA, Bevan MW (1987) GUS fusions: beta-glucuronidase as a sensitive and versatile gene fusion marker in higher plants. EMBO J **6:** 3901-3907

Jones JDG, Dangl JL (2006) The plant immune system. Nature **444:** 323-329

Kapeller R, Moriarty A, Strauss A, Stubdal H, Theriault K, Siebert E, Chickering T, Morgenstern JP, Tartaglia LA, Lillie J (1999) Tyrosine phosphorylation of tub and its association with Src homology 2 domain-containing proteins implicate tub in intracellular signaling by insulin. J Biol Chem **274:** 24980-24986

Keminer O, Peters R (1999) Permeability of Single Nuclear Pores. Biophys J **77:** 217-228

Khatabi B, Molitor A, Lindermayr C, Pfiffi S, Durner J, von Wettstein D, Kogel KH, Schäfer P (2012) Ethylene supports colonization of plant roots by the mutualistic fungus *Piriformospora indica*. PLoS One **7:** e35502

Kiefer F, Arnold K, Künzli M, Bordoli L, Schwede T (2009) The SWISS-MODEL Repository and associated resources. Nucleic Acids Res **37:** D387-392

Kile BT, Schulman BA, Alexander WS, Nicola NA, Martin HME, Hilton DJ (2002) The SOCS box: a tale of destruction and degradation. Trends Biochem Sci **27:** 235-241

Kipreos ET, Pagano M (2000) The F-box protein family. Genome Biol **1:** REVIEWS3002

Kleyn PW, Fan W, Kovats SG, Lee JJ, Pulido JC, Wu Y, Berkemeier LR, Misumi DJ, Holmgren L, Charlat O, Woolf EA, Tayber O, Brody T, Shu P, Hawkins F, Kennedy B, Baldini L, Ebeling C, Alperin GD, Deeds J, Lakey ND, Culpepper J, Chen H, Glücksmann-Kuis MA, Carlson GA, Duyk GM, Moore KJ (1996) Identification and characterization of the mouse obesity gene *tubby*: a member of a novel gene family. Cell **85:** 281-290

Kloppholz S, Kuhn H, Requena N (2011) A Secreted Fungal Effector of *Glomus intraradices* Promotes Symbiotic Biotrophy. Curr Biol **21:** 1204-1209

Ko JH, Yang SH, Han KH (2006) Upregulation of an Arabidopsis RING-H2 gene, *XERICO*, confers drought tolerance through increased abscisic acid biosynthesis. Plant J **47:** 343-355

Komari T, Hiei Y, Saito Y, Murai N, Kumashiro T (1996) Vectors carrying two separate T-DNAs for co-transformation of higher plants mediated by *Agrobacterium tumefaciens* and segregation of transformants free from selection markers. Plant J **10:** 165-174

Koornneef A, Pieterse CMJ (2008) Cross talk in defense signaling. Plant Physiol **146:** 839-844

Kost B, Lemichez E, Spielhofer P, Hong Y, Tolias K, Carpenter C, Chua NH (1999) Rac homologues and compartmentalized phosphatidylinositol 4, 5-bisphosphate act in a common pathway to regulate polar pollen tube growth. J Cell Biol **145:** 317-330

Kottke I, Beiter A, Weiss M, Haug I, Oberwinkler F, Nebel M (2003) *Heterobasidiomycetes* form symbiotic associations with hepatics: *Jungermanniales* have sebacinoid mycobionts while *Aneura pinguis* (*Metzgeriales*) is associated with a *Tulasnella* species. Mycol Res **107:** 957-968

Kou Y, Qiu D, Wang L, Li X, Wang S (2009) Molecular analyses of the rice tubby-like protein gene family and their response to bacterial infection. Plant Cell Rep **28:** 113-121

Kunze G, Zipfel C, Robatzek S, Niehaus K, Boller T, Felix G (2004) The N terminus of bacterial elongation factor Tu elicits innate immunity in Arabidopsis plants. Plant Cell **16:** 3496-3507

Kwak JM, Mori IC, Pei ZM, Leonhardt N, Torres MA, Dangl JL, Bloom RE, Bodde S, Jones JDG, Schroeder JI (2003) NADPH oxidase *AtrbohD* and *AtrbohF* genes function in ROS-dependent ABA signaling in *Arabidopsis*. EMBO J **22:** 2623-2633

Lai CP, Chen PH, Huang JP, Tzeng YH, Chaw SM, Shaw JF (2012) Functional diversification of the Tubby-like protein gene families (TULPs) during eukaryotic evolution. Biocatalysis and Agricultural Biotechnology **1:** 2-8

Lai CP, Lee CL, Chen PH, Wu SH, Yang CC, Shaw JF (2004) Molecular analyses of the Arabidopsis TUBBY-like protein gene family. Plant Physiol **134:** 1586-1597

Laloi C, Apel K, Danon A (2004) Reactive oxygen signalling: the latest news. Curr Opin Plant Biol **7:** 323-328

Larkin MA, Blackshields G, Brown NP, Chenna R, McGettigan PA, McWilliam H, Valentin F, Wallace IM, Wilm A, Lopez R, Thompson JD, Gibson TJ, Higgins DG (2007) Clustal W and clustal X version 2.0. Bioinformatics **23:** 2947-2948

Lechner E, Achard P, Vansiri A, Potuschak T, Genschik P (2006) F-box proteins everywhere. Curr Opin Plant Biol **9:** 631-638

Lee SH, Ahsan N, Lee KW, Kim DH, Lee DG, Kwak SS, Kwon SY, Kim TH, Lee BH (2007) Simultaneous overexpression of both CuZn superoxide dismutase and ascorbate peroxidase in transgenic tall fescue plants confers increased tolerance to a wide range of abiotic stresses. J Plant Physiol **164:** 1626-1638

Legendre L, Yueh YG, Crain R, Haddock N, Heinstein PF, Low PS (1993) Phospholipase C activation during elicitation of the oxidative burst in cultured plant cells. J Biol Chem **268:** 24559-24563

Lemmon MA (2004) Pleckstrin homology domains: not just for phosphoinositides. Biochem Soc Trans **32:** 707-711

Lemmon MA, Ferguson KM, O'Brien R, Sigler PB, Schlessinger J (1995) Specific and high-affinity binding of inositol phosphates to an isolated pleckstrin homology domain. Proc Natl Acad Sci USA **92:** 10472-10476

Letunic I, Doerks T, Bork P (2012) SMART 7: recent updates to the protein domain annotation resource. Nucleic Acids Res **40:** D302-305

Lewis CA, Batlle IR, Batlle KGR, Banerjee P, Cideciyan AV, Huang J, Alemán TS, Huang Y, Ott J, Gilliam TC, Knowles JA, Jacobson SG (1999) Tubby-like protein 1

homozygous splice-site mutation causes early-onset severe retinal degeneration. Invest Ophthalmol Vis Sci **40:** 2106-2114

Li QZ, Wang CY, Shi JD, Ruan QG, Eckenrode S, Davoodi-Semiromi A, Kukar T, Gu Y, Lian W, Wu D, She JX (2001) Molecular cloning and characterization of the mouse and human *TUSP* gene, a novel member of the tubby superfamily. Gene **273:** 275-284

Link K, Vogel F, Sonnewald U (2011) PD Trafficking of Potato Leaf Roll Virus Movement Protein in Arabidopsis Depends on Site-specific Protein Phosphorylation. Front Plant Sci **2:** 18

Liu JX, Howell SH (2010) Endoplasmic reticulum protein quality control and its relationship to environmental stress responses in plants. Plant Cell **22:** 2930-2942

Liu JX, Srivastava R, Che P, Howell SH (2007) Salt stress responses in Arabidopsis utilize a signal transduction pathway related to endoplasmic reticulum stress signaling. Plant J **51:** 897-909

Liu Q (2008) Identification of rice TUBBY-like genes and their evolution. FEBS J **275:** 163-171

Luhua S, Ciftci-Yilmaz S, Harper J, Cushman J, Mittler R (2008) Enhanced tolerance to oxidative stress in transgenic Arabidopsis plants expressing proteins of unknown function. Plant Physiol **148:** 280-292

Lunn JE (2007) Compartmentation in plant metabolism. J Exp Bot **58:** 35-47

Mano S, Miwa T, Nishikawa S, Mimura T, Nishimura M (2009) Seeing is believing: on the use of image databases for visually exploring plant organelle dynamics. Plant Cell Physiol **50:** 2000-2014

Mathur J (2007) The illuminated plant cell. Trends Plant Sci **12:** 506-513

Mauch-Mani B, Mauch F (2005) The role of abscisic acid in plant–pathogen interactions. Curr Opin Plant Biol **8:** 409-414

Meijer HJG, Munnik T (2003) Phospholipid-based signaling in plants. Annu Rev Plant Biol **54:** 265-306

Melin PM, Sommarin M, Sandelius AS, Jergil B (1987) Identification of Ca^{2+}-stimulated polyphosphoinositide phospholipase C in isolated plant plasma membranes. FEBS Lett **223:** 87-91

Mengiste T, Chen X, Salmeron J, Dietrich R (2003) The *BOTRYTIS SUSCEPTIBLE1* gene encodes an R2R3MYB transcription factor protein that is required for biotic and abiotic stress responses in Arabidopsis. Plant Cell **15:** 2551-2565

Mittler R, Vanderauwera S, Gollery M, Van Breusegem F (2004) Reactive oxygen gene network of plants. Trends Plant Sci **9:** 490-498

Mittler R, Vanderauwera S, Suzuki N, Miller G, Tognetti VB, Vandepoele K, Gollery M, Shulaev V, Van Breusegem F (2011) ROS signaling: the new wave? Trends Plant Sci **16:** 300-309

Moreno AA, Orellana A (2011) The physiological role of the unfolded protein response in plants. Biol Res **44:** 75-80

Mukhopadhyay S, Jackson PK (2011) The tubby family proteins. Genome Biol **12:** 225

Mukhopadhyay S, Wen X, Chih B, Nelson CD, Lane WS, Scales SJ, Jackson PK (2010) TULP3 bridges the IFT-A complex and membrane phosphoinositides to promote trafficking of G protein-coupled receptors into primary cilia. Genes Dev **24:** 2180-2193

Munnik T, Irvine RF, Musgrave A (1998) Phospholipid signalling in plants. Biochim Biophys Acta **1389:** 222-272

Munnik T, Vermeer JEM (2010) Osmotic stress-induced phosphoinositide and inositol phosphate signalling in plants. Plant Cell Environ **33:** 655-669

Munns R (2002) Comparative physiology of salt and water stress. Plant Cell Environ **25:** 239-250

Nanjo Y, Oka H, Ikarashi N, Kaneko K, Kitajima A, Mitsui T, Munoz FJ, Rodriguez-Lopez M, Baroja-Fernandez E, Pozueta-Romero J (2006) Rice plastidial *N*-glycosylated nucleotide pyrophosphatase/phosphodiesterase is transported from the ER-Golgi to the chloroplast through the secretory pathway. Plant Cell **18:** 2582-2592

Nash MS, Young KW, Willars GB, Challiss RA, Nahorski SR (2001) Single-cell imaging of graded Ins(1,4,5)P3 production following G-protein-coupled-receptor activation. Biochem J **356:** 137-142

Navarro L, Bari R, Achard P, Lisón P, Nemri A, Harberd NP, Jones JDG (2008) DELLAs Control Plant Immune Responses by Modulating the Balance of Jasmonic Acid and Salicylic Acid Signaling. Curr Biol **18:** 650-655

Nelson BK, Cai X, Nebenführ A (2007) A multicolored set of *in vivo* organelle markers for co-localization studies in Arabidopsis and other plants. Plant J **51:** 1126-1136

Nelson CP, Nahorski SR, Challiss RAJ (2008) Temporal profiling of changes in phosphatidylinositol 4,5-bisphosphate, inositol 1,4,5-trisphosphate and diacylglycerol

allows comprehensive analysis of phospholipase C-initiated signalling in single neurons. J Neurochem **107:** 602-615

Newton AC, Fitt BDL, Atkins SD, Walters DR, Daniell TJ (2010) Pathogenesis, parasitism and mutualism in the trophic space of microbe–plant interactions. Trends Microbiol **18:** 365-373

Nibau C, Gibbs DJ, Bunting KA, Moody LA, Smiles EJ, Tubby JA, Bradshaw SJ, Coates JC (2011) ARABIDILLO proteins have a novel and conserved domain structure important for the regulation of their stability. Plant Mol Biol **75:** 77-92

Nishina PM, North MA, Ikeda A, Yan Y, Naggert JK (1998) Molecular characterization of a novel tubby gene family member, *TULP3*, in mouse and humans. Genomics **54:** 215-220

Noben-Trauth K, Naggert JK, North MA, Nishina PM (1996) A candidate gene for the mouse mutation *tubby*. Nature **380:** 534-538

Noctor G, Foyer CH (1998) ASCORBATE AND GLUTATHIONE: Keeping Active Oxygen Under Control. Annu Rev Plant Physiol Plant Mol Biol **49:** 249-279

Norman RX, Ko HW, Huang V, Eun CM, Abler LL, Zhang Z, Sun X, Eggenschwiler JT (2009) Tubby-like protein 3 (TULP3) regulates patterning in the mouse embryo through inhibition of Hedgehog signaling. Hum Mol Genet **18:** 1740-1754

North MA, Naggert JK, Yan Y, Noben-Trauth K, Nishina PM (1997) Molecular characterization of *TUB*, *TULP1*, and *TULP2*, members of the novel tubby gene family and their possible relation to ocular diseases. Proc Natl Acad Sci USA **94:** 3128-3133

Nürnberger T, Brunner F, Kemmerling B, Piater L (2004) Innate immunity in plants and animals: striking similarities and obvious differences. Immunol Rev **198:** 249-266

Oelmüller R, Sherameti I, Tripathi S, Varma A (2009) *Piriformospora indica*, a cultivable root endophyte with multiple biotechnological applications. Symbiosis **49:** 1-17

Ohlemiller KK, Hughes RM, Mosinger-Ogilvie J, Speck JD, Grosof DH, Silverman MS (1995) Cochlear and retinal degeneration in the tubby mouse. Neuroreport **6:** 845-849

Okumoto S, Jones A, Frommer WB (2012) Quantitative imaging with fluorescent biosensors. Annu Rev Plant Biol **63:** 663-706

Panstruga R (2004) A golden shot: how ballistic single cell transformation boosts the molecular analysis of cereal–mildew interactions. Mol Plant Pathol **5:** 141-148

Parida AK, Das AB (2005) Salt tolerance and salinity effects on plants: a review. Ecotoxicol Environ Saf **60:** 324-349

Parniske M (2008) Arbuscular mycorrhiza: the mother of plant root endosymbioses. Nat Rev Micro **6:** 763-775

Pazour GJ, Rosenbaum JL (2002) Intraflagellar transport and cilia-dependent diseases. Trends Cell Biol **12:** 551-555

Pei ZM, Murata Y, Benning G, Thomine S, Klüsener B, Allen GJ, Grill E, Schroeder JI (2000) Calcium channels activated by hydrogen peroxide mediate abscisic acid signalling in guard cells. Nature **406:** 731-734

Pei ZM, Kuchitsu K, Ward JM, Schwarz M, Schroeder JI (1997) Differential abscisic acid regulation of guard cell slow anion channels in Arabidopsis wild-type and *abi1* and *abi2* mutants. Plant Cell **9:** 409-423

Peitsch MC (1995) Protein modeling by E-mail. Nat Biotechnol **13**: 658-660

Peškan-Berghöfer T, Shahollari B, Giong PH, Hehl S, Markert C, Blanke V, Kost G, Varma A, Oelmüller R (2004) Association of *Piriformospora indica* with *Arabidopsis thaliana* roots represents a novel system to study beneficial plant–microbe interactions and involves early plant protein modifications in the endoplasmic reticulum and at the plasma membrane. Physiol Plantarum **122:** 465-477

Pfannschmidt T (2003) Chloroplast redox signals: how photosynthesis controls its own genes. Trends Plant Sci **8:** 33-41

Pieterse CMJ, Leon-Reyes A, Van der Ent S, Van Wees SCM (2009) Networking by small-molecule hormones in plant immunity. Nat Chem Biol **5:** 308-316

Pieterse CM, van der Does D, Zamioudis C, Leon-Reyes A, van Wees SC (2012) Hormonal Modulation of Plant Immunity. Annu Rev Cell Dev Biol

Pieterse CMJ, van Wees SCM, Hoffland E, van Pelt JA, van Loon LC (1996) Systemic resistance in Arabidopsis induced by biocontrol bacteria is independent of salicylic acid accumulation and pathogenesis-related gene expression. Plant Cell **8:** 1225-1237

Pieterse CMJ, van Wees SCM, van Pelt JA, Knoester M, Laan R, Gerrits H, Weisbeek PJ, van Loon LC (1998) A novel signaling pathway controlling induced systemic resistance in Arabidopsis. Plant Cell **10:** 1571-1580

Pingret JL, Journet EP, Barker DG (1998) *Rhizobium* nod factor signaling: Evidence for a G protein-mediated transduction mechanism. Plant Cell **10:** 659-672

Potuschak T, Lechner E, Parmentier Y, Yanagisawa S, Grava S, Koncz C, Genschik P (2003) EIN3-Dependent Regulation of Plant Ethylene Hormone Signaling by Two *Arabidopsis* F Box Proteins: EBF1 and EBF2. Cell **115:** 679-689

Qiang X, Weiss M, Kogel KH, Schäfer P (2012) *Piriformospora indica*-a mutualistic basidiomycete with an exceptionally large plant host range. Mol Plant Pathol **13:** 508-518

Qiang X, Zechmann B, Reitz MU, Kogel KH, Schäfer P (2012) The mutualistic fungus *Piriformospora indica* colonizes *Arabidopsis* roots by inducing an endoplasmic reticulum stress-triggered caspase-dependent cell death. Plant Cell **24:** 794-809

Quan LJ, Zhang B, Shi WW, Li HY (2008) Hydrogen Peroxide in Plants: a Versatile Molecule of the Reactive Oxygen Species Network. J Integr Plant Biol **50:** 2-18

Quinn KV, Behe P, Tinker A (2008) Monitoring changes in membrane phosphatidylinositol 4,5-bisphosphate in living cells using a domain from the transcription factor tubby. J Physiol **586:** 2855-2871

Rafiqi M, Bernoux M, Ellis JG, Dodds PN (2009) In the trenches of plant pathogen recognition: Role of NB-LRR proteins. Semin Cell Dev Biol **20:** 1017-1024

Rentel MC, Lecourieux D, Ouaked F, Usher SL, Petersen L, Okamoto H, Knight H, Peck SC, Grierson CS, Hirt H, Knight MR (2004) OXI1 kinase is necessary for oxidative burst-mediated signalling in *Arabidopsis*. Nature **427:** 858-861

Riechmann JL, Heard J, Martin G, Reuber L, Jiang CZ, Keddie J, Adam L, Pineda O, Ratcliffe OJ, Samaha RR, Creelman R, Pilgrim M, Broun P, Zhang JZ, Ghandehari D, Sherman BK, Yu GL (2000) *Arabidopsis* transcription factors: genome-wide comparative analysis among eukaryotes. Science **290:** 2105-2110

Risseeuw EP, Daskalchuk TE, Banks TW, Liu E, Cotelesage J, Hellmann H, Estelle M, Somers DE, Crosby WL (2003) Protein interaction analysis of SCF ubiquitin E3 ligase subunits from *Arabidopsis*. Plant J **34:** 753-767

Rodriguez RJ, Redman RS, Henson JM (2004) The Role of Fungal Symbioses in the Adaptation of Plants to High Stress Environments. Mitigation and Adaptation Strategies for Global Change **9:** 261-272

Sahay NS, Varma A (1999) *Piriformospora indica*: a new biological hardening tool for micropropagated plants. FEMS Microbiol Lett **181:** 297-302

Santagata S, Boggon TJ, Baird CL, Gomez CA, Zhao J, Shan WS, Myszka DG, Shapiro L (2001) G-protein signaling through tubby proteins. Science **292:** 2041-2050

Schäfer P, Kogel KH (2009) The Sebacinoid Fungus *Piriformospora indica*: an Orchid Mycorrhiza Which May Increase Host Plant Reproduction and Fitness. In: *The Mycota, Vol. 5, Plant Relationships* (Deising, HB, Esser, K, eds) pp 99-112. Heidelberg: Springer Verlag.

Schäfer P, Pfiffi S, Voll LM, Zajic D, Chandler PM, Waller F, Scholz U, Pons-Kühnemann J, Sonnewald S, Sonnewald U, Kogel KH (2009) Manipulation of plant innate immunity and gibberellin as factor of compatibility in the mutualistic association of barley roots with *Piriformospora indica*. Plant J **59:** 461-474

Schmittgen TD, Livak KJ (2008) Analyzing real-time PCR data by the comparative C_T method. Nat Protocols **3:** 1101-1108

Scholl RL, May ST, Ware DH (2000) Seed and molecular resources for Arabidopsis. Plant Physiol **124:** 1477-1480

Schultz J, Milpetz F, Bork P, Ponting CP (1998) SMART, a simple modular architecture research tool: Identification of signaling domains. Proc Natl Acad Sci USA **95:** 5857-5864

Schwacke R, Fischer K, Ketelsen B, Krupinska K, Krause K (2007) Comparative survey of plastid and mitochondrial targeting properties of transcription factors in Arabidopsis and rice. Mol Genet Genomics **277:** 631-646

Schwechheimer C, Willige BC (2009) Shedding light on gibberellic acid signalling. Curr Opin Plant Biol **12:** 57-62

Schweizer P, Pokorny J, Abderhalden O, Dudler R (1999) A transient assay system for the functional assessment of defense-related genes in wheat. Mol Plant Microbe In **12:** 647-654

Selosse MA, Dubois MP, Alvarez N (2009) Do Sebacinales commonly associate with plant roots as endophytes? Mycol Res **113:** 1062-1069

Selosse MA, M Weiß, Jany JL, Tillier A (2002) Communities and populations of sebacinoid basidiomycetes associated with the achlorophyllous orchid *Neottia nidus-avis* (L.) L.C.M. Rich. and neighbouring tree ectomycorrhizae. Mol Ecol **11:** 1831-1844

Selosse MA, Setaro S, Glatard F, Richard F, Urcelay C, Weiß M (2007) Sebacinales are common mycorrhizal associates of Ericaceae. New Phytol **174:** 864-878

Serfling A, Wirsel SGR, Lind V, Deising HB (2007) Performance of the Biocontrol Fungus *Piriformospora indica* on Wheat Under Greenhouse and Field Conditions. Phytopathology **97:** 523-531

Sherameti I, Tripathi S, Varma A, Oelmüller R (2008) The root-colonizing endophyte *Pirifomospora indica* confers drought tolerance in *Arabidopsis* by stimulating the expression of drought stress-related genes in leaves. Mol Plant Microbe In **21:** 799-807

Sherameti I, Venus Y, Drzewiecki C, Tripathi S, Dan VM, Nitz I, Varma A, Grundler FM, Oelmüller R (2008) PYK10, a β-glucosidase located in the endoplasmatic reticulum, is crucial for the beneficial interaction between *Arabidopsis thaliana* and the endophytic fungus *Piriformospora indica*. Plant J **54:** 428-439

Simon-Plas F, Elmayan T, Blein JP (2002) The plasma membrane oxidase NtrbohD is responsible for AOS production in elicited tobacco cells. Plant J **31:** 137-147

Sirrenberg A, Göbel C, Grond S, Czempinski N, Ratzinger A, Karlovsky P, Santos P, Feussner I, Pawlowski K (2007) *Piriformospora indica* affects plant growth by auxin production. Physiol Plant **131:** 581-589

Smaldone S, Laub F, Else C, Dragomir C, Ramirez F (2004) Identification of MoKA, a novel F-box protein that modulates Krüppel-like transcription factor 7 activity. Mol Cell Biol **24:** 1058-1069

Smaldone S, Ramirez F (2006) Multiple pathways regulate intracellular shuttling of MoKA, a co-activator of transcription factor KLF7. Nucleic Acids Res **34:** 5060-5068

Smith RJ, Sam LM, Justen JM, Bundy GL, Bala GA, Bleasdale JE (1990) Receptor-coupled signal transduction in human polymorphonuclear neutrophils: effects of a novel inhibitor of phospholipase C-dependent processes on cell responsiveness. J Pharmacol Exp Ther **253:** 688-697

Soll J, Schleiff E (2004) Protein import into chloroplasts. Nat Rev Mol Cell Biol **5:** 198-208

Sorek N, Bloch D, Yalovsky S (2009) Protein lipid modifications in signaling and subcellular targeting. Curr Opin Plant Biol **12:** 714-720

Spartz AK, Gray WM (2008) Plant hormone receptors: new perceptions. Genes Dev **22:** 2139-2148

Stauffer TP, Ahn S, Meyer T (1998) Receptor-induced transient reduction in plasma membrane PtdIns(4,5)P_2 concentration monitored in living cells. Curr Biol **8:** 343-346

Stein E, Molitor A, Kogel KH, Waller F (2008) Systemic resistance in *Arabidopsis* conferred by the mycorrhizal fungus *Piriformospora indica* requires jasmonic acid signaling and the cytoplasmic function of NPR1. Plant Cell Physiol **49:** 1747-1751

Stolc V, Samanta MP, Tongprasit W, Marshall WF (2005) Genome-wide transcriptional analysis of flagellar regeneration in *Chlamydomonas reinhardtii* identifies orthologs of ciliary disease genes. Proc Natl Acad Sci USA **102:** 3703-3707

Stothard P (2000) The sequence manipulation suite: JavaScript programs for analyzing and formatting protein and DNA sequences. Biotechniques **28:** 1102, 1104

Stubdal H, Lynch CA, Moriarty A, Fang Q, Chickering T, Deeds JD, Fairchild-Huntress V, Charlat O, Dunmore JH, Kleyn P, Huszar D, Kapeller R (2000) Targeted deletion of the *tub* mouse obesity gene reveals that *tubby* is a loss-of-function mutation. Mol Cell Biol **20:** 878-882

Sun TP (2008) Gibberellin metabolism, perception and signaling pathways in Arabidopsis. Arabidopsis Book **6:** e0103

Sutherland MW (1991) The generation of oxygen radicals during host plant responses to infection. Physiol Mol Plant P **39:** 79-93

Szentpetery Z, Balla A, Kim YJ, Lemmon MA, Balla T (2009) Live cell imaging with protein domains capable of recognizing phosphatidylinositol 4,5-bisphosphate; a comparative study. BMC Cell Biol **10:** 67

Tang RH, Han S, Zheng H, Cook CW, Choi CS, Woerner TE, Jackson RB, Pei ZM (2007) Coupling diurnal cytosolic Ca^{2+} oscillations to the CAS-IP3 pathway in *Arabidopsis*. Science **315:** 1423-1426

Tedersoo L, Kõljalg U, Hallenberg N, Larsson KH (2003) Fine scale distribution of ectomycorrhizal fungi and roots across substrate layers including coarse woody debris in a mixed forest. New Phytol **159:** 153-165

Thatcher LF, Manners JM, Kazan K (2009) *Fusarium oxysporum* hijacks COI1-mediated jasmonate signaling to promote disease development in Arabidopsis. Plant J **58:** 927-939

The Arabidopsis Genome Initiative (2000) Analysis of the genome sequence of the flowering plant Arabidopsis thaliana. Nature **408:** 796-815

Torres MA (2010) ROS in biotic interactions. Physiol Plantarum **138:** 414-429

Torres MA, Dangl JL, Jones JDG (2002) *Arabidopsis* gp91^{phox} homologues *AtrbohD* and *AtrbohF* are required for accumulation of reactive oxygen intermediates in the plant defense response. Proc Natl Acad Sci USA **99:** 517-522

Torres MA, Jones JDG, Dangl JL (2005) Pathogen-induced, NADPH oxidase-derived reactive oxygen intermediates suppress spread of cell death in *Arabidopsis thaliana*. Nat Genet **37:** 1130-1134

Toulza E, Shin MS, Blanc G, Audic S, Laabir M, Collos Y, Claverie JM, Grzebyk D (2010) Gene expression in proliferating cells of the dinoflagellate *Alexandrium catenella* (Dinophyceae). Appl Environ Microbiol **76:** 4521-4529

Triantaphylidès C, Havaux M (2009) Singlet oxygen in plants: production, detoxification and signaling. Trends Plant Sci **14:** 219-228

Trujillo M, Ichimura K, Casais C, Shirasu K (2008) Negative Regulation of PAMP-Triggered Immunity by an E3 Ubiquitin Ligase Triplet in *Arabidopsis*. Curr Biol **18:** 1396-1401

Ueguchi-Tanaka M, Ashikari M, Nakajima M, Itoh H, Katoh E, Kobayashi M, Chow TY, Hsing YIC, Kitano H, Yamaguchi I, Matsuoka M (2005) *GIBBERELLIN INSENSITIVE DWARF1* encodes a soluble receptor for gibberellin. Nature **437:** 693-698

Ülker B, Peiter E, Dixon DP, Moffat C, Capper R, Bouché N, Edwards R, Sanders D, Knight H, Knight MR (2008) Getting the most out of publicly available T-DNA insertion lines. Plant J **56:** 665-677

Urban A, Weib M, Bauer R (2003) Ectomycorrhizas involving sebacinoid mycobionts. Mycol Res **107:** 3-14

Vadassery J, Tripathi S, Prasad R, Varma A, Oelmüller R (2009) Monodehydroascorbate reductase 2 and dehydroascorbate reductase 5 are crucial for a mutualistic interaction between *Piriformospora indica* and *Arabidopsis*. J Plant Physiol **166:** 1263-1274

Van Breusegem F, Vranová E, Dat JF, Inzé D (2001) The role of active oxygen species in plant signal transduction. Plant Sci **161:** 405-414

Van Der Biezen EA, Jones JDG (1998) Plant disease-resistance proteins and the gene-for-gene concept. Trends Biochem Sci **23:** 454-456

Van Leeuwen W, Vermeer JEM, Gadella TWJ, Jr., Munnik T (2007) Visualization of phosphatidylinositol 4,5-bisphosphate in the plasma membrane of suspension-cultured tobacco BY-2 cells and whole Arabidopsis seedlings. Plant J **52:** 1014-1026

Van Wees SCM, Van der Ent S, Pieterse CMJ (2008) Plant immune responses triggered by beneficial microbes. Curr Opin Plant Biol **11:** 443-448

Varma A, Savita V, Sudha, Sahay N, Bütehorn B, Franken P (1999) *Piriformospora indica*, a cultivable plant-growth-promoting root endophyte. Appl Environ Microbiol **65:** 2741-2744

Várnai P, Balla T (1998) Visualization of phosphoinositides that bind pleckstrin homology domains: calcium- and agonist-induced dynamic changes and relationship to myo-[^{3}H]inositol-labeled phosphoinositide pools. J Cell Biol **143:** 501-510

Várnai P, Balla T (2006) Live cell imaging of phosphoinositide dynamics with fluorescent protein domains. BBA - Mol Cell Biol L **1761:** 957-967

Verma S, Varma A, Rexer KH, Hassel A, Kost G, Ashok S, Bisen P, Bütehorn B, Franken P (1998) *Piriformospora indica*, gen. et sp. nov., a New Root-Colonizing Fungus. Mycologia **90:** 896-903

Villarejo A, Burén S, Larsson S, Déjardin A, Monné M, Rudhe C, Karlsson J, Jansson S, Lerouge P, Rolland N, von Heijne G, Grebe M, Bako L, Samuelsson G (2005) Evidence for a protein transported through the secretory pathway *en route* to the higher plant chloroplast. Nat Cell Biol **7:** 1224-1231

Vincent P, Chua M, Nogue F, Fairbrother A, Mekeel H, Xu Y, Allen N, Bibikova TN, Gilroy S, Bankaitis VA (2005) A Sec14p-nodulin domain phosphatidylinositol transfer protein polarizes membrane growth of *Arabidopsis thaliana* root hairs. J Cell Biol **168:** 801-812

Waller F, Achatz B, Baltruschat H, Fodor J, Becker K, Fischer M, Heier T, Hückelhoven R, Neumann C, von Wettstein D, Franken P, Kogel KH (2005) The endophytic fungus *Piriformospora indica* reprograms barley to salt-stress tolerance, disease resistance, and higher yield. Proc Natl Acad Sci USA **102:** 13386-13391

Wang L, Tsuda K, Sato M, Cohen JD, Katagiri F, Glazebrook J (2009) Arabidopsis CaM Binding Protein CBP60g Contributes to MAMP-Induced SA Accumulation and Is Involved in Disease Resistance against *Pseudomonas syringae*. PLoS Pathog **5:** e1000301

Wardhan V, Jahan K, Gupta S, Chennareddy S, Datta A, Chakraborty S, Chakraborty N (2012) Overexpression of CaTLP1, a putative transcription factor in chickpea (*Cicer arietinum* L.), promotes stress tolerance. Plant Mol Biol **79:** 479-493

Weigel D, Nilsson O (1995) A developmental switch sufficient for flower initiation in diverse plants. Nature **377:** 495-500

Weiß M, Oberwinkler F (2001) Phylogenetic relationships in *Auriculariales* and related groups—hypotheses derived from nuclear ribosomal DNA sequences. Mycol Res **105:** 403-415

Weiß M, Selosse MA, Rexer KH, Urban A, Oberwinkler F (2004) *Sebacinales*: a hitherto overlooked cosm of heterobasidiomycetes with a broad mycorrhizal potential. Mycol Res **108:** 1003-1010

Weiß M, Sýkorová Z, Garnica S, Riess K, Martos F, Krause C, Oberwinkler F, Bauer R, Redecker D (2011) Sebacinales everywhere: previously overlooked ubiquitous fungal endophytes. PLoS One **6:** e16793

Wente SR, Rout MP (2010) The nuclear pore complex and nuclear transport. Cold Spring Harb Perspect Biol **2:** a000562

Wiederkehr A, Avaro S, Prescianotto-Baschong C, Haguenauer-Tsapis R, Riezman H (2000) The F-box protein Rcy1p is involved in endocytic membrane traffic and recycling out of an early endosome in *Saccharomyces cerevisiae*. J Cell Biol **149:** 397-410

William DA, Su Y, Smith MR, Lu M, Baldwin DA, Wagner D (2004) Genomic identification of direct target genes of LEAFY. Proc Natl Acad Sci USA **101:** 1775-1780

Williamson B, Tudzynski B, Tudzynski P, Van Kan JAL (2007) *Botrytis cinerea*: the cause of grey mould disease. Mol Plant Pathol **8:** 561-580

Wilson D (1995) Endophyte: The Evolution of a Term, and Clarification of Its Use and Definition. Oikos **73:** 274-276

Winck FV, Riao-Pachón DM, Sommer F, Rupprecht J, Mueller-Roeber B (2012) The nuclear proteome of the green alga *Chlamydomonas reinhardtii*. Proteomics **12:** 95-100

Wittstock U, Gershenzon J (2002) Constitutive plant toxins and their role in defense against herbivores and pathogens. Curr Opin Plant Biol **5:** 300-307

Yan J, Zhang C, Gu M, Bai Z, Zhang W, Qi T, Cheng Z, Peng W, Luo H, Nan F, Wang Z, Xie D (2009) The *Arabidopsis* CORONATINE INSENSITIVE1 protein is a jasmonate receptor. Plant Cell **21:** 2220-2236

Yang Z, Zhou Y, Wang X, Gu S, Yu J, Liang G, Yan C, Xu C (2008) Genomewide comparative phylogenetic and molecular evolutionary analysis of tubby-like protein family in *Arabidopsis*, rice, and poplar. Genomics **92:** 246-253

Yee D, Goring DR (2009) The diversity of plant U-box E3 ubiquitin ligases: from upstream activators to downstream target substrates. J Exp Bot **60:** 1109-1121

Zarea MJ, Hajinia S, Karimi N, Mohammadi Goltapeh E, Rejali F, Varma A (2012) Effect of *Piriformospora indica* and *Azospirillum strains* from saline or non-saline soil on mitigation of the effects of NaCl. Soil Biol Biochem **45:** 139-146

Zhou Q, Ben-Efraim I, Bigcas JL, Junqueira D, Wiedmer T, Sims PJ (2005) Phospholipid scramblase 1 binds to the promoter region of the inositol 1,4,5-triphosphate receptor type 1 gene to enhance its expression. J Biol Chem **280:** 35062-35068

Zhou Q, Zhao J, Stout JG, Luhm RA, Wiedmer T, Sims PJ (1997) Molecular cloning of human plasma membrane phospholipid scramblase. A protein mediating transbilayer movement of plasma membrane phospholipids. J Biol Chem **272:** 18240-18244

Zhu JK (2003) Regulation of ion homeostasis under salt stress. Curr Opin Plant Biol **6:** 441-445

Zipfel C (2008) Pattern-recognition receptors in plant innate immunity. Curr Opin Immunol **20:** 10-16

Zipfel C, Kunze G, Chinchilla D, Caniard A, Jones JDG, Boller T, Felix G (2006) Perception of the bacterial PAMP EF-Tu by the receptor EFR restricts *Agrobacterium*-mediated transformation. Cell **125:** 749-760

Zuccaro A, Lahrmann U, Güldener U, Langen G, Pfiffi S, Biedenkopf D, Wong P, Samans B, Grimm C, Basiewicz M, Murat C, Martin F, Kogel KH (2011) Endophytic life strategies decoded by genome and transcriptome analyses of the mutualistic root symbiont *Piriformospora indica*. PLoS Pathog **7:** e1002290

7. Supplement

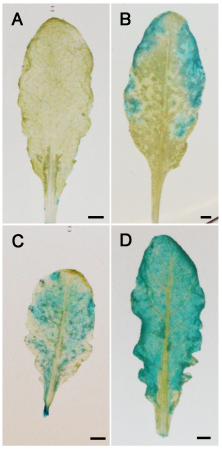

Fig. 7.1: Histochemical GUS-analysis of rosette leaves from AtTLP5$_{Prom}$:*GUS* transgenic plants. Rosette leaves were harvested from 4-6-week-old soil grown plants and kept in GUS staining solution for about four hours. Detected GUS activity varied strongly between different leaves. Bars: 2 mm. Highly similar results were obtained from two independent transgenic lines.

ERKLÄRUNG

Ich erkläre:

„Ich habe die vorgelegte Dissertation selbstständig, ohne unerlaubte fremde Hilfe und nur mit den Hilfen angefertigt, die ich in der Dissertation angegeben habe. Alle Textstellen, die wörtlich oder sinngemäß aus veröffentlichten oder nicht veröffentlichten Schriften entnommen sind, und alle Angaben, die auf mündlichen Auskünften beruhen, sind als solche kenntlich gemacht. Bei den von mir durchgeführten und in der Dissertation erwähnten Untersuchungen habe ich die Grundsätze guter wissenschaftlicher Praxis wie sie in der „Satzung der Justus-Liebig-Universität Gießen zur Sicherung guter wissenschaftlicher Praxis“ niedergelegt sind, eingehalten.“

Gießen, im September 2012

Marco Uwe Reitz

Danksagung

Mein erster Dank gilt Prof. Dr. Kogel für die Gelegenheit, meine Promotion am IPAZ durchführen zu können, für die Unterstützung und das mir entgegengebrachte Vertrauen das ich während meiner Zeit am Institut erfahren durfte.

Ebenso danke ich Prof. Dr. van Bel, der sich bereit erklärt hat, meine Arbeit als Zweitgutachter zu begleiten.

Ein ganz besonderes Dankeschön auch an Patrick Schäfer für die direkte Betreuung meiner Promotion. Ohne die vielen Ideen, die Unterstützung und generell die immerwährende Bereitschaft mit mir über mein Thema zu diskutieren, wäre die Arbeit nicht möglich gewesen.

Bei Dr. Ruth Eichmann möchte ich mich für die Durchführung der Mehltau Experimente bedanken. Dr. Agnès Attard danke ich für die Versuche mit *Phytophtora*. Außerdem, danke ich Dr. Kathleen Zocher für die Erstellung der 3D Struktur für AtTLP3 und Dr. Jafargholi Imani für die Transformation von *Arabidopsis* Pflanzen für die GUS Experimente.

Jeff K. Bissue und Subhash Pai haben im Rahmen ihrer Master-Arbeiten zu meinem Thema beigetragen. Danke für die Mithilfe!

Viele weitere Leute haben dafür gesorgt, dass ich mich am IPAZ sehr wohl gefühlt habe. Ausdrücklich möchte ich Daggi und Rebekka für die Unterstützung bei den Versuchen und der Lösung so vieler kleiner und größerer Probleme danken. Ein Dankeschön auch an Martina, die mir sehr dabei geholfen hat mich in die molekularbiologischen Methoden einzufinden. Sophie, Adam, Sebastian, Anna und einige mehr: Danke für die schöne Zeit auch außerhalb des Instituts. Und auch allen anderen danke ich für die letzten Jahre, die Hilfe und die anregenden und lehrreichen Diskussionen.

Speziellen Dank auch noch einmal an Sabrina, Sebastian und Anna für die Durchsicht meines Manuskripts und die vielen hilfreichen Anmerkungen.

Meine Eltern und Geschwister haben mich immer unterstützt und mussten viel Verständnis für meine oft fehlende Zeit aufbringen. Ich danke euch für alles!

Und am Ende möchte ich mich ganz besonders bei meiner Freundin Dina bedanken. Ohne deine Geduld, Ermutigung und Unterstützung hätte ich es nicht geschafft.